Functional Biomarkers to Assess Visual System Integrity

An eye tracking based approach

NAJIYA SUNDUS K. MEETHAL

Functional Biomarkers to Assess Visual System Integrity
An eye tracking based approach

Najiya Sundus Kadavath Meethal

Functional Biomarkers to Assess Visual System Integrity
An eye tracking based approach

Functionele Biomarkers om
Visuele Systeem Integriteit te Beoordelen
Een op eye tracking gebaseerde aanpak

Thesis

To obtain the degree of Doctor from the Erasmus University Rotterdam
By command of the rector magnificus

Prof. Dr. A.L. Bredenoord

And in accordance with the decision of the Doctorate Board.
The public defence shall be held on

Tuesday 21 February 2023 at 10:30 hrs

By

Najiya Sundus Kadavath Meethal
Born in the "Land of Spices"
Kerala | India

Erasmus University Rotterdam

Promotion Commission:

Promotors: Prof. Dr. J. van der Steen
                                    Prof. Dr. R.J. George

Other members: Prof. Dr. M.A. Frens
                                      Prof. Dr. J.T. Erichsen
                                      Prof. Dr. C.C.W. Klaver

Copromotor: Dr. ir. J.J.M. Pel

"The sun casts light on things, and through that light,
it is possible to see. The purpose of light is to see."

"If everything around you seems dark, look again, you
may be the LIGHT."

|Rumi

TABLE OF CONTENTS

CHAPTER 1

General Introduction

1.1 Human visual system: Hierarchical organisation and neural elements

The primary senses provide us with a deep perceptual understanding of the real world among which we predominantly rely on sight as the foremost one. Our eyes function as a portal through which information from the surrounding environment is captured. They are exquisitely evolved with the ability to transduce light reflected from an object located in the external physical world into the brain's internal language of electrical signals (Figure 1.1).

1st Neuron: Light entering the eye triggers photochemical reaction in the photoreceptors (rods and cones)

2nd Neuron: Activation of bipolar cells triggered by the photochemical reaction

Cross sectional image of the retina

Light

Cones

Neural impulse

Ganglion cell

Bipolar cell

Light

Rods

Optic Nerve

3rd Neuron: Transfer of visual information to processing centres within the brain via the axonal fibres of RGCs

Figure 1.1: A schematic diagram demonstrating the path of light rays entering the eye, passing through its optical components, reaching the neural retina, and getting transmitted to the brain via the optic nerve.
(Image reproduced from Stangor et al., 2014)

Quanta of light are detected and later transformed into electrochemical impulses by means of a complex process facilitated by specialised retinal cells (~150 million) known as photoreceptors (rods and cones). Each photoreceptor generates a graded electrical potential that is proportional to the amount

of light sensed. These signals are further pre-processed in the layer of Retinal Ganglion Cells (RGCs) and propagated as action potentials along the Optic Nerve (ON) to the cortical and subcortical visual processing areas of the brain. Hence, in summary, in order to allow us to see the light-reflecting objects around us as a visual image, the intricate synchronisation of the ocular elements that initiate a cascade of biochemical reactions and the visual processing in the corresponding brain centres is necessary (Stangor et al., 2014; De Nava et al., 2021).

1.1.1 Optic Nerve and its linkage to the brain for visual processing

The ON is the second cranial nerve that transmits visual information from the retina to the higher centres in the brain. It is a cable-like grouping of ~ 770,000 to 1.7 million axons/nerve fibres, which are the extensions of a specific type of neuron set in the inner surface of the retina called the RGCs. The bundle of RGC axons receive their input from bipolar cells, makes a nearly 90° sharp turn, and projects through the Optic Nerve Head (ONH) or Optic disc (Figure 1.2). The ONH is the beginning of the ON and the exit point for axonal fibres. After reaching the ONH, the axons continue as a series of bundles/fascicles parted from one another by helical columns of glial cells, and vascular connective tissue septa, to form the ON (Hayreh, 1974; Monkhouse, 2005).

The ON leaves the orbit and enters the cranium (the skull), via the optic canal (~ 5 to 12 mm passage), running posteromedially towards the middle cranial fossa where the ON from each eye merge to form an 'x' shaped structure called 'the optic chiasm' (Figure 1.3). At the chiasm, nasal retinal fibres cross over to the contralateral optic tract, while fibres from the temporal halves stay ipsilateral (partial decussation). Several distinct and parallel visual pathways code the propagation and processing of retinal information within the Central Nervous System (CNS) wherein ON acts as a highway that connects our eyes to the brain via different projections (Hayreh, 1974; Monkhouse, 2005). The projections of ON endow the visual system with an exceptionally complex organisation composed of multiple pathways managing both hierarchical and analogous visual processing. If there is a disruption to one of the

components of these multiple pathways due to disease, lesion, or trauma, it has a significant impact on the visual system (Sadun, 1986). Hence, the specific functional properties of these multiple pathways can be used as potential biomarkers to evaluate the integrity of afferent and/or efferent conduction thereby aiding in disease detection and even prognosis assessment. To explore or rely on the biomarkers in diseases that affect the visual system/pathways, we need precise knowledge of the anatomy of these extensive neural paths concerning the to-and-fro transmission of visual information.
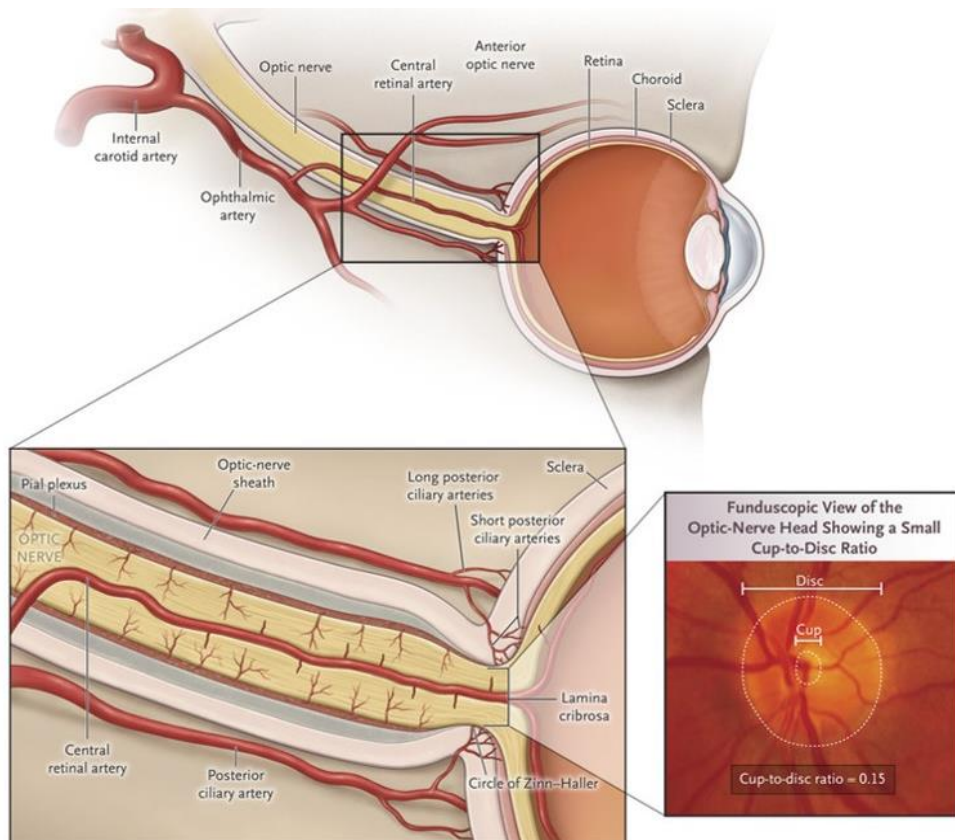

Figure 1.2: Sagittal section of the eye and the Optic Nerve (ON) illustrating the nerve exiting at the Optic Nerve Head (ONH) via the optic canal with the blood supplies by the branches of the central artery of the retina, pial branches from the choroidal arteries, circle of Zinn, and the ophthalmic artery.
(Image reproduced from Biousse et al., 2015)

1.1.2 Cortical/Striate projections of the Optic Nerve

The ON axons carrying neuronal signals from the retina terminate at different brain structures depending on their function. The majority of ON axons cease at a relay centre called the Lateral Geniculate Nucleus (LGN) of the midbrain, a posterolateral extension of the thalamus. The LGN consists of six specific layers organised into an explicit retinotopic map (point-by-point representation of the retinal surface in the higher centres of the visual system).
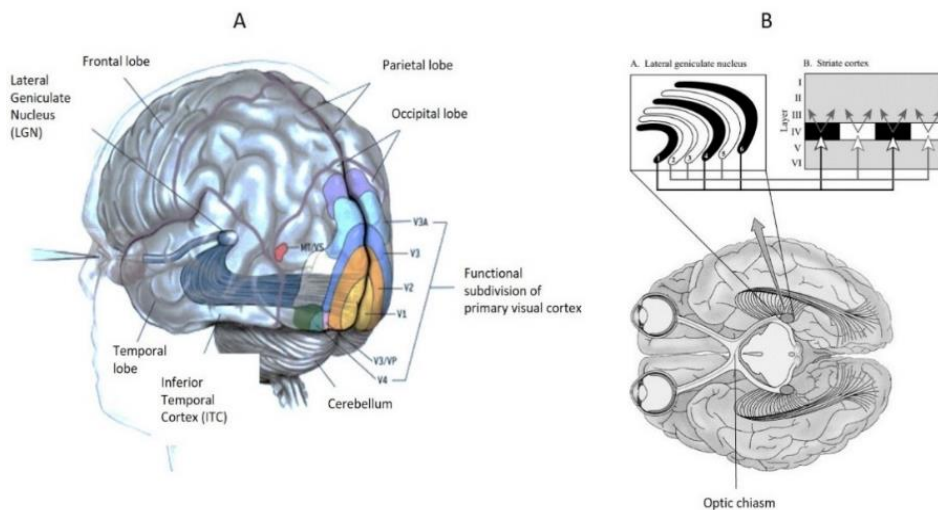
Figure 1.3: Schematic diagram of the human visual system displaying the main connections originating in the retina, synapsing in the Lateral Geniculate Nucleus (LGN), and projecting to the primary visual cortex.
(Image reproduced from www.gatsby.ucl.ac.uk (Panel A) and (Panel B: View from the ventral surface of the brain) from Wiencken-Barger et al., 2002)

The Optic Radiations (OR), a projection tract, connects the LGN with the primary visual cortical areas (Brodmann's area 17/V1 or striate) positioned along and within the calcarine fissure in the occipital lobe. OR is also known as the geniculocalcarine tract, the geniculostriate pathway, or posterior thalamic radiation. OR constitute ventral, medial, and dorsal bundles in which they transmit input from the superior quadrants of the retina, from the macula, and the lower quadrants of the retina respectively (Voets et al., 2017). Each of these bundles travels to the visual cortex where the signals converge

and are analysed with regard to form, movement, disparity, and colour (Daw, 2006). This is termed the retinogeniculostriate pathway or primary visual pathway (Figure 1.3). After the initial analysis of signals at the primary visual cortex, they are further processed by two parallel pathways that are dedicated to dealing with different aspects of visual information in subcortical/extrastriate areas (Figure 1.4). These are called the ventral stream (What pathway: Analysis of contour, orientation, texture, colour, and brightness) and a dorsal stream (Where pathway: Analysis of location, movement, and spatial relationships). The ventral stream projects to the inferior temporal cortex beginning from V1 running via V4 and Fusiform Face Area (FFA). Meanwhile the dorsal stream projects to the networks of the posterior parietal cortex beginning from V1 running through the motion-sensitive areas of V5 and V3a. In addition to these feedback projections to the extrastriate areas, V1 has a large number of neural connections with other cerebral and subcortical areas pertaining to attention, emotional regulations, etc., and other cortical areas associated with memory and motor movements (Daw & Daw, 2006; Kravitz et al., 2011; Atkinson & Braddick, 2012).
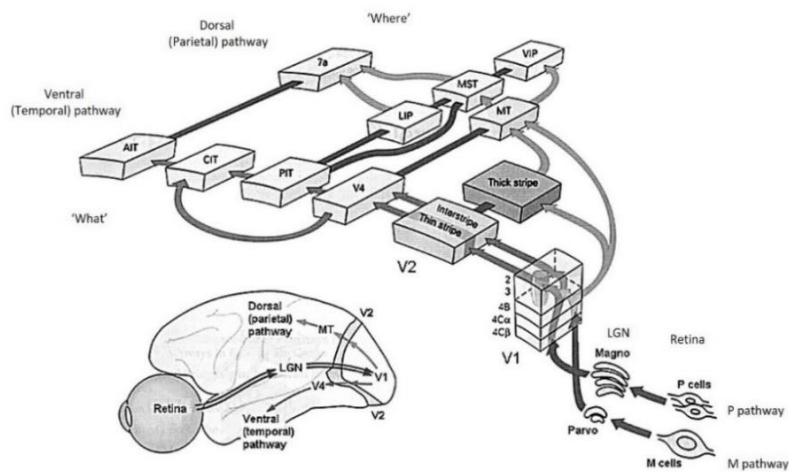
Figure 1.4: Schematic diagram of the human visual system projections from the retina to the primary visual cortex (V1) to the extrageniculostriate areas (V2, V3, V4, and MT+/V5) via the dorsal and ventral visual stream for higher-level processing. (Image reproduced from Behnke, 2003)

1.1.3 Sub-cortical/Extrastriate projections of the Optic Nerve

A second major subclass of RGC axons projects to the pretectum, a coordinating centre in the midbrain to regulate/control the Pupillary Light Reflexes (PLR). The nasally aligned fibres intersect at the chiasm and transfer the signal to the contralateral pretectal (pertaining to the other side) nucleus. Meanwhile, the temporally aligned fibres relay the information to the ipsilateral pretectal nucleus (pertaining to the same side). Each pretectal nucleus projects bilaterally and synapses in both Edinger-Westphal nuclei (EW). The activated EW nuclei open the efferent limb of the reflex by generating action potentials. The preganglionic parasympathetic neurons' axons conduct the signals along the oculomotor nerve (Cranial Nerve III) to the post-ganglionic nerve fibres of the ciliary ganglion. Subsequently, the short ciliary nerves stimulate the sphincter muscle of the pupil and cause pupillary constriction (Figure 1.5).

Figure 1.5: Schematic representation of the afferent and efferent pathways involved in pupillary reactions that responds to the photic/accommodative stimulus. (Image reproduced from fbnotebook.com)

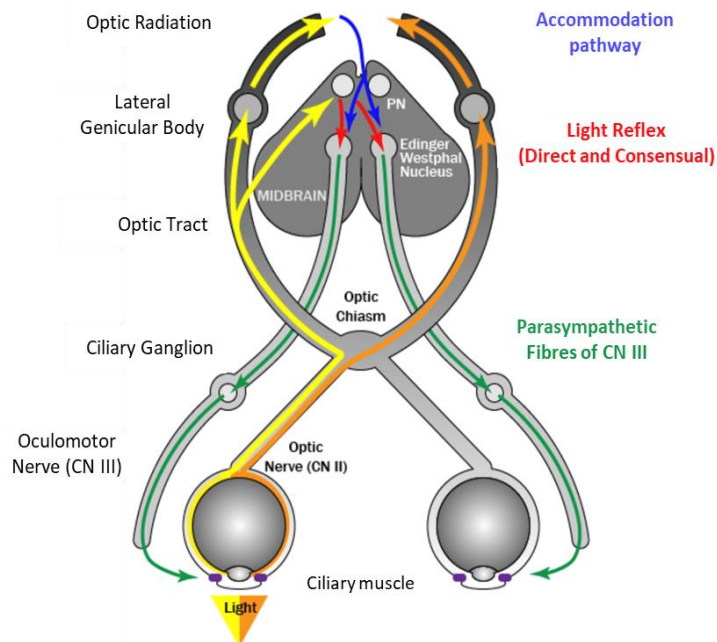Conversely, pupillary dilatation depends on sympathetic coordination which consists of pre-ganglionic fibres projecting from the hypothalamus to the superior cervical ganglion and post-ganglionic fibres projecting to the iris dilator muscles, via ciliary nerves (Yoo & Mihaila, 2020; Zele & Gamlin, 2020). Although the PLR is the main mechanism regulating the Pupil Diameter (PD), mediated by the subcortical pathways, the cognitive or emotional processes that influence pupillary dynamics are based on the feedback from the cortical innervation (Peinkhofer et al., 2019).

1.1.4 Role of oculomotor circuitries in visual processing

The human retina is not uniformly distributed but has its highest spatial resolution at the fovea. Therefore, in order to perceive new information, the visual system requires a constant sampling of signals from different parts of the external space by means of eye movements. These functional eye movements can be grossly classified as saccades (rapid shift of gaze between two locations), smooth pursuits (smooth tracking of moving objects), fixation (looking at a stationary object), and vergence (simultaneous movement of both eyes in opposite directions to obtain/maintain single binocular vision) eye movements (Kowler, 2011; Leigh & Zee, 2015). While saccadic movements direct the eyes to a region of interest, fixation is necessary for the process of stable visual perception. The performance of the oculomotor system undertakes constant recalibration and readjustment mediated by the subcortical and cortical regions acting as the prerequisite for optimal visual capabilities. The registration and evaluation of visually mediated eye movements is an important asset for understanding the integrity of the underlying neural substrate and a vital aid in the diagnosis of neuronal loss.

Eye movements are initiated voluntarily or triggered by the appearance of a detectable stimulus within the Visual Field (VF). Saccades are defined as rapid movements of the eye between fixation points generated by a network of cortical and brain stem structures and executed by a set of six extraocular muscles (Perry & Cowey, 1985). Excitatory input from the Frontal Eye Field (FEF), Parietal Eye Field (PEF), and Supplementary Eye Field (SEF) in combination with the inhibitory input from the basal ganglia are fed into the

Superior Colliculus (SC). From the SC, these signals are propagated to the saccade burst generator in the reticular formation (Figure 1.6) to initiate a specific type of saccade (Perry & Cowey, 1985).
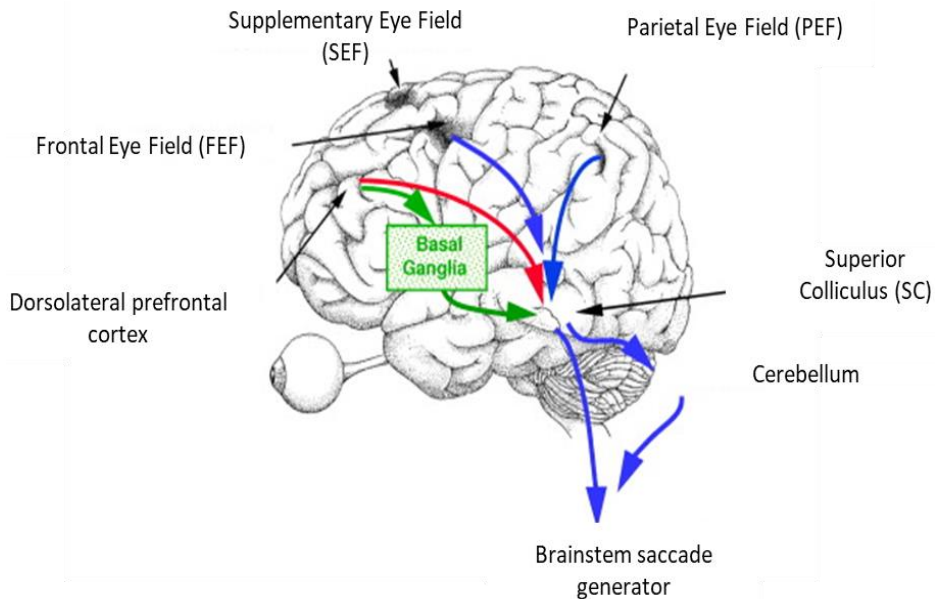
Figure 1.6: Illustration of the cortical and subcortical regions involved in the generation of eye movements. (Image reproduced from Gaymard, 2012)

1.2 Clinical assessment methods for visual system integrity

Eyes being labelled as a window to the soul is rather a cliché since eternities, which was later addressed by various vision researchers to determine and define its logical basis, clinical significance, and applicability. The anatomical and developmental aspects of the visual system show that the neurosensory retina is an extension of the CNS, and the myelinated orbital portion of the ON is considered more like a tract of the brain than a real cranial nerve. Hence, the ON is susceptible to a variety of both ocular and CNS diseases as it is linked at one end to the retina and the other end to the brain (Daw et al., 2006). Many neurodegenerative (progressive loss of structure and function of neurons) conditions involving the CNS have manifestations in the eye wherein several ocular-specific pathologies share characteristic features of

other CNS pathologies. In certain cases, the ocular-related symptoms often precede the actual clinical diagnosis of such CNS disorders wherein ophthalmic/optometry consultation becomes the first line of the medical zone where the patient approaches. Structural damage to the ON can be caused by trauma/injury or as a result of underlying CNS/ocular conditions.

The ON is susceptible to damage from intrinsic, intraorbital, intracranial, or systemic disease. ON disorders encompass diverse life as well as sight-threatening conditions (Montaleone, 2010). Permanent or even temporary damage can eventually disturb the functional integrity of the system leading to a decline in visual functions. Among the various ON disorders, Glaucomatous Optic Neuropathy (GON) is one of the leading causes of global visual impairment. It is a complex disease in which the ON damage leads to slow, progressive, and irreversible vision loss. In most types of glaucoma, the damage is associated with an elevation in Intra Ocular Pressure (IOP) as a result of the building up of the aqueous humor fluid inside the eye, which in usual circumstances flows out through the Trabecular Meshwork (TM), a mesh-like drainage channel. Glaucoma is often called the 'silent thief of sight' because most types typically present as an asymptomatic form until the occurrence of an evident vision-related loss (Foster et al., 2002).

In addition to glaucoma, neuro-ophthalmic conditions including optic neuritis often associated with Multiple Sclerosis (MS) or infectious/para infectious diseases, Anterior Ischemic Optic Neuropathy (AION), traumatic optic neuropathy, compressive lesions/tumors, etc. also can cause damage to the ON leading to a complete/partial loss of vision (Montaleone, 2010). The classical clinical signs include a decline in high and low contrast Visual Acuity (VA), pupillary reflex defects, colour vision defects, Visual Field Defects (VFDs), delayed latency of Visual Evoked Potentials (VEP), etc. (Wilhelm et al., 2015; Ravi Thomas et al., 2011). The integrity of functional vision has a significant impact on patients' lives affecting their overall life activities and eventually their Quality of life (QoL). Conventional ophthalmic evaluation entails various methods to assess the ON integrity including VF evaluation using perimetry and pupillary evaluation.

1.2.1 Visual field intactness: The conventional testing method

The entire area that can be visualised when our eyes focus on a central point (fixation) is the field of vision. Typically, a human eye can detect visual stimuli up to 60° superiorly, 70° inferiorly, 60° nasally, and 100° temporally from the point of fixation, a point corresponding to the fovea.
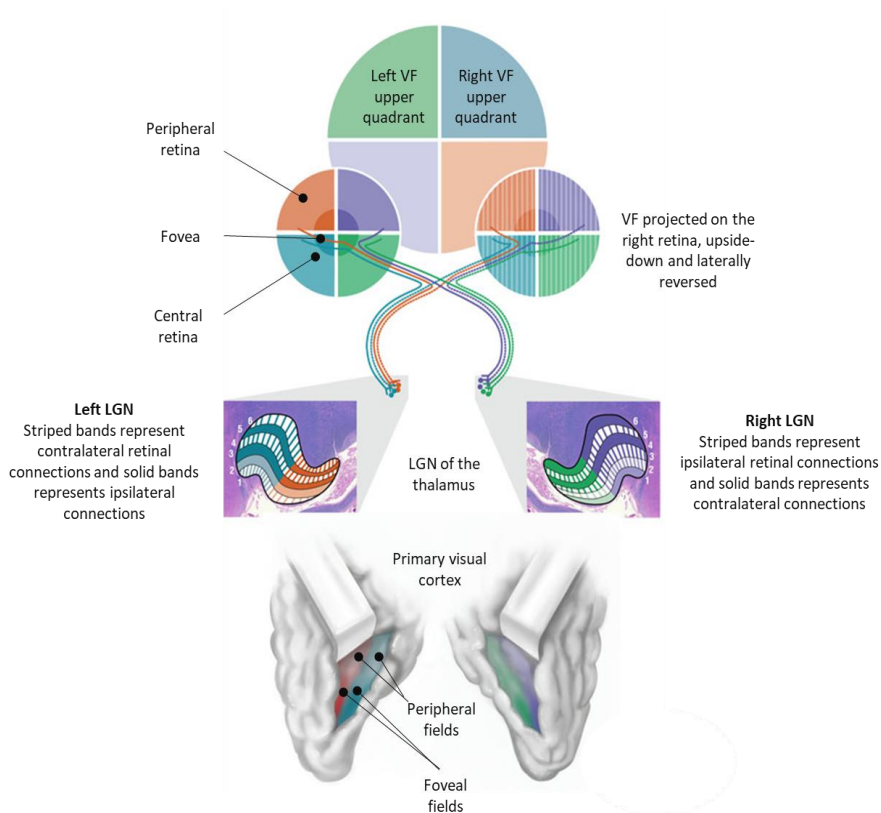
Figure 1.7: Representation of the primary visual cortices that receive visual signals from the four quadrants of the Visual Fields via the Lateral Geniculate Nuclei. (Image reproduced from Linda Wilson-Pauwels, 2013)

The field of vision is often depicted as a three-dimensional hill, where the peak sensitivity to a visual stimulus lies at the point of fixation. This sensitivity level diminishes rapidly within the 10° area around fixation, and then gradually subsides for the peripheral locations. Each point of the VF maps onto a

defined group of neurons in the primary visual cortex where the remapping of the retinal image onto the cortical surface takes place. That means the intactness of the VF relies on a sound neural pathway beginning with retinal receptors, visual neurons in the brain extending from LGN to the visual cortex (Figure 1.7). Hence, a method termed perimetry is used to detect the extent and integrity of VF as an index measure for the intactness of the visual pathway. Perimetry is considered a mainstream technique to detect the presence and progression of VFDs concomitant with any damage involving the components of the visual pathway (Figure 1.8).
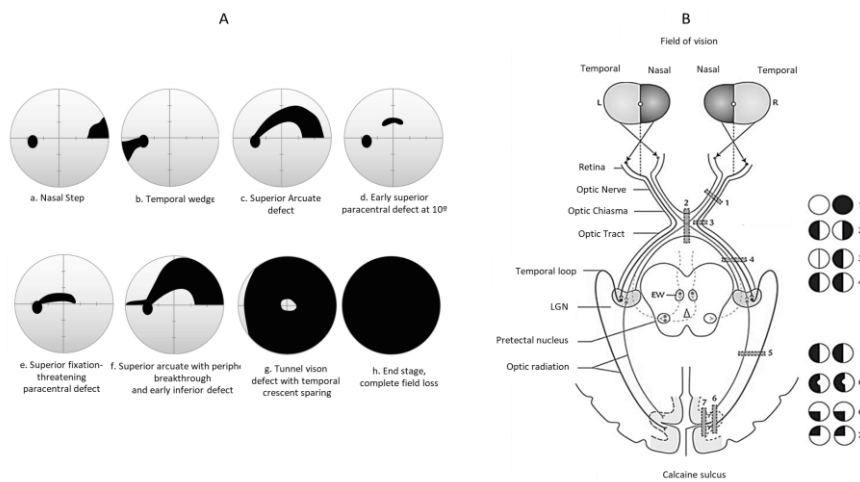
Figure 1.8: Schematic illustration of the location and pattern of visual field defects associated with glaucoma (Panel A) and non-glaucomatous diseases (Panel B) affecting various parts of the visual system.
(Image reproduced from Broadway, 2012)

Even though during the past years, diverse perimeters and test strategies have been established, Standard Automated Perimetry (SAP) with the Humphrey Field Analyser (HFA, Carl-Zeiss Meditec, Dublin, CA, USA) is regarded as the current clinical standard. During the testing procedure, the patient is positioned appropriately against the forehead and chin rest, the non-tested eye is occluded with a patch. The analyser projects a series of white circular light stimuli of varying intensities, throughout a uniformly illuminated bowl (Figure 1.9).
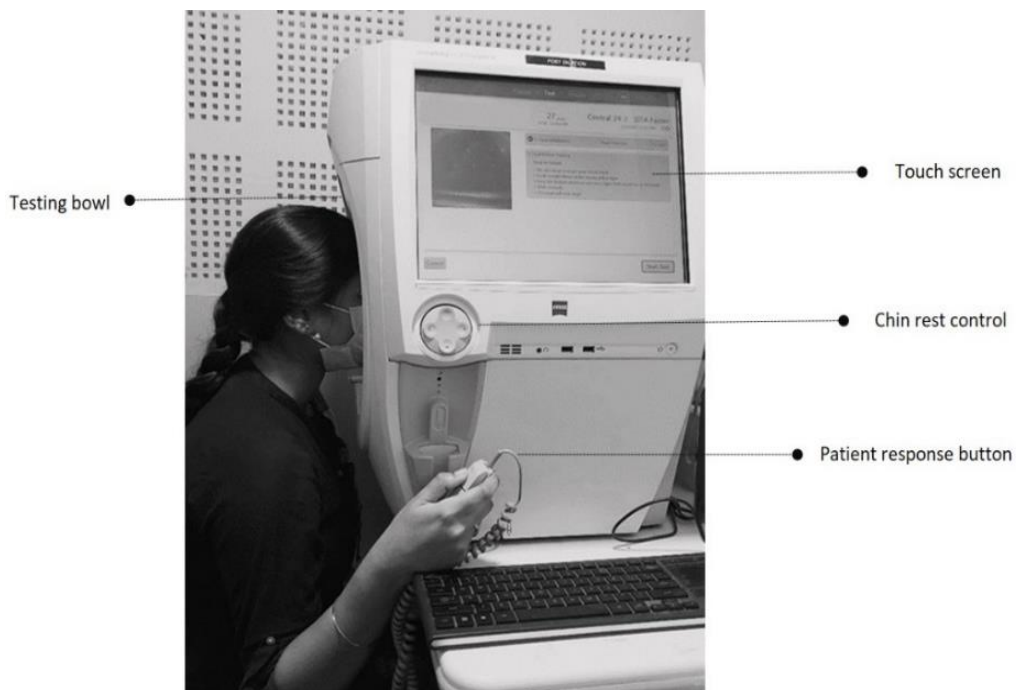
Figure 1.9: Image showing a study participant sitting in front of the HFA machine with forehead and chin stabilised using the forehead and chin rest, a response button in hand, and performing the test.

(Note: Participant shown is a volunteer from whom an additional informed consent was obtained for publishing this photograph. The room illumination is ambient for the purpose of photography).

The patient is instructed to maintain a steady fixation on the central target and respond to each peripheral stimulus by pressing a button ("White on White" testing where a white stimulus is projected on a white background). The varying stimuli are projected to test the visual threshold at different locations for different levels of contrast. Based on the patient's responses, the retinal sensitivity is recorded in 'decibels' (dB) along with the reliability indices (False positives and negatives, Fixation losses, Gaze tracking signals). In addition to the raw threshold values, HFA projects probability plots based on the comparison with the normative database to identify the presence, extent, and depth of the VFDs. The latest advances in its test strategies and the introduction of progression analysis algorithms have further settled it as the

preferred and ideal method for diagnosis and follow-up of functional loss (Heijl & Patella, 2002). When SAP (white-on-white perimetry using HFA) is considered a diagnostic standard, a commercial device called Frequency Doubling Perimeter (FDP) is also available as a screening perimetry method. FDP is a portable device that works on a similar basis as that of SAP except for the use of low spatial frequency sinusoidal grating for determining the contrast sensitivity loss (Johnson & Samuels, 1997). Beyond glaucoma screening and progression monitoring, FDP is also used in other ophthalmic pathologies as it correlates well with SAP in detecting VFDs secondary to neuro-ophthalmic disorders.

1.2.2 Pupillary Light Reflex (PLR): The conventional testing method

The extensive neural pathway resulting in the constriction and dilatation of pupils is subserved by the parasympathetic and sympathetic arms of the autonomic nervous system. This assessment is a mandatory part of the ophthalmic evaluation as it is crucial to provide valuable information regarding the sensory and motor functions of not just the ocular system but also the general nervous system. Conventionally we use a procedure called the 'Swinging Flashlight Test (SFT)' in general neuro/neuro-ophthalmic clinics. Using the flashlight, we evaluate the pupils by including a general observation of their shape, location, and size as well as their reactivity to light. To compare the symmetry in the reaction between the eyes a torchlight is shone to the right followed by the left eye, and the examiner looks for the pupil responses. There can be instances where both pupils get light stimulation or only one receives the light, in both these conditions it is normal for both pupils to constrict briskly and simultaneously.

The responses are customarily described using terminologies relating to the a) laterality (unilateral/bilateral), b) pupil diameter or size (miotic/mid-dilated/dilated), c) and reactivity (brisk/sluggish/non-reactive) that are often applied in the absence of any standardised clinical protocol or consistent definition. So here, the right pathway is compared with the left in terms of symmetry in their responses. So if there is a difference in reactivity that means

either of these pathways is asymmetrically disrupted and referred to as a Relative Afferent Pupillary Defect (RAPD), which is graded into different levels based on the severity (Mathôt, 2018; Couret et al., 2016). Due to the proximity of the pupillary pathway to various anatomic structures, pupillary dysfunctions/abnormalities, especially anisocoria (a condition characterised by unequal pupil sizes), can be indicative of life-threatening emergencies. Hence, apart from RAPD (afferent defect due to lesions of the optic nerve, chiasm, and the tract), efferent pupillary defects also gain clinical importance for their ability to predict the occurrence of potentially life-threatening emergencies such as aneurysms causing oculomotor nerve palsy, Horner's syndrome, etc. (Kawasaki, 1999). Thus, well-controlled instruments that precisely quantify the pupil parameters and monitor the same over a period of time to assess the disease prognosis have a role.

1.3 The problem statements

Conventional perimetry (SAP) and pupillary evaluation methods (SFT), indeed play a vital role in the diagnosis of visual dysfunctions and monitoring of disease prognosis. However, these approaches definitely raise some challenges thereby compromising the reliability of the outcome measures. With regard to SAP, its onerous testing procedures mandate an adequate level of cognitive and motor function. Maintaining a steady central fixation for a prolonged duration tends to result in image fading, an optical illusion affecting visual perception known as the Ganzfeld blank out or Troxler's fading effect (Martinez-Conde et al., 2004; Poletti & Rucci, 2010). This triggers the patients' complaints such as discomfort, blurry vision, double vision, and fatigue. This requirement for a steady fixation, subduing the natural impulse of the person to look towards the target makes the test challenging to do, in turn compromising the reliability of the perceptual measurement (Toepfer et al., 2008).

Similarly, the conclusions from the SFT, a deceptively simple test to evaluate pupillary reactions, are prone to substantial inconsistency and inter-examiner variability due to its dependency on the examiner's judgment and clinical expertise. Since pupillary responses are so delicate, even an unequal retinal bleaching or off-axis light stimulation of the retina can induce pupil reactions

that mimic true afferent pupillary defects causing false positive conclusions (Mathôt, 2018; Couret et al., 2016).

1.4 New functional biomarkers to quantify visual system integrity

In the field of ocular diagnostics, the current conventional methods of VF and pupillary evaluation have certain constraints due to the tedious testing method demanding absolute patient cooperation and dependency on the manual observation skills of the examiner respectively. These pitfalls restrict the methods to reliably and accurately deliver conclusions in clinical as well as community-based screening. Alternative technological interventions can supplement the current approaches by the development of automated, standardised, and rapid systems for the purpose of screening specific diseases as well as a follow-up or progression assessment. With the advancements in technology over the past decades, the capabilities have increased enormously. Among many such progresses, the Eye Tracking Technology (ETT) based approaches offer one of the most potent ways of assessing visual functional biomarkers. ETT set forth the possibilities in analytical and interactive applications in which a device estimates the point of gaze of a participant with high accuracy using image sensing technology integrated with a mathematical algorithm. These approaches encompass navigation that can aid in ocular diagnostics, telemedicine applications, community screening, and home-based monitoring (Kozak & Rahn, 2021). Eye Movement Perimetry (EMP) is an alternative approach of automated perimetry. EMP addresses some of the concerns that were raised in the section where we discussed SAP since it is based on natural human reflexes.

In EMP, Saccadic Eye Movements (SEMs) initiated by the participants during a prosaccade task is captured by an eye tracking device. EMP incorporates test protocols that encourage participants to initiate SEM towards visual stimuli projected in the surrounding periphery rather than restricting the natural urge of the individuals to look at any randomly appearing targets in their vicinity. Thus, EMP exploits the reflexive properties of the oculomotor system to generate SEM and uses its reliable parameters as a clinical index to plot

the VF rather than a manual or verbal response. The eye movement responses (seen/unseen) are recorded and from the 'seen' responses a reliable index of SEM known as the Saccadic Reaction Time (SRT) is quantified. The SRT (saccade latency) is used as a functional index to describe the responsiveness and intactness of the VF. This technique was evaluated for feasibility and applicability among infants (Jones et al., 2014; Satgunam et al., 2017; Perperidis et al., 2021), children (Murray et al., 2013; Pel et al., 2013), and adults. This method is technically feasible in a clinical setting to provide sensitive, quantitative, and objective data to aid in detecting and monitoring a range of patients with various diseases ranging from glaucoma (Mazumdar et al., 2014; Toepfer et al., 2008) to other neuro-ophthalmic conditions (Clark et al., 2019).

Likewise, with regard to pupillometry, certain advancements in technology have transpired in the recent past for objectifying pupillary reactions using well-controlled systems called pupillometers. Automated pupillometry is used to increase the validity, consistency, and reproducibility compared to the manual pupillary examination. Previous reports suggest that this non-invasive technique successfully detects subtle and early pupillary variations and it is a useful diagnostic and prognostic indicator. This expansion has increased the scope of its use not only in diagnosing glaucoma and neurological diseases but also to monitor the advancement/prognosis over a course of time (Hall & Chilcott, 2018). Since the pupil responses are also cortically mediated it aids in a better understanding of language and cognitive processing, investigating reading behaviour, evaluating mood disorders, assessing learning disabilities, and also obtaining unique insights about how an individual perceives and interacts with his/her environment.

1.5 Aim of the thesis

The aim of this thesis was to quantify potential functional biomarkers to assess the integrity of the visual system on the basis of ETT. It was postulated

that the application of ETT at eye care centres can provide a supplementary/surrogate way of studying oculomotor behaviour to diagnose visual system defects in comparison to current clinical techniques and can be translated into population-based screening strategies.

1.5.1 Study sites and ethical considerations

The research work described in this thesis was developed and executed at the collaborative institutes: 1) Erasmus Medical Centre, Rotterdam, The Netherlands, and 2) Sankara Nethralaya, a unit of Medical Research Foundation, Chennai, India. To explore the generated research questions, a well-defined set of samples that included adults and pediatric participants were enrolled. All the eligible adult participants were explained the purpose of the research, the flow, and the pattern of the testing protocol, and the battery of measurements commenced only after obtaining written informed consent. Besides, for the pediatric participants, who are by definition too young (< 18 years) to give informed consent, the details of the research and its protocol were described to the participants as well as to their parents/legal guardians and the assent forms were obtained. This study had a cross-sectional descriptive design and all procedures performed were in accordance with the ethical standards of the Institutional Research Boards (IRB) of both the institutions and with the 1964 Declaration of Helsinki and its later amendments.

1.5.2 Main objectives and Research questions

As a part of the course of designing and developing a novel eye tracker-based ocular diagnostics/screening system, it was mandatory to explore a set of Research Questions (RQs). The RQs aimed at investigating the system's feasibility and clinical applicability in a diverse set of populations (Among adults and children) and the distinct nature of ON dysfunctions. All the RQs included a set of well-defined healthy controls and patients clinically diagnosed with visual system dysfunctions (due to either glaucoma or neuro-ophthalmic diseases).

The initial stages of the research considered the development and evaluation of a perimetry protocol (EMP) on the basis of eye movement behavior (Chapters 2 to 6) which later progressed into the integration of a pupillometry protocol (Chapter 7).

1. **Research Question 1**: What is the effect of ethnic diversity on SRT among healthy controls and glaucoma patients while performing a prosaccade task during EMP? (Chapter 2).

    Statement of purpose: For the development and evaluation of an EMP protocol, the first step focused on enrolling a set of adult patients diagnosed with Glaucomatous Optic Neuropathy (GON) and their age-matched healthy controls. The condition of 'Glaucoma' was considered because of its highly prevalent status globally (2nd leading cause of blindness) and the asymptomatic nature due to which the majority of the cases in the community remain undetected. Hence, the development of rapid and reliable screening protocols for glaucoma in an at-risk population can enable the commencement of early intervention, thereby reducing visual morbidity and decline in QoL. To introduce the customised EMP method and evaluate its feasibility and applicability in ethnically different populations this step enrolled two different ethnic cohorts (Indian and Dutch). This aided in understanding the influence of ethnicity on eye movement behaviour specifically while performing a prosaccade task in EMP.

    Study participants: Healthy controls were defined as those with Best Corrected Visual Acuity (BCVA) of ≥ 20/40 for distance and N6 for near, spherical ametropia of less than ± 5.00 D, and cylindrical ametropia of less than −2.00 D, normal pupils that were equally round and reacting to light, normal extraocular motility, an IOP ≤ 21 mmHg, and a healthy anterior and posterior segment. Glaucoma patients were defined on the basis of the International Society of Geographical and Epidemiologic Ophthalmology (ISGEO) classification who presented with characteristic structural defects with corresponding, repeatable, and reliable perimetry reports (HFA).

2. **Research Question 2:** What is the reliability of SRT as a screening index to detect visual function loss associated with ON damage and the pattern of participants' preference and perception toward the proposed EMP-based screening approach when compared to conventional clinical methods? (Chapters 3 and 4).

   Statement of purpose: This was planned to further understand the prospect of using eye movement behavior as a discriminatory index for identifying glaucoma among adults. The full field protocol in EMP that is described in the RQ1 required substantial alterations with respect to the testing grid, duration, and pattern to introduce it as a screening modality. There are certain features that need to be considered while investigating the clinical applicability of a newly proposed diagnostic/screening device. Hence, in addition to HFA (clinical standard), this research considered a conventional VF screening device, FDP, as a comparative method. Furthermore, it seemed essential to evaluate the patient preference and attitudes toward the newly designed psychophysical testing method.

   Study participants: Adult participants (20 – 70 years of age) diagnosed with GON and their age-matched healthy controls were recruited from the collaborative research centre in India. Participants were defined based on the criteria mentioned above (RQ1: Study participants).

3. **Research Question 3:** What is the feasibility of the SRT-based EMP protocol among the pediatric population and the clinical reliability of using SRT as a basis for detecting the presence and extent of VFDs associated with neuro-ophthalmic conditions in the pediatric population? (Chapter 5)

   Statement of purpose: This step was to explore the possibility of extending the proposed method to the pediatric population. The viability of the method was evaluated in healthy controls as well as in children diagnosed with neuro-ophthalmic manifestations due to lesions compromising the visual system.

Study participants: Patient group was defined as those (4 – 15 years of age) diagnosed with Intracranial Lesions (IL), with and without genetic mutation of Neurofibromatosis-1 (NF-1) presenting with specific ophthalmic manifestations. Healthy controls were defined as those born between 37 to 42 weeks of gestation, with no significant history of visual or ocular problems, and with no evidence of brain injury/damage.

4. **Research Question 4:** What is the clinical reliability of using SRT as a basis to detect and monitor the presence and extent of VFDs associated with neuro-ophthalmic conditions in the adult population? (Chapter 6)

   Statement of purpose: This step was considered a pilot exploration of the EMP protocol (detection and prognosis evaluation) in an individual who was diagnosed with a neuro-ophthalmic condition and presented to the clinic with significant ophthalmic manifestations. This step was initiated to evaluate the applicability of SRT as a detection and prognostic index in ON disorders.

   Study participant: An adult diagnosed with optic neuritis and associated neuro-ophthalmic manifestations including a corresponding VFD and pupillary abnormality.

5. **Research Question 5:** What is the scope of integrating pupil-based parameters as an additional index to SRT to evaluate the integrity of the visual system and the clinical applicability of the customised pupillometer system in detecting pupillary defects associated with neuro/neuro-ophthalmic conditions? (Chapter 7)

   Statement of purpose: The RQ that explored the viability of EMP in adult and pediatric populations in glaucoma and neuro-ophthalmic conditions relied on a single screen stimulus presentation system. But to integrate a pupil stimulation protocol, a binocular (dual screen) system was necessary to simultaneously or alternatively stimulate the visual system. Hence this step aimed at detailing the design and organisation of a haploscope-based binocular system.

Study participants*:* Healthy controls were defined based on the criteria mentioned based on the criteria mentioned above (RQ1: Study participants). Neuro ophthalmic patients were defined as those who presented with characteristic structural defects with corresponding, repeatable, and reliable perimetry reports (HFA) and definite afferent pupillary defects.

1

CHAPTER 2

Effect of ethnic diversity on the pro-saccade reaction time between Indian and Dutch healthy controls and glaucoma patients

Najiya Sundus K. Meethal [1,2], Deepmala Mazumdar [1,2], Gijs Thepass [1], H.G. Lemij [3], J. van der Steen [1,4], Johan. J. M. Pel [1], Ronnie George [2]

1. Vestibular and Ocular Motor Research group, Dept. of Neuroscience, Erasmus MC, Rotterdam, The Netherlands
2. Medical Research Foundation, Chennai, India
3. Dept. of Glaucoma, The Rotterdam Eye Hospital, Rotterdam, The Netherlands
4. Royal Dutch Visio, Huizen, The Netherlands

ABSTRACT

Background

Eye Movement Perimetry (EMP) expresses the decline in Visual Field (VF) responsiveness on the basis of deviation in Saccadic Reaction Times (SRTs) from their expected age-matched responses (normative database). Since ethnic dissimilarities tend to affect saccade parameters, the current study aimed to evaluate the effect of ethnic diversity on SRT and its interaction with age, stimulus eccentricity, and intensity.

Materials and Methods

Participants including healthy controls and glaucoma patients (n = 215) drawn from Indian and Dutch ethnicities underwent a customised EMP protocol. Participants were instructed to look at a fixation target and respond to peripheral visual stimuli with eye movements. The gaze trials were inspected and from the reliably 'seen' responses, the SRTs were calculated. To determine the influence of ethnic differences in combination with factors such as age, stimulus eccentricity, and intensity, a Generalised Linear Mixed Model (GLMM) analysis was used. Receiver Operating Characteristic (ROC) analysis was used to compare the classification accuracies of SRT based decision algorithm.

Results

The GLMM analysis considered SRT as a dependent variable and revealed an overall statistically significant interaction between the tested factors ($p < 0.001$). During the posthoc analysis, only 6% of the pair-wise estimates showed statistical significance. ROC analysis revealed promising and comparable areas under the curve values for both the ethnic cohorts with the ethnic-specific as well as the swapped normative databases (> 0.95).

Conclusions

The global mean SRT values could be a reliable index to discriminate healthy controls from glaucoma in both Indian and Dutch study cohorts. The normative databases (Indian and Dutch) adjusted for the age and stimulus-related factors showed an influence only on 6% of the pairwise interactions, hence ethnic-specific SRT normative databases are not mandatory to estimate the VF responsiveness using the proposed EMP protocol.

2

2

2

2

2

2

2

CHAPTER 3

Development of a test grid using Eye Movement Perimetry for screening glaucomatous visual field defects

Najiya Sundus K. Meethal [1,2], Deepmala Mazumdar [1,2], Rashima Asokan [2], Manish Panday [2], J. van der Steen [1,3], K.A. Vermeer [4], H.G. Lemij [5], Ronnie George [2], Johan J.M. Pel [1]

1. Vestibular and Ocular Motor Research group, Dept. of Neuroscience, Erasmus MC, Rotterdam, The Netherlands
2. Medical Research Foundation, Chennai, India
3. Royal Dutch Visio, Huizen, The Netherlands
4. Rotterdam Ophthalmic Institute, The Rotterdam Eye Hospital, Rotterdam, The Netherlands
5. Dept. of Glaucoma, The Rotterdam Eye Hospital, Rotterdam, The Netherlands
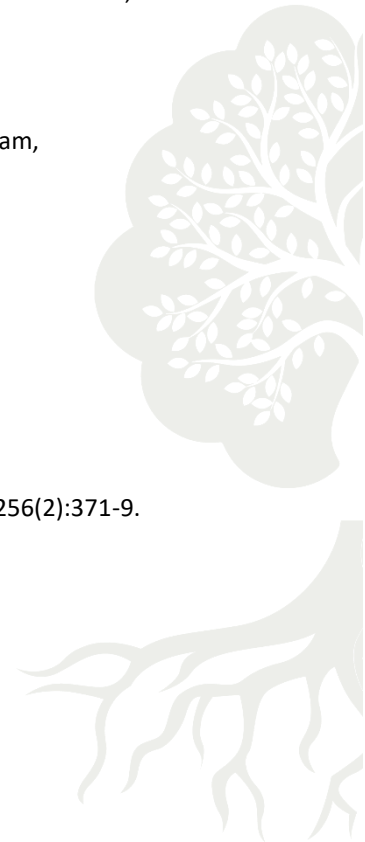
ABSTRACT

Background
Eye Movement Perimetry (EMP) uses Saccadic Eye Movement (SEM) responses for Visual Field (VF) evaluation. Previous studies have demonstrated significant delays in the initiation of SEMs among glaucoma patients. The aim of the current study was to develop an EMP-based screening grid to identify glaucomatous visual field defects.

Materials and Methods
An interactive test with 36 locations and two stimulus intensities (214 cd/m^2 and 276 cd/m^2) was evaluated in 54 healthy controls and 50 glaucoma patients. Participants were presented with a central fixation target combined with the random projection of Goldmann size III peripheral stimuli. Instructions were given to fixate the central fixation target and look at each peripheral stimulus on detection while the saccades were assessed using an infrared based eye tracker. From each of the reliably 'seen' responses, the Saccadic Reaction Time (SRT) was calculated which were used to plot Receiver Operating Characteristic (ROC) curves. The Area under the Curve (AUC) values were used to identify the locations with the highest susceptibility to glaucomatous damage. Each stimulus location with an AUC less than 0.75 along with its mirrored test locations around the horizontal axis was eliminated from the grid.

Results
The mean age was 48.1 ± 16.6 years and 50.0 ± 14.5 years for the controls and patients respectively. A significant delay in SRT values by 76.5% (p < 0.001) was found in glaucoma patients. From the ROC analysis, ten out of 36 locations meeting the cut-off criteria of AUC were eliminated resulting in a new grid containing 26 test locations. SRT values were significantly different (p < 0.05) between the healthy controls and glaucoma patients irrespective of the grids used.

Conclusions
The present study resulted in a screening grid consisting of 26 locations predominantly focusing on the nasal, superior, and inferior areas of the VF. An internal validation of the modified grid showed 90.4% of screening accuracy, which makes it a potential approach for population-based screening.

INTRODUCTION

Glaucoma is a progressive optic neuropathy characterised by typical structural alterations of the optic nerve associated with concomitant Visual Field Defects (VFDs) (Weinreb & Khaw, 2004; Foster et al., 2002). Based on a recent estimate, there are 11.2 million people aged 40 years and above with glaucoma in India (George et al., 2010). Because of its asymptomatic nature, 90% of glaucoma in the community remains undetected (Weinreb & Khaw, 2004; George et al., 2010). The requirement for additional infrastructure along with financial constraints makes it yet more challenging for developing countries like India to deal with a large number of individuals with glaucoma (George et al., 2010; Thomas et al., 2002). Rapid screening for glaucoma in an at-risk population can enable early intervention, thereby reducing visual morbidity and decline in the quality of life of an individual with the manifest disease (Weinreb & Khaw, 2004). Functional evaluations using perimetry techniques have been considered one such potential approach in glaucoma screening (Quigley, 1998).

Standard Automated Perimetry (SAP) is the most accepted diagnostic procedure to quantify glaucomatous VFDs (Foster et al., 2002). In conventional perimetry tests, patients are required to sustain a steady central fixation throughout the course of testing. This might result in Ganzfeld blank out or Troxler's fading effect due to neural adaptation (Toepfer et al., 2008; Jernigan, 1980; Kim et al., 1995; Trope et al., 1989; Warren et al., 2013; Martinez-Conde, 2006). This often leads to complaints such as blurred vision, diplopia, inattention, discomfort, hallucination, and fatigue. In addition, the fixation requirement contradicts the natural urge of the person to look at new peripheral stimuli, thus complicating the task. Overall, the approach sets up an unnatural environment for the measurement of human perceptual performance, which can affect the precise measurement of the field of vision (Toepfer et al., 2008; Kim et al., 1995).

Eye Movement Perimetry (EMP) addresses some of these concerns since it is based on natural human reflexes. A person's performance relied on

Saccadic Eye Movements (SEMs), which means the test results include the properties of the oculomotor control system (Toepfer et al., 2008; Kim et al., 1995). A key parameter of detected stimuli is the Saccadic Reaction Time (SRT). Past studies have demonstrated reliable and comparable results between SAP and EMP in terms of the ability to detect Visual Field (VF) loss (Kim et al., 1995). A major benefit of this approach is the elimination of the need for testing for false positive responses (Mazumdar et al., 2014). Although a small learning curve exists (Pel et al., 2013), EMP has the potential to become the standard in perimetry for young children and people who have mental or physical limitations to perform conventional perimetry (Murray et al., 2009; Pel et al., 2010).

We have previously shown delayed SRT values in primary glaucoma patients compared to healthy controls across different eccentricities throughout the tested field of vision (Mazumdar et al., 2014). The protocol included all 54 locations tested on the Swedish Interactive Thresholding Algorithm (SITA) standard 24–2 test pattern of the Humphrey Field Analyser (HFA). Each point was presented at four different stimulus intensities, thus 216 stimuli in total were shown to each of the participants (Mazumdar et al., 2014). The test duration of the fixed protocol was 12 minutes (min) per eye, which limited rapid screening for any VF loss. Therefore, the current study aimed to develop an EMP based rapid and novel screening grid to identify glaucomatous VFDs in patients with primary glaucoma and age-matched healthy controls.

MATERIALS AND METHODS

The full threshold grid (54 locations) used in our previous study (Figure 3.1: Right panel) followed a fixed stimulus presentation pattern in which each peripheral stimulus appeared for a constant duration of 1.2 seconds (s) with a 0.2 s time gap between subsequent projections with a total test duration of 12 min (Mazumdar et al., 2014). An interactive test version was created wherein each stimulus projection time varied based on the person's response. The protocol was programmed in such a way that peripheral stimulus

disappeared immediately after the obtainment of an eye movement response from the participant. The EMP test initially consisted of four stimulus intensities varying from subthreshold stimuli (Intensity: 192 cd/m^2) to suprathreshold stimuli (Intensity: 276 cd/m^2) plotted against a 152 cd/m^2 background. We have previously shown that significant differences in SRTs between healthy controls and patients with glaucoma were obtained at an intensity level of 214 cd/m^2. Therefore, we decided to include only 214 cd/m^2 and 276 cd/m^2 intensity levels for screening purpose.

Reduction of test locations

A reduction of the tested locations was obtained in two phases. The first phase was to eliminate irrelevant locations based on the literature and on clinical observation followed by the second phase that focused on an evaluation study in healthy controls and glaucoma patients using the reduced grid. Based on the evaluation outcomes, another reduction in test locations was obtained by identifying those locations with the highest susceptibility to glaucomatous damage. The loss of sensitivity near the foveal region occurs relatively late in the process of glaucomatous damage when tested with the SAP 24–2 test algorithm (Hitchings & Spaeth, 1976; Harwerth et al., 1999). We, therefore, decided to put more emphasis on locations in the peripheral areas of the VF.

The first reduction of the full threshold 54-point grid (Figure 3.1: Left panel) was obtained by replacing 16 central stimulus locations (four most central locations in each of the quadrants) with four new test locations. The eccentricity of these four locations was calculated as the mean eccentricity of all 16 locations. In addition, the farthest locations (x = ± 15, y = ± 15) in each quadrant were eliminated along with the two test locations adjacent to the blind spot region i.e. 15° temporal to fixation (Varay, 1969) thereby achieving an overall 66.7% reduction of test locations (from 54 locations tested four times to 36 locations tested twice), as illustrated in Figure 3.1.
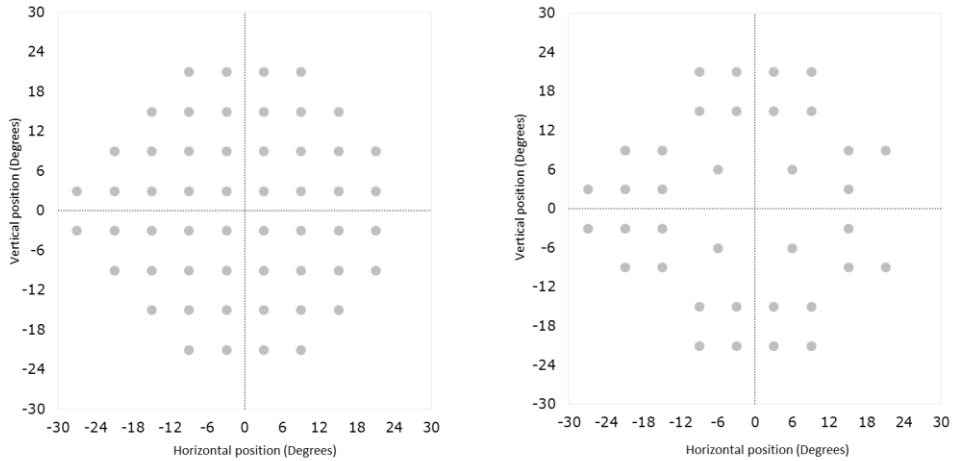
Figure 3.1: The left panel illustrates the full test grid consisting of 54 locations and the right panel illustrates the modified test grid consisting of 36 locations.

Evaluation of the 36-point grid

Study Participants:

Healthy controls and patients diagnosed with primary glaucoma aged between 20 to 70 years were recruited at the outpatient department and the glaucoma clinic of Sankara Nethralaya (a tertiary eye care centre located in Chennai, India). Healthy controls were defined as those with Best Corrected Visual Acuity (BCVA) ≥ 20/40 for distance and N6 for near, an Intra Ocular Pressure (IOP) of ≤ 21 mmHg, and a healthy anterior and posterior segment. A dilated posterior segment evaluation was carried out, including an assessment of the optic disc by a glaucoma specialist along with VF evaluation by means of the 24–2 SITA standard protocol in the HFA to rule out any clinically evident structural or functional signs of glaucoma. Exclusion criteria were the presence of spherical ametropia greater than ±5.00 D and cylindrical ametropia of > −2.00 D, cataract with a grade more than N2, C1, P1 based on the Lens Opacification Classification System (LOCS) II (Chylack et al., 1989) and any presence of strabismus, nystagmus or retinal diseases (Mazumdar et al., 2014). Glaucoma patients were defined on the basis of the International

Society of Geographical and Epidemiologic Ophthalmology (ISGEO) classification (Foster et al., 2002). Patients with primary open angle or angle closure glaucoma who had glaucomatous optic disc changes and corresponding reliable and repeatable VFDs on HFA were included. Reliability criteria were as recommended by the instrument's algorithm (Fixation Losses (FL) < 20%, False Positive (FP) and False Negative (FN) errors < 33%). Patients with glaucoma were classified into mild, moderate, and severe glaucoma based on their VFDs by using the Hodapp, Parrish, and Anderson's classification (Hitchings & Spaeth, 1976).

All the study participants underwent a comprehensive ophthalmic evaluation that included a VF examination by means of two perimetry techniques. The first assessment of each individual's monocular VF was done using HFA (model 750; Carl Zeiss Meditec, Dublin) with SITA Standard 24–2 white-on-white protocol followed by our customised and interactive EMP test (Tobii T120, Tobii, Sweden). Written informed consent was obtained from all the participants before enrolment. The study adhered to the tenets of the Declaration of Helsinki and the experimental measures were reviewed and accepted by the Institutional Review Board (IRB) and Ethics Committee (EC) of Vision Research Foundation (VRF), Chennai.

Measurement setup and procedures:
The EMP setup consisted of a Tobii T120 infrared eye-tracking device integrated in a 17 inches Thin Film Transistor (TFT) monitor with a refresh rate of 60 Hertz (Hz) as illustrated in Figure 3.2. Each participant was seated in front of the monitor at a fixed working distance of 60 cm. A chin rest was provided to minimise any head movements during the test. A constant testing environment was maintained for all the participants with a dim room illumination and a minimal level of auditory distractions. The right eye was tested first, followed by the left. The non-tested eye was covered with a black Polymethyl methacrylate (PMMA) occluder that allowed the infrared eye tracking of the non-tested eye. Customised testing protocol developed for the current study integrated three procedures: A tracking status estimation, a calibration procedure, and an interactive EMP test. Each measurement procedure started

with a tracking status estimation that was necessary to ensure appropriate eye alignment and proper gaze tracking. Every participant was instructed to look at all four corners of the screen to ensure negligible eye tracking data loss at each corner. Minor alignment adjustments were done when eye tracking was not optimal. Next, a nine-point calibration procedure was done by showing a red circular target to align the person's gaze with the presented calibration dots. The calibration procedure was repeated either for preferred locations or for all the nine locations, if poor calibration resulted from various factors such as inaccurate focusing of participants on the calibration dot, blink artefacts, or any hardware/tracking issues, etc. was noted.

Figure 3.2: Illustration of a participant sitting in front of the Eye Movement Perimetry (EMP) test set up consisting of an eye tracking device integrated into a Thin Film Transistor (TFT) monitor.

(Note: Participant shown is a volunteer from whom an additional informed consent was obtained for publishing this photograph).

After the calibration process, an interactive EMP test was started. A Software Development Kit (SDK) was used to assess real-time gaze positions at a 60 Hz sample rate. The test started with plotting a Goldmann size IV central fixation target (green colour) on the eye tracker's monitor with a background illumination of 152 cd/m^2. Meanwhile, real-time gaze tracking was used to monitor the correct central target fixation. A peripheral stimulus was projected after a consistent central target fixation for at least 0.5 s. Goldmann size III peripheral stimuli of intensity 214 cd/m^2 and 276 cd/m^2 appeared sequentially by using an overlap paradigm, which meant that the central fixation target was kept visible to the participants. A peripheral stimulus was plotted for a maximum duration of 1.2 s. Yet, this stimulus was removed when it was fixated within 1.2 s. All participants were encouraged to look at detected peripheral stimuli followed by refixating at the central fixation target. To test the VF up to visual angles of 27° horizontally and 21° vertically, the central fixation target was repositioned during the test to four eccentric locations. During the presentation of peripheral stimuli, gaze data were collected and stored for analysis.

Data analysis and statistics:
A custom-written Matlab program (Mathworks Inc., Natick, MA, USA) was used to analyse and calculate the properties of SEMs. Figure 3.3 illustrates the trajectory and time course of a saccade aimed at a peripheral stimulus projected at location x = 3, y = 15. A peripheral stimulus obtained was labelled as 'seen' if the following criteria were satisfied: (1) fixation of the central target was followed by a peripheral stimulus fixation, (2) the angular disparity between the direction of the primary SEM and the peripheral stimulus location was less than 45°, (3) the amplitude of the primary SEM covered more than 50% of the total target distance. A peripheral stimulus was classified as 'unseen' when: (1) fixation remained on the central fixation target; (2) the angular disparity between the direction of the primary SEM and the peripheral stimulus location was larger than 45° (indicating search behaviour). A peripheral stimulus was classified as 'invalid' when gaze data was poor due to blinking or pupil tracking failure, which was used as the preliminary reliability index.

An EMP test with more than 25% (> 6/26 gaze events) of invalid responses were considered 'unreliable', hence excluded from the analysis. For the events labelled as 'seen', SRT was defined as the time between the onset of the target stimulus and the initiation of the SEM (Figure 3.3). This was determined based on a velocity criterion by calculating the time at which the eye velocity crossed 50° per second (Pel et al., 2013; Thepass et al., 2015).

Statistical analyses were performed by using SPSS (Statistical Package for Social Sciences, version 15, Chicago, IL, USA). The right eye was considered for analysis. Tests for normality were carried out for all the continuous variables and appropriate parametric/non parametric tests were utilised. Type 1 error was kept at a 5% level and all the tests used were two-tailed. Logarithmic transformation of SRT values in milliseconds (ms) was done to reduce the skewness of the data, thereby achieving a normal data distribution.
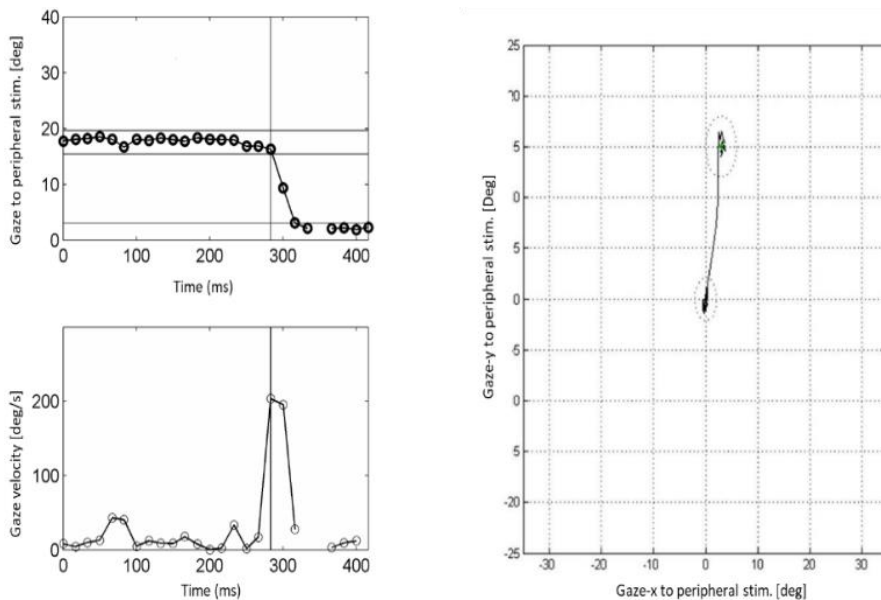

Figure 3.3: Illustration of the Matlab analysis window used for analysing the trajectory and time course of a saccade aimed at a peripheral stimulus projected at location x = 3, y = 15. At the moment of presenting this stimulus, the gaze was on the central fixation target (x = 0, y = 0).

An independent t-test was used to compare SRTs between healthy controls and glaucoma patients. The pattern of eye movement responses was compared between healthy controls and glaucoma patients by calculating the percentage of reliably seen, unseen, and invalid responses. The stimulus locations were divided into central and peripheral zones comprising of 4 locations and 32 locations respectively. All the 36 tested locations were represented by their 'x' and 'y' co-ordinates (Supplementary Figure 3.1). Of each location, the obtained SRTs by projecting 214 cd/m^2 stimuli were used to construct Receiver Operating Characteristic (ROC) curves. The Area Under the Curve (AUC) values obtained for 32 test locations in the peripheral zone were considered as an index of accuracy in classifying diseased and non-diseased individuals. The AUC values obtained for each location were inspected for determining the minimum AUC cut-off value below which the points were eliminated along with their mirrored test locations around the horizontal axis for the maintenance of horizontal symmetry.

After designing the reduced grid, SRT values were obtained from both the 36-point grid and the modified 26-point grid. Differences in mean SRT values between healthy controls and glaucoma patients were analysed using an independent t-test. One-way analysis of variance (ANOVA) was done to compare the mean SRTs across the four diagnostic categories (healthy, mild, moderate, and severe) using the SRT values obtained from both grids.

Some healthy controls had increased SRT values, and some glaucoma patients had SRT values that fell within the normal range. A five-fold cross-validation technique was adapted to estimate the classification accuracy as a means of internal validation of the modified grid. The analysis began with generating five (k = 5) equal sized random subsets from the original data set. Of the five samples, a single subsample was retained as the validation data for the testing model, and the remaining four subsamples (k-1) were used as training data. The cross-validation process was then repeated five times, with each of the five subsamples used exactly once as the validation data thereby calculating five SRT cut-off values using binary logistics (SPSS). These cut-off values were averaged to compute a single estimation of classification accuracy. Finally, to investigate the test duration of the modified grid, another

five healthy controls, and five glaucoma patients underwent the modified EMP screening test.

RESULTS

A total of 104 participants were recruited that included 54 age-matched healthy controls and 50 glaucoma patients. The demographic details of the controls are presented in Table 3.1. The glaucoma patients consisted of 24 (48%), 17 (34%), and 9 (18%) individuals with mild, moderate, and severe forms of the disease, respectively. In Table 3.2, the test performance is summarised by analysing the percentage of 'seen' points, 'unseen' points due to VFDs, and 'invalid' points due to blinks or poor gaze tracking. Supplementary Table 3.1 describes the AUC calculated for each stimulus location in the central and peripheral zones. An illustration of one of the point wise ROC analysis outputs is presented in Figure 3.4. The AUC values calculated for four central stimulus locations (x = +/−6 and y = +/−6) ranged from 0.71 to 0.81. By inspecting the range of AUC values obtained for the peripheral zone, a cut-off value of 0.75 was decided. We found ten peripheral locations with an AUC below this cut-off and these locations were eliminated from the test grid, resulting in a 26-point grid (Figure 3.5). This included two test locations at the blind spot region i.e. 15° temporal to fixation (Armaly, 1969) due to the high variability of reaction times reported in the literature (Pel et al., 2013).

Table 3.1: Demographics of the study population.

Participants' characteristics	Healthy controls (n = 54)	Glaucoma Patients (n = 50)
Mean age (SD) in years	48.1 (16.6)	50.0 (14.5)
Gender, n (%)		
Male	31 (57)	38 (76%)
Female	23 (43)	12 (24%)
Mean (SD) Intra Ocular Pressure (mmHg)	14.3 (2.6)	16.2 (3.7)
Mean Cup-to-Disc ratio (SD)	0.4 (0.1)	0.7 (0.2)

SD – Standard Deviation

Comparison of SRT values obtained from the 36-point and 26-point grids

The mean SRT values obtained in the 36-point grid were 427 ± 113 ms and 754 ± 194 ms among healthy controls and glaucoma patients, respectively which were statistically significantly different (p < 0.001; Independent t-test). In the 26-point grid, the mean SRT values were 435 ± 116 ms for healthy controls and 806 ± 234 ms for glaucoma patients. Again, this difference was statistically significantly different (p < 0.001; Independent t-test). SRT values obtained from both grids did not show any significant difference. One-way ANOVA was performed to compare the SRT values within each diagnostic category obtained from both the grids. When the 36-point grid was analysed, a significant difference in SRT values (p < 0.05) was noted between each of the diagnostic categories (healthy and mild, moderate and severe glaucoma). The same results were found when this analysis was carried out with the SRT values obtained from the 26-point grid (p < 0.05). The Tukey posthoc test revealed that increasing disease severity resulted in increased SRT values. No significant difference in SRT values was noted between 36 and 26-point grids.

Table 3.2: Pattern of eye movement response for healthy controls and glaucoma patients in both the stimulus intensity levels.

Eye movement responses	Seen		Unseen		Invalid	
	214 cd/m^2	276 cd/m^2	214 cd/m^2	276 cd/m^2	214 cd/m^2	276 cd/m^2
Percentage of response from healthy controls (n = 54)	90.5	97.7	6.9	1.4	2.6	0.9
Percentage of response from glaucoma patients (n = 50)	57.3	68.6	30.8	22.2	11.9	9.2

Stimulus Intensity is denoted using cd/m^2

Although significant on a group level, not all glaucoma patients had a delayed reaction time. Based on a five-fold cross-validation analysis, an overall

classification accuracy of 90.4% (10.9) was considered as an internal valida-tion of the modified grid. Finally, the average test duration (per eye) using the 36-point grid was 3.2 ± 0.3 min and 5.3 ± 0.6 min respectively among healthy controls and glaucoma patients. After the modification, a small pilot in five healthy controls and five glaucoma patients showed a test duration of 1.2 ± 0.3 min and 2.9 ± 0.6 min, respectively.
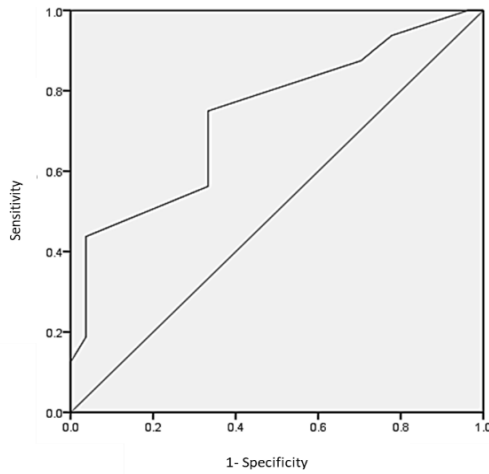
Figure 3.4: Receiver Operating Characteristic (ROC) curve obtained for location x = 21, y = 9 with an Area Under the Curve (AUC) of 0.73.
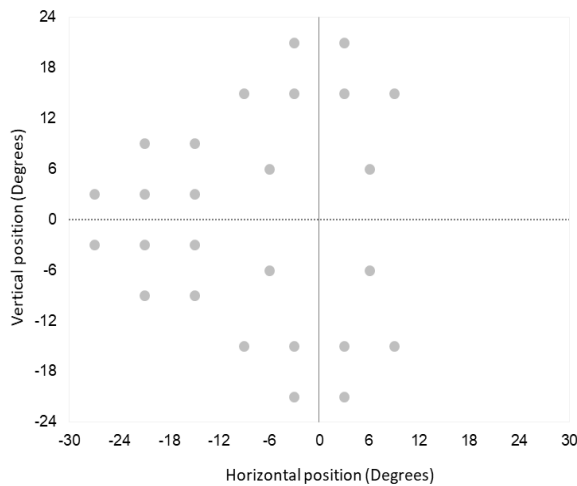
Figure 3.5: Illustration of the new stimulus grid for the right eye with 26 test loca-tions.

DISCUSSION

This study aimed at developing a screening protocol for detecting glaucomatous VF loss by utilising an ideal screening approach, which can be economical, easily administrable, rapid, and reliable. The use of eye tracking technology offers a non-invasive, low-cost, easily administrable, and objective method for measuring SRT that can be used as an index for evaluating the functional visual aspects (Jernigan ME, 1980; Kim et al., 1995).
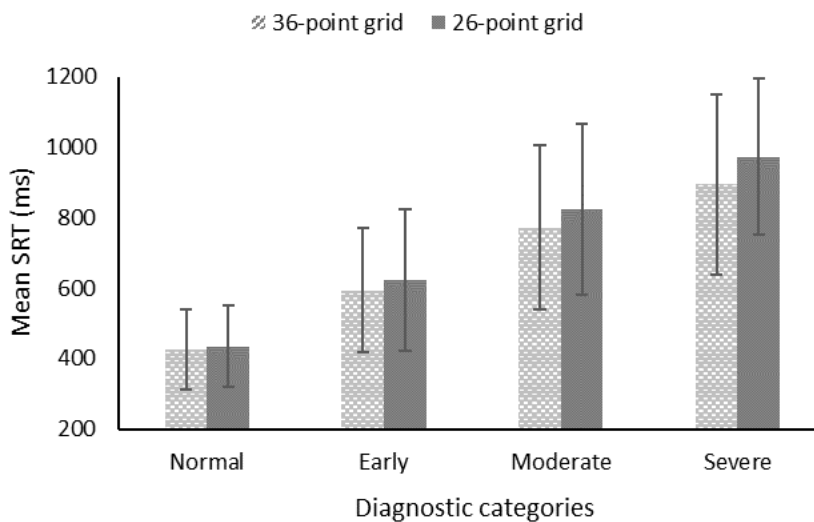
Figure 3.6: A cluster bar graph that displays the comparison between the mean SRT (ms) obtained in four diagnostic categories using 36-point and 26-point grids. The error bars represent the Standard Deviation.

As the intention was to screen for glaucomatous defects, maximum preference was given to evaluate the peripheral VF areas. Therefore, the developed test grid had 26 stimulus locations comprising four central locations and 22 test locations in the peripheral zones, predominantly testing nasal, superior, and inferior of the VF. The four central test locations were placed at slightly eccentric positions, i.e. 8° from the grid centre. This might trigger the false categorisation of glaucomatous defects involving only central VF as healthy ones, but this proportion might be insignificant, as the early glaucomatous defects tend to affect the Bjerrum area (Hitchings & Spaeth, 1976; Harwerth et al., 1999). The evaluation of the remaining 36-point grid was carried out

among healthy controls and glaucoma patients who were sub-classified into mild, moderate and severe stages of glaucoma. The study sample intentionally had a high proportion of mild followed by moderate cases with relatively few severe cases. The inclusion of a large proportion of severe defects of glaucoma would have resulted in the elimination of valuable test locations since in this group the number of unseen points due to VFDs is higher. Using this approach, we optimised the screening grid for detecting early glaucomatous defects.

To improve the reliability of assessing saccades, certain specific features were integrated into the test protocol. A peripheral stimulus was projected only when central fixation was stable. In addition, an overlap paradigm was used, meaning that the central fixation stimulus was kept visible even during the projection of subsequent peripheral stimuli, which is a similar approach used in HFA. When a central stimulus disappears, it might trigger search behaviour. Despite this, a significant difference in eye movement responses was noted between healthy controls and glaucoma patients (Table 3.2). In spite of instructions to not search for peripheral stimuli, glaucoma patients still exhibited more searching behaviour than healthy ones, which is in agreement with previous studies (Kim et al., 1995). This behaviour might reflect the visual adaptation that glaucoma patients develop as a compensatory action for their field defects. Observation of these eye movement patterns may give insight into the real-life impact of Glaucomatous Optic Neuropathy (GON). The percentage of false negative responses was expected to be minimal as EMP depended on the natural eye movement reflex response. The current algorithm could not incorporate an index for monitoring the possible false negative responses as we felt it would lengthen the test duration. The test administration was noted to be examiner friendly, as the need for continuous monitoring of the participants' response and repeated instructions were minimal.

Since perimetry is a psychophysical procedure that shows intra-test and inter-test fluctuations and variability, the ROC curve was considered to be an efficient approach to identifying the test locations for developing the

screening grid. The AUC values summarise the entire location of the ROC curve instead of considering single measures of sensitivity and specificity (Hajian-Tilaki K, 2013). Therefore, AUC values were considered as an index of accuracy. We interpreted the AUC of a particular stimulus location as the probability to have a high risk of glaucomatous damage. From Figure 3.6 and Supplementary Table 3.1, it is apparent that this strategy did result in the elimination of locations, which are suspected to have a poor discriminating value from clinical evidence. Faster reaction times were noted for stimulus projected at 276 cd/m^2 in comparison with 214cd/m^2 and this observation was in accordance with the previous literature (Pel et al., 2013). Mean SRT values obtained from 36 and 26 point grids were compared across four diagnostic categories, i.e. healthy, mild, moderate and severe glaucoma (Figure 3.6). The difference in mean SRT (obtained from two grids) ranged from 7.5-76.8 ms, which was not statistically significant, i.e. the mean SRT values did not show a significant change even after the removal of ten locations. Even though Pel et al. measured the SRT values using comparable background and stimulus intensity levels we used in our set up, our healthy controls exhibited higher SRT values (Pel et al., 2013). A possible explanation could be the higher mean age of our study sample. A similar approach was used in the work published by Thepass et al. on the effect of cataract on EMP. Here, higher luminance intensity levels were used, up to 450 cd/m^2, which presumably explains the faster SRT values they reported compared to our results (Thepass et al., 2015).

A five-fold cross-validation analysis was done on the global SRT values of all participants to have a first evaluation of the classification ability of the 26-point grid. In this method, the original data sample (n = 104) was randomly partitioned into five subsamples, and one was left out in each iteration. This method was adopted because repeated random subsampling results in eventually using all subsets as both training and validation data whereas they are considered exactly once for validation. In this study, a single mean global SRT value per participant, as calculated from the 26 locations, was used for calculating the accuracy, which is a rough estimate of the tested VF responsiveness. A refinement might be achieved when a point-wise analysis is done to

further evaluate its screening ability in identifying healthy controls and pa-tients with different grades of glaucoma. A clinical comparison of the EMP screening grid should be done preferably with the current standard method (Frequency Doubling Perimetry) and the test-retest variability has to be ana-lysed (Thomas et al., 2002; Hess et al., 2012). A 90.4% of average classifica-tion accuracy was calculated while using global SRT obtained using the 26-point grid for categorising healthy controls and glaucoma. This suggests that SRT values can be a promising index for the detection of glaucomatous VFDs. The simplicity of testing technique and strategy could potentially reduce the need for close supervision thereby allowing an easier administration of the test without relying on trained personnel. This can be a reliable approach for static perimetry specifically in paediatric and geriatric participants.

CONCLUSIONS

The current study resulted in an interactive EMP test grid with 26 locations, which were predominantly placed in the nasal, superior and inferior areas of the VF. The reduction of tested points resulted in a reduction of test times with no significant changes in mean SRT values compared to a larger grid. The fivefold cross-validation, technique revealed the ability of the grid to accu-rately classify 90.4% of participants into healthy and glaucoma on the basis of mean global SRT values.

APPENDIX – Chapter 3

Supplementary Figure 3.1:
Illustration of the test in which all 36 locations were denoted using xy co-ordinates based on their positioning.
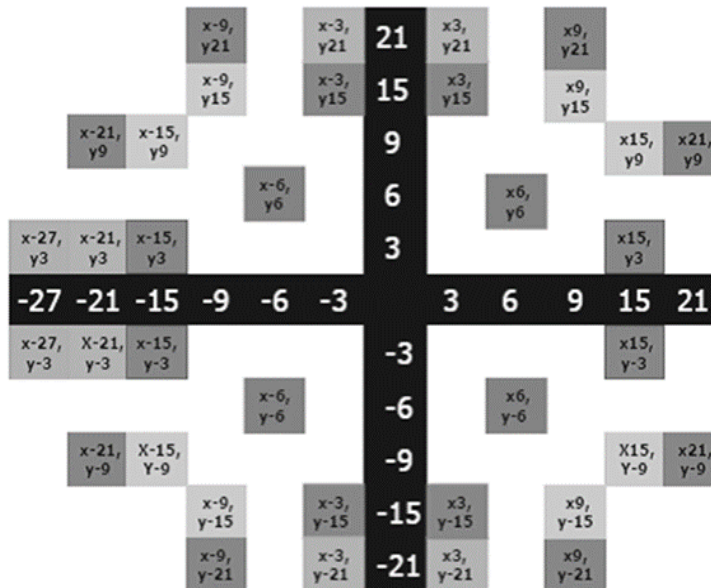
Supplementary Table 3.1:

Enumeration of the list of tested location ('x' and 'y' co-ordinates) with their corresponding Area Under the Curve values (obtained from the ROC analysis), 95% Confidence Interval limits, Cut off values, sensitivity (%), specificity (%), and associated p-values.

AUC values for four central locations

Tested locations	AUC	95 % CI		Cut offs	p-values	Sensitivity (%)	Specificity (%)
		Lower	Upper				
x6,y6	0.73	0.66	0.81	0.70	**<0.001**	0.70	0.71
x6,y-6	0.72	0.65	0.80	0.70	**<0.001**	0.69	0.71
x-6,y-6	0.71	0.62	0.78	0.65	**<0.001**	0.62	0.77
x-6,y6	0.81	0.76	0.88	0.70	**<0.001**	0.74	0.81

AUC values for peripheral locations

Tested locations	AUC	95 % CI		Cut offs	p-values	Sensitivity (%)	Specificity (%)
		Lower	Upper				
x3,y15	0.75	0.68	0.80	0.65	**<0.001**	0.60	0.69
x3,y-15	0.75	0.66	0.79	0.70	**<0.001**	0.66	0.70
x-3,y-15	0.77	0.73	0.85	0.70	**<0.001**	0.66	0.71
x-3,y15	0.78	0.72	0.83	0.70	**<0.001**	0.65	0.75
x15,y3*	0.68	0.60	0.76	0.70	**<0.001**	0.69	0.71
x15,y-3*	0.52	0.43	0.61	0.60	**<0.001**	0.60	0.69
x-15,y-3	0.79	0.72	0.86	0.70	**<0.001**	0.71	0.75
x-15,y3	0.80	0.72	0.87	0.70	**<0.001**	0.71	0.75
x9,y15	0.75	0.66	0.80	0.70	**<0.001**	0.65	0.71
x9,y-15	0.81	0.76	0.86	0.70	**<0.001**	0.68	0.75
x-9,y-15	0.76	0.69	0.82	0.70	**<0.001**	0.67	0.69
x-9,y15	0.80	0.71	0.86	0.70	**<0.001**	0.68	0.72
x15,y9*	0.79	0.73	0.86	0.80	**<0.001**	0.76	0.74

x15,y-9*	0.73	0.66	0.82	0.70	**<0.001**	0.68	0.73
x-15,y-9	0.76	0.70	0.82	0.70	**<0.001**	0.69	0.70
x-15,y9	0.81	0.74	0.87	0.70	**<0.001**	0.70	0.78
x3,y21	0.76	0.68	0.81	0.80	**<0.001**	0.76	0.74
x3,y-21	0.76	0.67	0.80	0.70	**<0.001**	0.66	0.71
x-3,y-21	0.76	0.70	0.82	0.80	**<0.001**	0.66	0.67
x-3,y21	0.79	0.73	0.85	0.80	**<0.001**	0.69	0.80
x-21,y3	0.76	0.70	0.83	0.70	**<0.001**	0.66	0.74
x-21,y-3	0.78	0.73	0.84	0.70	**<0.001**	0.68	0.76
x9,y21*	0.71	0.65	0.78	0.65	**<0.001**	0.66	0.65
x9,y-21*	0.77	0.71	0.83	0.70	**<0.001**	0.69	0.73
x-9,y-21*	0.70	0.63	0.77	0.65	**<0.001**	0.75	0.62
x-9,y21*	0.77	0.73	0.85	0.70	**<0.001**	0.70	0.77
x21,y9*	0.73	0.65	0.78	0.65	**<0.001**	0.67	0.65
x21,y-9*	0.74	0.67	0.80	0.65	**<0.001**	0.66	0.71
x-21,y-9*	0.77	0.71	0.83	0.80	**<0.001**	0.68	0.78
x-21,y9	0.77	0.71	0.84	0.70	**<0.001**	0.65	0.77
x-27,y3	0.75	0.69	0.81	0.70	**<0.001**	0.70	0.78
x-27,y-3	0.79	0.73	0.85	0.70	**<0.001**	0.69	0.80

*Denotes the eliminated locations

3

CHAPTER 4

Eye Movement Perimetry and Frequency Doubling Perimetry: Clinical performance and patient preference during Glaucoma screening

Najiya Sundus K. Meethal[1,2], Johan J.M. Pel[1], Deepmala Mazumdar[1,2], Rashima Asokan[2], Manish Panday[2], J. van der Steen[1,3], Ronnie George[2],

1. Vestibular and Ocular Motor Research group, Dept. of Neuroscience, Erasmus MC, Rotterdam, The Netherlands
2. Medical Research Foundation, Chennai, India
3. Royal Dutch Visio, Huizen, The Netherlands

ABSTRACT

Background

To evaluate the screening accuracy of an Eye Movement Perimetry (EMP) in comparison with Frequency Doubling Perimetry (FDP) and to investigate the patient preference and perception towards these Visual Field (VF) screening methods.

Materials and Methods

A total of 104 healthy controls [mean age (SD) of 48 (14) years] and 73 glaucoma patients [mean age (SD) of 52 (13) years] were recruited. All the participants underwent a comprehensive ophthalmic evaluation including the 24-2 SITA standard protocol on the Humphrey Field Analyser. This was followed by the 26-point protocol in EMP and the C-20-1 protocol in FDP. During EMP, all participants were instructed to fixate a central target and to look at the detected peripheral target, followed by refixation of the central target, and Saccadic Reaction Time (SRT) was calculated. Next, a questionnaire was administered to evaluate the participants' preference and perception towards the perimetry techniques. Mean SRTs and Robin's scores were used to plot Receiver Operating Characteristics (ROC) curves. From the questionnaire survey, the frequency distributions of the responses were calculated.

Results

Robin's scores and SRT values were significantly increased in glaucoma patients in comparison with the age-matched healthy controls ($p < 0.001$). The ROC analysis revealed comparable Area Under the Curve (AUC) values (0.95, $p = 0.81$) with a specificity of 95.2% for FDP and 96.2% for EMP with a sensitivity of 87.7%. Thirty-seven percent of the older age group (≥ 40 years) and 65% of severe glaucoma patients showed a preference for EMP over FDP.

Conclusions

This study results indicate that the customised protocol in EMP provides efficient and raid means of screening VF defects, which compared well with FDP. Elderly healthy controls and patients with moderate and severe glaucomatous defects preferred EMP as it permitted natural reflexive eye movements thereby resembling a real-life test setting.

INTRODUCTION

Glaucoma is a chronic, multifactorial optic neuropathy that causes the impairment of vision-related functions eventually leading to irreversible blindness (Foster et al., 2002). Due to its asymptomatic nature and subtle clinical signs, a significant proportion of glaucoma remains undetected in people worldwide (George et al., 2010). To date, the global prevalence of glaucoma is 64.3 million which is predicted to increase by 18% in 2020 and 74% in 2040, predominantly affecting the inhabitants from Asian and African ethnicity (Tham et al., 2014). These statistics emphasise the necessity for increasing the rate of early case identification and improving glaucoma care services, especially in the developing world (George et al., 2010; Tham et al., 2014; Varma et al., 2011).

Various glaucoma screening techniques have been devised for detecting structural or functional glaucomatous damage to enable early detection and intervention in order to control the rate of disease progression (Sharma et al., 2008). Screening for characteristic glaucomatous Visual Field Defects (VFDs) using perimetry is one such potential approach. Standard Automated Perimetry (SAP) is the current clinical standard for screening and diagnosing functional glaucomatous loss (Foster et al., 2002 and Sharma et al., 2008). However, in conventional perimetry tests, patients are required to sustain a steady central fixation throughout the course of testing. This might lead to test induced fatigue and certain visual complaints, which in turn compromises the test reliability and the precise quantification of the Visual Field (VF). Eye Movement Perimetry (EMP) was developed as a viable alternative by addressing some of these constraint (Kim et al., 1995; Toepfer et al., 2008; Mazumdar et al., 2014; Murray et al., 2009; Meethal et al., 2018).

Our study group has developed a testing protocol in EMP by adopting the 54-point grid tested on the SITA Standard 24–2 protocol of the Humphrey Field Analyser (HFA). Each point was tested by presenting stimuli at four different intensity levels; thus, 216 stimuli in total were presented to each participant. The protocol relied on eye tracking technology for the real-time monitoring of the participant's gaze responses to each of the peripheral stimuli, with the

advantage of negating the requirement for pressing the response button. Still, the test duration of this fixed protocol was ~12 min per eye, which limited the rapid screening for any VFDs. This paved way for the development of an EMP screening protocol that evaluated a 26-point grid (Meethal et al., 2018). These locations predominantly focus on areas in the VF with a maximum susceptibility for glaucomatous damage. The protocol assesses the extent of the VF using the binary responses (seen/unseen) for each tested location. Then the Saccadic Reaction Time (SRT) to the 'seen' location is derived which is used as an index to quantify the VF responsiveness. When evaluated in a set of healthy controls and glaucoma patients, the screening protocol calculated the mean SRT values (SD) to be 435 ± 116 ms and 806 ± 234 ms respectively. Based on this statistically significant delay in SRT ($p < 0.001$), an overall classification accuracy of 90.4% was found (Meethal et al., 2018).

The aim of this study was to compare the clinical performance of this EMP method with that of an existing standard method. As glaucoma screening lacks a legitimate clinical standard with an appropriate diagnostic ability (sensitivity and specificity), the Frequency Doubling Perimeter (FDP) which has a reasonable performance in clinical and community-based evaluation studies (Thomas et al., 2002) was used for the comparative analysis.

The first phase of this study focused on the comparative analysis of the screening accuracy of the 26-point grid protocol in EMP and the C-20-1 protocol in FDP. The subsequent part of the study focused on a questionnaire-based assessment of the perimetry systems, test target characteristics, and physical/mental factors that can have a possible impact on the psychophysical test performance.

MATERIALS AND METHODS

A written informed consent was attained from all the participants before the commencement of any clinical evaluation. The study adhered to the tenets of the Declaration of Helsinki and was approved by the Institutional Review Board (IRB) of Vision Research Foundation (VRF), Chennai.

Study participants

This cross-sectional study enrolled 112 healthy controls and 80 glaucoma patients aged above 20 years. Participants were either volunteers or recruited from a non-consecutive series of patients attending the outpatient department and glaucoma clinic of a tertiary eye care centre situated in southern India. Healthy controls were defined as those who were bilaterally phakic with normal extraocular motility, normal anterior segment, and Intra Ocular Pressure (IOP) ≤ 21 mmHg. A dilated posterior segment evaluation and perimetry (SAP) were done to rule out any structural or functional glaucomatous damage or any neurological defect that might affect the VF.

All participants underwent a comprehensive ophthalmic evaluation including VF assessment using 24-2 Swedish Interactive Threshold Algorithm (SITA) standard protocol in HFA (model 750; Carl Zeiss Meditec, Dublin). Reliability indices and the criteria considered for accepting the test results were based on the Humphrey perimetry algorithm, which was Fixation Loss (FL) and False Positive (FP) less than 20% and False Negative (FN) less than 33%. Glaucoma patients were defined on the basis of the International Society of Geographical and Epidemiologic Ophthalmology (ISGEO) classification (Foster et al., 2002). Patients with primary glaucoma who had characteristic structural defects with corresponding, repeatable, and reliable VF deficits were included. They were classified into mild, moderate, and severe glaucoma based on disease severity assessed using VF reports based on the Hodapp, Parrish, and Anderson's (HAP) classification (Anderson & Patella, 1999). This was followed by VF testing using the C-20-1 screening protocol in FDP (Welch Alyn, Skaneateles Falls, NY, USA, and Carl Zeiss Meditec, Dublin, CA, USA) and a 26-point grid interactive EMP test (Tobii 120, Tobii, Sweden). The order of performing FDP and EMP was randomised using a block randomisation technique and a minimum gap of 15 minutes. Verbal instructions were given by a single examiner before and during the testing in the vernacular language or in English. The right eye was tested first in all the cases except for those patients with interocular differences in visual acuity or severity of VFDs. In those

instances, the better eye was tested first followed by the fellow eye. Testing was performed with dim room illumination and a minimal level of voice or other interruptions.

Frequency Doubling Perimetry

During the FDP procedure, no optical correction was used and the participants were instructed to rest their forehead on the forehead rest and maintain a steady central fixation while low spatial frequency sinusoidal grating targets (Figure 4.1: Left panel) were presented in the near periphery on a Cathode Ray Tube (CRT) monitor display (Figure 4.1: Right panel). The viewing canopy automatically covered the non-tested eye. Participants were encouraged to act in response to the near threshold targets by pressing a button without making searching eye movements. The screening protocol (C-20-1) reviewed a grid of 17 points (16 targets zones and a central foveal point, Figure 4.1: Left panel) and the missed points were re-evaluated and bracketed for the severity of the defect. As FDP incorporates only three trials to calculate each reliability index, any test result with even one FP/FL was repeated to ensure accurate results. FDP results with excess FP/FL errors even on repetition were classified as 'unreliable' hence excluded from the final analysis.

The presence of two depressed points anywhere in the tested field (including the central point), with at least one point depressed to < 1% p level and the other to < 1%, < 0.5% p level, or the most severe level, was considered to differentiate healthy individuals and glaucoma (Thomas et al., 2002; Quigley, 1998 and Johnson & Samuels, 1997) A final Robin's score was calculated for each patient by including all abnormal points on the basis of number, location, and depth of the defect, i.e., normal, mild, moderate, or severe (Patel et al., 2000). Final scores ranged from zero for a completely normal test to 87 for a test in which all points were missed at the maximum threshold. Robin's score was used as an index to classify each VF as normal or glaucomatous on FDP. A score of 0 to 2 was considered as the range for healthy, whereas 3–87 was considered for glaucoma (Patel et al., 2000).
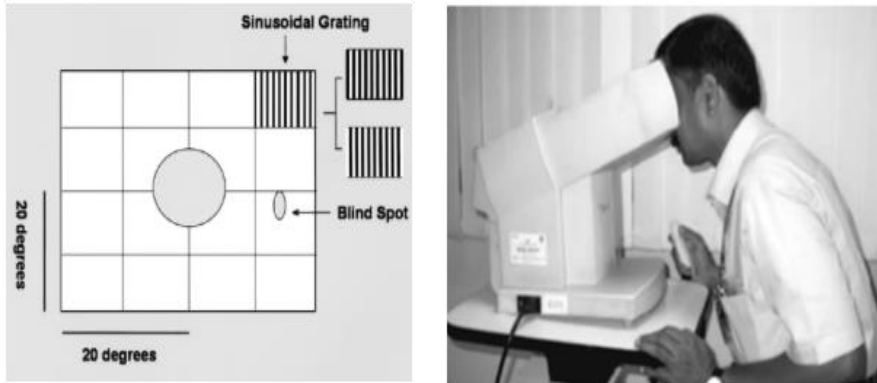
Figure 4.1: The left panel illustrates the test grid used in the C-20-1 protocol consisting of 17 locations along with the sinusoidal gating stimulus whereas the right panel displays the measurement setup used in the study showing a volunteer sitting in front of the perimeter with his forehead resting on the visor facing the monitor through the viewing canopy (Note: Participant shown is a volunteer from whom an additional informed consent was obtained for publishing this photograph).

Eye Movement Perimetry

The EMP setup comprised of a Tobii 120 eye tracking device integrated into a 17-in Thin Film Transistor Liquid Crystal Display (TFT-LCD) monitor of 1280 × 1024 pixels (Mazumdar et al., 2014; Meethal et al., 2018). Each participant was seated at a fixed test distance of 60 cm with a chin rest (Figure 4.2: Left panel). The non-tested eye was covered with a black Polymethyl methacrylate (PMMA) blocker that was transmissible to infrared light. This permitted binocular gaze tracking with no visual stimuli on the screen being visible to the non-tested eye. The interactive EMP screening test used in the study (Meethal et al., 2018) commenced with a tracking status estimation followed by a nine-point calibration procedure that lasted for ~ 13 to 15 s per eye (Mazumdar et al., 2014; Meethal et al., 2018). The calibration procedure was repeated either for all the nine locations or for any preferred locations, if the calibration accuracy was poor due to blink artifacts, inaccurate focusing of participants on the calibration dot, or any hardware/tacker-related

issues, etc. Participants with unsuccessful calibration even on repetition were exempted from further measurements and final analysis. The test plotted Goldmann size IV central fixation target against a background illumination of 152 cd/m². Peripheral targets (Goldmann size III) of intensity 214 cd/m² and 276 cd/m² were projected sequentially based on an overlap paradigm at 26 test locations (Figure 4.2: Right panel). Each target appeared for a maximum duration of 1.2 seconds (s). All participants were encouraged to maintain a central target fixation and respond to the appearance of a peripheral target on detection with an eye movement followed by refixation of the central target. The central target was repositioned at four eccentric positions to cover a maximum testing angle of 27° horizontally and 21° vertically. For each of the presented stimuli, gaze data was collected and stored for analysis.
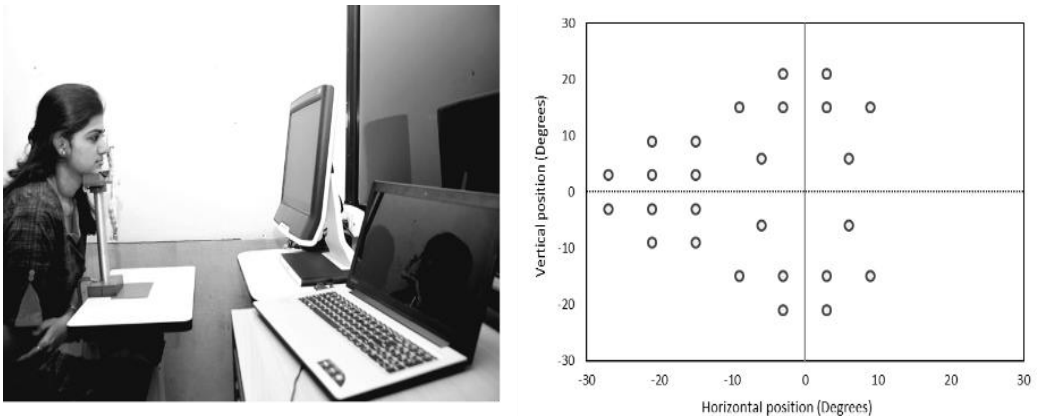
Figure 4.2: Left panel shows the Eye Movement Perimetry setup used in the study showing a participant sitting with her chin rested on the chin rest provided at a fixed testing distance of 60 cm (Note: The participant in the photograph is a volunteer from whom an additional informed consent was obtained for publishing this photograph). Right panel illustrates the Screening grid for the right eye with 26 test locations, which are predominantly placed in the nasal, superior, and inferior areas of the visual field.

A customised Matlab program was used to analyse the trajectory and time course of a Saccadic Eye Movement (SEM) initiated towards each peripheral

target. A peripheral stimulus was labelled as 'seen' if the following criteria were fulfilled: (1) fixation of the central target was followed by a peripheral stimulus fixation, (2) the angular disparity between the direction of the primary SEM and the peripheral stimulus location was less than 45°, (3) the amplitude of the primary SEM covered more than 50% of the total target distance. A peripheral stimulus was classified as 'unseen' when these criteria were not followed. An event where insufficient eye movement data was available due to blinking or pupil-tracking failure was labelled as 'invalid'. This was used as the preliminary reliability index. An EMP test with more than 25% (> 6/26 gaze events) of invalid responses were considered 'unreliable', hence excluded from the analysis.

Table 4.1: Enumeration of the centroid points obtained from the k-means cluster analysis for healthy and glaucoma groups (Cluster limits calculated from a previously published dataset, Meethal et al., 2018).

Age group (in years)	Centroid (in milliseconds)	
	Healthy (n=54)	Glaucoma (n=50)
20 - 29	378	586
30 - 39	403	611
40 - 49	444	678
50 - 59	524	700
> 60	560	729

For the events labelled as 'seen', SRT was calculated as the time between the onset of a peripheral target and the initiation of the SEM, which was done, based on the gaze velocity criterion by calculating the reaction time at which the eye velocity crossed 50°/s.

A k-means cluster analysis was performed on a different set of sample (54 healthy controls and 50 glaucoma patients) from a previously published study (Meethal et al., 2018). The analysis helped to identify the most representative SRT value within the group called 'centroid', which was used to discriminate between healthy controls and glaucoma patients (Table 4.1).

Questionnaire administration

Upon completion of VF screening tests using FDP and EMP, a previously validated questionnaire (Meethal et al., 2019) was administered by a single examiner to evaluate the patient preference, views, and perception about perimetry techniques. The questionnaire had 13 questions (Appendix 4.1) which assessed (a) patient preference for test techniques and test targets, (b) factors influencing the patient attentiveness during perimetry performance, and (c) their impression about the level of difficulty in performing perimetry. Questions for assessing ease/comfort of perimetry procedures, preference for central fixation, and peripheral test targets used in the perimetry techniques in terms of recognition, etc. were framed for assessing the patient preference. Factors like noise distraction, fear of failing or repeating the test, room ambiance, placement of patch/occluder, and fatigue or lack of sleep were included to understand the factors that could influence attentiveness while performing perimetry. Questions to verify the reliability of the participant's response were also included. The impression about the level of task difficulty was analysed by including questions related to difficulty in maintaining steady central fixation for an extended duration, difficulty in recognising peripheral targets against the background, and difficulty in pressing the response button. The responses were obtained using a five-point Likert scale.

Statistical analysis

Statistical analyses were performed using SPSS (Statistical Package for Social Sciences, version 15, Chicago, IL, USA). The right eye of each participant and the SRT obtained for the stimulus intensity 214 cd/m^2 were considered for analysis. Type 1 error was kept at a 5% level and all the tests used were two-tailed. A descriptive analysis of the demographic details, and the two outcome measures, i.e., Robin's score and SRT values, were done. Test duration was quantified as the time taken per eye (seconds) to complete the examination.

Pearson correlation was performed between Robin's score and SRT values against the duration of that particular screening test protocol. One-way Analysis of Variance (ANOVA) was used to analyse the variation of Robin's score and SRT between different diagnostic categories (healthy, mild, moderate, and severe). Bonferroni posthoc test was used to compare the mean values between the sub-groups by considering a conservative p-value. Classification of the sample into two diagnostics categories (healthy and glaucomatous) was done based on Robin's score and SRT limits and the counts or frequencies were represented in 2 × 2 contingency tables. The cell frequencies observed in each category were used to indicate the discrimination accuracy by means of True Positive (TP) and True Negative (TN) outcomes. Receiver Operating Characteristic (ROC) curves were plotted to describe the screening ability of FDP and EMP and the area under the curve (AUC) values were considered as a measure to quantify the relative performance.

The coded and five-point Likert scale responses were obtained from the survey and their frequency distributions were used to summarise the outcome variables. The questions pertaining to the 'ease of task performance' and 'comfortable perimetry machine' were combined to state the overall patient preference for the perimetry techniques. These references were analysed in the overall sample specifically in the healthy group (n = 103) by categorising them based on their age (below and above 40 years) and in those with glaucoma by classifying them based on the disease severity in order to identify any contributory factors.

RESULTS

A total of 196 participants were recruited of whom 19 were excluded due to eye tracking failure/poor calibration (n = 8), error during post-processing of data (n = 1), unreliable (> 25% of invalid responses) EMP results (n = 6), and unreliable FDP results (n = 4). The final analysis included a total of 177 partcipants comprising 104 healthy controls and 73 glaucoma patients. The proportion of males was 56% (n = 58) and 74% (n = 54) among the healthy controls and glaucoma patients respectively. The demographic details of the

study controls are presented in Table 4.2. There was no statistically significant difference in mean age between the two groups (p = 0.06). The glaucoma patient group comprised 33 (45%), 23 (32%), and 17 (23%) individuals with mild, moderate, and severe forms of the disease respectively.

Frequency Doubling Perimetry

Robin's scores ranged from 0 to 67, with high scores found in individuals with increased severity of VFDs. The mean Robin's score for healthy s controls was 1 (SD: 2) which was statistically significantly different (Independent t-test, p < 0.001) from the glaucoma patients who had a mean score of 29 (SD: 20). A positive correlation was observed between Robin's score and the test duration of the FDP screening protocol (r = 0.98, p < 0.001). The mean test duration of FDP was 50 s and 113 s for healthy controls and glaucoma patients respectively (Figure 4.3: Left panel).

Table 4.2: Demographics of the study population stratified as healthy controls and glaucoma patients

Participants' characteristics (mean ± SD)	Healthy controls (n = 104)	Glaucoma patients (n = 73)	p-values*
Age (years)	49 ± 14	52 ± 13	0.06
Intraocular Pressure (mm Hg)	14 ± 3	16 ± 4	**< 0.001**
Mean Cup-to-Disc Ratio	0.4 ± 0.1	0.7 ± 0.2	**< 0.001**

*Independent t-test, SD – Standard Deviation

Eye Movement Perimetry

SRT values obtained for each individual ranged from 340 to 870 ms. The mean SRT (SD) for healthy controls was 467 (76) ms, whereas glaucoma patients had a delayed mean SRT (SD) of 683 (99) ms which was a statistically significant difference (Independent t-test, p < 0.001). A positive correlation was observed between mean SRT values and the test duration of EMP screening protocol (r = 0.97, p < 0.001). The mean test duration of EMP was 88 s and 151 s for healthy controls and glaucoma patients respectively (Figure 4.3: Right panel).

Outcome measures of FDP and EMP in diagnostic categories

A significant increase in Robin's score and delay in mean SRT was found when compared between healthy and different severity levels of glaucoma (Table 4.3). Segregation of participants was done (healthy and glaucoma) based on Robin's scores and age-corrected SRT limits (Table 4.4) and was compared with that of the HFA diagnosis (HAP criteria).
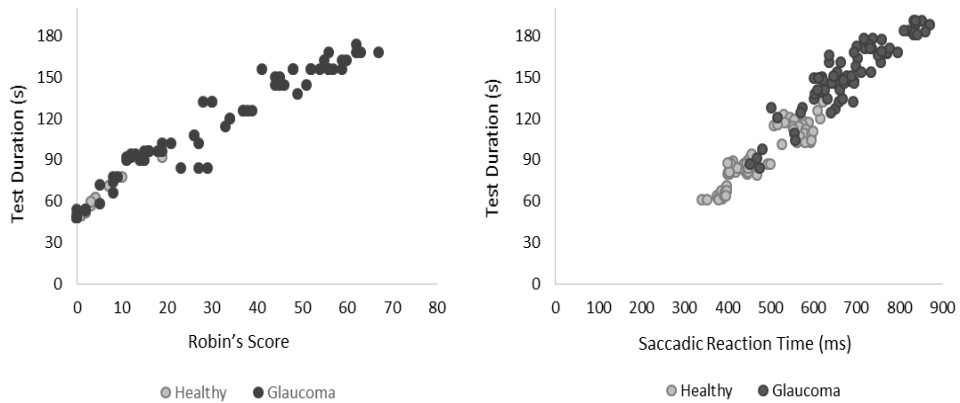
Figure 4.3: Scatter plot showing the positive correlation between Robin's score and the test duration in FDP (Left panel) and between the mean SRT values and the test duration in EMP (Right panel).

Table 4.3: Comparison of Robin's Scores and SRT values between healthy controls, mild, moderate and severe glaucoma patients

FDP and EMP outcomes	Healthy (n = 104)	Mild (n = 33)	Moderate (n = 23)	Severe (n = 17)	p-values
Robin's Score (Mean ± SD)	1.0 (2)	16 (13)	31 (16)	54 (11)	**< 0.001***
SRT values (Mean ± SD)	467 (76)	607 (62)	683 (57)	798 (42)	**< 0.001***

*One-way ANOVA

SRT – Saccadic Reaction Time in ms; SD – Standard Deviation

The Area under the ROC curves was comparable (Figure 4.4) for the FDP and EMP which were 0.952 and 0.958 respectively (p = 0.81). Figure 4.4 shows the ROC curves for both the screening methods. By keeping a minimum cut-off of 95% specificity (Fixed specificity), the optimum sensitivity was 87.7% for FDP and EMP with a specificity of 95.2% and 96.2% respectively.
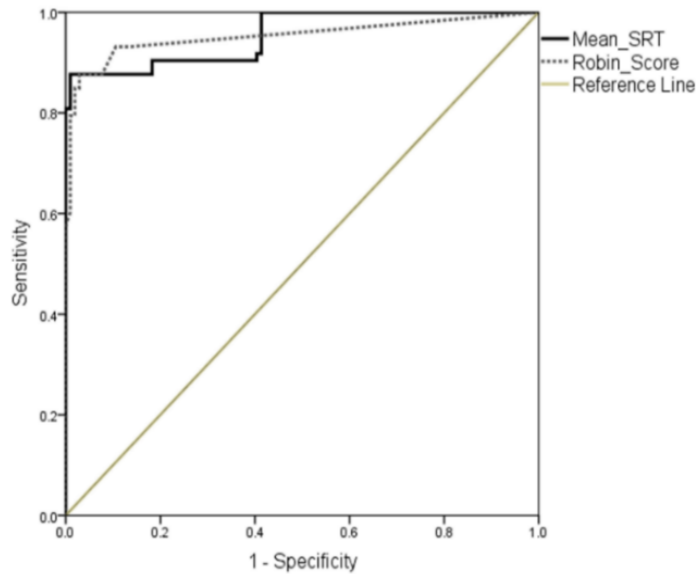
Figure 4.4: ROC curves plotted for the screening protocols in Frequency Doubling Perimetry and Eye Movement Perimetry.

Table 4.4: Study participants segregated into two diagnostic groups based on the Robin's score in FDP and Saccadic Reaction Time (SRT) limits in EMP and its comparison with HFA diagnosis (HAP criteria).

FDP and EMP outcomes	Diagnosis based on HFA (HAP*) criteria	
	Glaucoma (n = 73)	Healthy (n = 104)
FDP Robin's Score > 2	64 (88%)	8 (8%)
FDP Robin's Score ≤ 2	9 (12%)	96 (92%)
EMP Delayed SRT	72 (99%)	17 (16%)
EMP Normal SRT	1 (1%)	87 (84%)

*HAP criteria – Hodapp, Parrish and Anderson's criteria. Table shows: n (%)

Questionnaire responses

One hundred seventy-four respondents were included for the final analysis whereas three participants (one healthy control and two glaucoma patients) who had inconvenience to respond or complete the survey were excluded (response rate 98.3%). Among the healthy participants, 82.5% (n = 85), 91.3% (n = 94), and 78.8% (n = 82) had no prior experience of performing the perimetry tasks using FDP, EMP, and HFA respectively. Among glaucoma patients, the percentages were 88.7% (n = 63) for FDP, 83.1% (n = 59) for EMP, and 21.1% (n = 15) for HFA.

a.   Test preference

Among the healthy controls, the preference for FDP and EMP methods was compared between two different age groups, i.e., below and above 40 years (Figure 4.5). 45.7% of the younger age group (< 40 years) reported an equal preference for EMP and FDP, whereas 36.8% of the older age group (≥ 40 years) preferred EMP. Among the glaucoma patients, the preference pattern was compared between the three different severity levels (Figure 4.6). 56% (n = 18) of mild glaucoma patients reported equal preference for EMP and FDP, whereas 50% (n = 11) of moderate and 64.7% (n = 11) of severe glaucoma patients showed a preference for EMP over FDP. Overall, 61.5% (n = 107) of all the respondents preferred vertical sine-wave grating stimuli used in FDP over the white circular stimuli used in EMP.

b.   Factors influencing test performance

Among the healthy controls, 25.7% (n = 9) of the younger age group and 52.9% (n = 36) of the older age group reported difficulty in maintaining the central fixation while performing FDP and HFA. The percentage of patients who reported difficulty in maintaining prolonged central fixation was 71.9% (n = 23), 72.7% (n =16), and 76.5% (n = 13) among mild, moderate, and severe glaucoma respectively. 23.6% (n = 41) of all respondents reported difficulty in pressing the button in response to the peripheral test stimulus in HFA and FDP. Figure 4.7 illustrates the responses obtained from the healthy controls and glaucoma patients concerning the various factors that might have an

influence on perimetry performance. 38.0% (n = 27) of glaucoma patients reported that the 'fear factor of failing the test' was their main concern which influenced their performance.

Figure 4.5: Bar diagram illustrates the percentage of responses attained for perimetry preference assessment question (Questions 5 and 6, Appendix 4.1) from the healthy controls below and above 40 years. The responses were EMP, FDP, Neither (no preference) and both (equal preference).
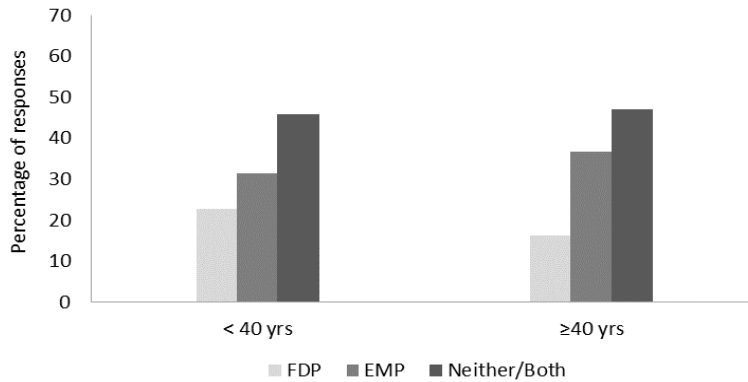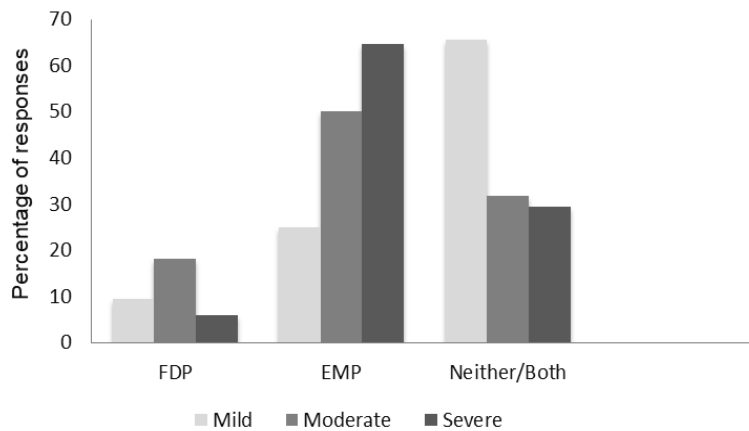
Figure 4.6: Bar diagram illustrates the percentage of responses attained for perimetry preference assessment question (Questions 5 and 6, Appendix 4.1) from the glaucoma patients. The responses were EMP, FDP, Neither (no preference) and both (equal preference).

DISCUSSION

The prime aim of our study was to estimate the screening accuracy of the 26-point grid screening protocol in EMP and perform a comparative analysis with the C-20-1 protocol in FDP. FDP and EMP correctly classified 64 (88%) and 72 (99%) patients respectively. The ROC analysis revealed AUC values (0.95) with a comparable specificity of 97% and sensitivity of 88% ($p = 0.81$).

Comparison of the outcome measures of FDP and EMP

To determine the screening accuracy of FDP, our study relied on the scoring system proposed by Patel et al. that considered the location of the defect as well as the depth of severity (Patel et al., 2000). The peripheral locations were given less weightage (value of 1) as they were expected to evoke FP responses and were prone to high variability (Patel et al., 2000). Using this age-corrected scoring system, the screening ability results of FDP in this mixture of healthy, mild, moderate, and severe glaucoma cases were comparable to those reported (Thomas et al., 2002; Johnson et al., 1997 and Patel et al., 2000).

For EMP, instead of a scoring method, eye movement responses were considered for estimating the extent of VF, and means of the location-wise SRT was considered as an index of VF responsiveness. This was irrespective of the location and depth of the defect. Instead of giving a location-wise weightage, equal emphasis was given to each response as SRT variance was reported to be independent of stimulus location (Pel et al., 2013). For the cluster analysis, age-corrected SRT limits were determined for five age bins as SRT has a dependency on the participant's age and those limits were used for categorising the participants into two diagnostic groups (Munoz et al., 1998). The correlation analysis between the Robin's score and SRT was carried out to determine the direction and strength of association between the two measured quantitative variables. The analysis indicated that the two variables were strongly related in a positive linear manner ($p < 0.001$).
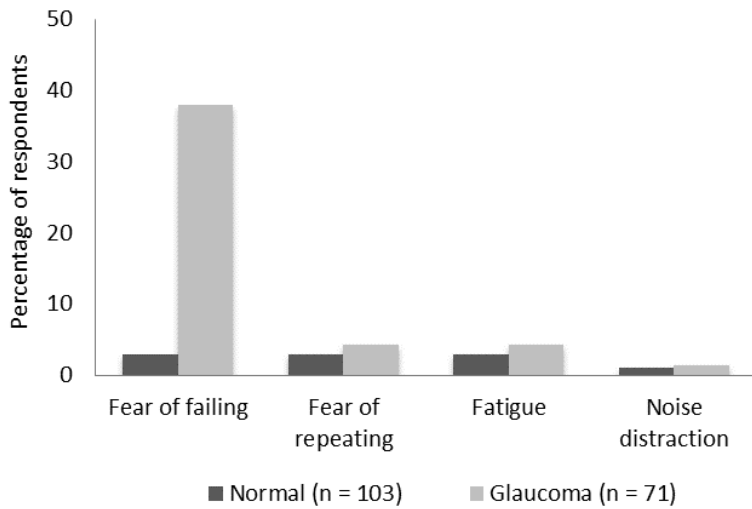
Figure 4.7: Bar graph illustrating the percentage of respondents for four different factors (noise/conversation in the testing room, fear of failing the test, fear of repeating the test and Fatigue) that were reported to influence the perimetry task performance.

Reliability of eye movement responses

In the customised algorithm of EMP, each peripheral stimulus was projected only after obtaining a stable central fixation. The central fixation target was kept visible even during the projection of peripheral stimuli (overlap paradigm). The probability of a stimulus appearing at any of the test locations was balanced by randomising the order of presentation. These specific features were integrated in order to improvise the reliability of SEMs. This was intended to avoid any biases introduced by the observer's prior expectation of stimuli locations, to minimalise the possibility of search behaviour or express/anticipatory saccades (Mazumdar et al., 2014; Meethal et al., 2018 and Pel et al., 2013). FDP has incorporated catch trails to estimate the rates of FL and FP responses but not FN. Since the number of catch trials is inadequate, it is recommended to repeat the FDP measurement even with the presence of a single false response. Instead, in EMP, definite criteria are incorporated

for evaluating the reliability of eye movement responses (FL, FP, and FN) during the post-processing analysis. This helped to consider only the reliably 'seen' locations for mean SRT calculation.

Effect of refractive error and cataract

All the study participants were either emmetropic or had a spherical and cylindrical ametropia of less than ± 5.00 D and − 2.00 D respectively and a visually insignificant cataract (grade less than N2, C1, P1 based on the Lens Opacification Classification System (LOCS) II (Chylack et al., 1989). Even though we have limited the range of refractive error and grades of cataract during the inclusion of study participants, the effect of these factors should be addressed. FDP uses a sinusoidal pattern stimulus that is less affected by refractive defocus. Due to the relatively larger stimulus size, refractive errors up to six dioptres are not considered to significantly influence the test results (Contestabile et al., 2013); similarly, the detection of peripheral stimuli in EMP might be difficult in the presence of a high magnitude of the uncorrected refractive error.

Studies have shown that accurate recording of SRT can be performed regardless of the presence of mild or moderate refractive errors (Vikesdal et al., 2016); still, it might be advisable to use the corrective lenses in case of high ametropia to improvise the accuracy and reliability of the outcome measures in order to optimise the test performance. Aside from refractive error, the presence of cataract can also have an effect on perimetry results. In FDP, even the mild stage cataract is reported to cause FP results; hence, it is advised to consider that factor when interpreting the results (Casson et al., 20006). Likewise, a previous study has evaluated cataract as a probable confounding factor in EMP measurements. Although the difficulty level for detecting visual stimuli increases with cataract-induced loss of contrast, no correlation was found between mild and moderate cataract (LOCS III, grades I-IV) and SRT. It was recommended to cautiously interpret EMP results in the presence of denser cataracts (LOCS III) (Thepass et al., 2015).

Test duration for FDP and EMP

At any particular test location in the VF, perimetric thresholding is a much-abbreviated procedure; hence, it was beneficial to exploit all the available information from each stimulus presentation and responses to improve the test. Test duration is one such example of the information collected during VF testing that could potentially be used to evaluate the patient performance and test reliability (Adams et al., 1999). FDP and EMP have an inbuilt interactive nature with which the response time window can be dynamically altered according to the speed of the participant's response. This enables faster responders to have a shorter response window, thereby reducing the test duration. A significant difference in test duration was found between healthy and glaucoma patients when tested in FDP (50 ± 6 s for healthy and 113 ± 38 s for glaucoma) as well as in EMP (88 ± 19 s for healthy and 151 ± 25 s for glaucoma). An increase in test duration of FDP and EMP was found with increasing severity of glaucoma. Additionally, the EMP test duration was found to be prolonged with increasing age as well.

In comparison with FDP, the EMP screening grid consisted of nine (53%) additional test locations (26 versus 17) which can explain the marginal increase in its overall test duration. Yet, the 'per location test time' for both the perimetry methods was identical in healthy controls (~ 3 s) but in glaucoma patients, the mean duration taken to evaluate each test location was ~ 6 s in EMP whereas it was ~ 7 s in FDP. The mean 'per location test time' in FDP might be equal for all the test locations as it exhibits a uniform sensitivity irrespective of their eccentricity. This is probably due to the use of a large target size (10° diameter) (Adams et al., 1999). However, in the case of EMP (Goldmann size III target, 0.43°), the duration for testing locations at the paracentral locations might be rather faster when compared to the extreme periphery (Mazumdar et al., 2014). The test grid used in EMP was basically an adapted subset of the 24-2 grid in HFA considering the locations with the highest susceptibility to glaucomatous damage (Meethal et al., 2018). These optimised test locations resulted from a ROC analysis and might supplement the diagnostic ability of the EMP screening protocol when targeting the

glaucoma population. The EMP test protocol with nominal test duration has the added advantage that a re-examination of the patient is not going to be time-consuming or burdensome.

The lack of a clinically suitable 'standard' for identifying the presence of disease, particularly when dealing with the early-stage disease, is often a study limitation when evaluating the sensitivity and specificity (Sharma et al., 2008). Therefore, in our study, the categorisation of participants was done considering the definite structural defects of glaucoma in combination with corresponding and reproducible VF reports from HFA in order to minimalise the effect. Still, this may perhaps result in an overestimation of screening accuracy since only those with confined VFDs were included. A subset of this study sample (54 healthy controls and 50 glaucoma patients) was considered to identify the cluster limits for each age group and was applied to the overall sample set (104 healthy and 73 glaucoma patients) to categorise them into four diagnostic categories. A repetition of cluster analysis was done for the entire study sample (n = 177) to ensure the limits are comparable. A cluster limit calculation was done for further segregation of glaucoma patients into mild, moderate, and severe. A proportion of healthy individuals (17%) had delayed SRT and were categorised as mild glaucoma by EMP whereas 43% of mild glaucoma detected using HFA were categorised as moderate by EMP. The majority of these participants belonged to the highest age bin, i.e., 60 years and above.

Questionnaire responses

Younger participants (< 40 years) among the healthy group and patients with mild glaucomatous defects showed an equal preference for FDP and EMP, whereas a high preference for EMP was reported by the older age group and people with moderate and severe field defects. The preference pattern was in line with a previous study that evaluated the acceptability of eye tracking perimetry and SAP among glaucoma patients (McTrusty et al., 2017). This preference can be attributed to the ease of the test procedure. Factors contributing to the easiness were (1) allowance of reflexive eye movements instead of pressing the response button during the detection of peripheral

stimulus and (2) possibility of making refixation eye movements rather than a prolonged central fixation. The repositioning of central fixation targets to four eccentric positions in EMP was found to increase the confidence levels among participants with severe peripheral field loss.

Prior studies have evaluated the perception and experience of individuals regarding their glaucoma follow-up, specifically towards the conventional perimetry methods (McTrusty et al., 2017; Chew et al., 2016 and Glen et al., 2014). In our study, we also conducted a qualitative assessment of patients' perceptions regarding various factors that can potentially influence perimetry performance. 'Anxiety/fear of failing the test' was acknowledged as a predominant factor influencing the test performance, which was in line with the previous studies (Chew et al., 2016). A previous study has reported fatigue/tiredness to have a negative effect on test performance (Glen et al., 2014). But, this was not a significant factor in our study probably due to the shorter test duration of both the screening tests. As the quality of instruction prior to the VF test can significantly affect subsequent estimations of VFDs (Chew et al., 2016), clear instructions in vernacular language were provided to each participant and the comprehension was ensured. Approximately, 20% of our overall sample had a complaint of claustrophobia with conventional perimetry methods. Older participants reported a high preference for EMP with no postural restraints and mentioned it as a more natural testing setup that allows regular inherent reflex. This study has highlighted the preference and perception of people about the perimetry methods and certain factors that can compromise the success of VF testing. Addressing these identified barriers can be vital to devise and clinically implement a new VF testing method in the future.

Study limitations

There are some study limitations to be addressed. Sufficient tracking of the eyes is a necessity for using EMP and 4.6% of the participants had a failure of eye tracking during the calibration procedure. Even if this is a minimal dropout percentage, this issue should be taken into account during future testing using EMP. Even if the order of performing EMP and FDP was randomised

with ample time provided between tests, approximately 5% of the participants got confused with the testing pattern of EMP and FDP. In such cases, a demo test was re-run and the second test was considered for analysis. The preference questionnaire was framed in English and was administered by the interviewer either in English or in the vernacular language (Tamil). The Tamil translation was validated before its incorporation in this study (Meethal et al., 2019). In 10.3% of participants (n = 18) who were not comfortable with either of the language, assistance was taken from the translators for conveying the meaning of each question which could have raised a potential response bias.

CONCLUSIONS

This study demonstrated a customised protocol in EMP as a novel method for screening VFDs in glaucoma. EMP showed high sensitivity (87.7%) and specificity (96.2%) values which compared well with FDP when considering the screening accuracy. Elderly healthy participants preferred EMP and patients with moderate and severe glaucomatous defects as it permitted natural reflexive eye movements thereby resembling a real-life test setting.

4

APPENDIX – Chapter 4

Full version of the validated questionnaire that was administered to compare patient's comfort in taking the visual fields test using the EMP and FDP

1. How many times have you taken the eye tests using

FDP
a. 0
b. 1
c. 2
d. 3 or more

EMP
a. 0
b. 1
c. 2
d. 3 or more

2. Which of the following do you feel is easier to see, while taking the test?

a. Vertical lines
b. White spots
c. Both
d. None

3. Do you find it difficult to concentrate on the central fixation point while taking the test?

a. Yes
b. No
c. Unable to decide

4. Which amongst the two machines do you think is a faster method to take the test?

a. FDP
b. EMP
c. Neither/No preference
d. Both/Equal preference

5. Which machine are you more comfortable with when you are required to take the test?

a. FDP
b. EMP
c. Neither/No preference
d. Both/Equal preference

6. Which amongst the two machines do you think is an easier method to take the test?

a. FDP
b. EMP
c. Neither/No preference
d. Both/Equal preference

7. Do you get disturbed and hence not perform the test accurately because of any of the following reasons in your immediate environment?

    a. Noise from outside / Conversations that take place in the room where the test is conducted

Very High	High	Less	Very less	Not at all

    b. Fear of failing the test

Very High	High	Less	Very less	Not at all

c. Fear of being asked to repeat the test

Very High	High	Less	Very less	Not at all

d. Black / white patches on the other eye

Very High	High	Less	Very less	Not at all

e. Fatigue / Lack of enough sleep

Very High	High	Less	Very less	Not at all

8. If you have filled in option (e): How many hours of work do you put in on an average day?
a. 4-6 hours
b. 6-8 hours

Do you work overtime/ night shift etc. -----------?
a. Yes
b. No

9. Do you prefer to take the test in a
a. Dark room
b. Brightly illuminated room

10. How many times were you asked to repeat the test the last time you took it?
a. 0
b. 1
c. 2
d. Can't recall

11. How long a gap does you require before retaking the test? -----------

12. Which test did you take first?
a. EMP
b. FDP

13. Kindly grade the following test conditions with respect to the difficulty / comfort level

Factors	Procedure	Very easy	Easy	Mildly Difficult	Difficult	Very difficult
Testing posture	FDP					
	EMP					
Language of instruction	FDP & EMP					
Ability to comprehend instructions	FDP					
	EMP					
Chin/Forehead rest	FDP					
	EMP					
Room lighting	FDP					
	EMP					
Eye Patches	FDP					
	EMP					
Button pressing	FDP					

CHAPTER 5

Detection of visual field defects using Eye Movement Pediatric Perimetry in children with intracranial lesions: Feasibility and Applicability

Najiya Sundus K. Meethal [1, 2], Jasper Robben [1], Deepmala Mazumdar [1, 2],
S. Loudon [3], N. Naus [3], J.R. Polling [3], J. van der Steen [1, 4],
Ronnie George [2], Johan J. M. Pel [1]

1. Vestibular and Ocular Motor Research group, Dept. of Neuroscience, Erasmus MC, Rotterdam, The Netherlands
2. Medical Research Foundation, Chennai, India
3. Dept. of Ophthalmology, Erasmus MC, Rotterdam, The Netherlands
4. Royal Dutch Visio, Huizen, The Netherlands

ABSTRACT

Background

The study aimed at evaluating the feasibility of Eye Movement Pediatric Perimetry (EMPP) among children in detecting Visual Field Defects (VFDs) associated with Intracranial Lesions (IL).

Materials and Methods

Healthy controls (n = 35) and patients diagnosed with IL (n = 19) underwent a comprehensive clinical evaluation followed by a Goldmann Visual Field (GVF) and a customised EMPP protocol. During EMPP, all the participants were encouraged to fixate on a central target and initiate eye movement responses towards randomly appearing peripheral stimuli. The eye movement responses were recorded using an eye-tracking device and further inspected to calculate Performance Scores (PS), the Saccadic Reaction Times (SRTs), and an EMPP Index (EMPI).

Results

The mean age (years) of the controls and cases was 7.3 (SD: 1.5) and 9.4 (SD: 2.4) respectively. Among the controls, the older children (≥ 7 years) showed statistically significantly faster SRTs (p = 0.008) compared to the younger group. The binocular EMPP measurements compared between the controls and the cases revealed no statistically significant differences in PS (p = 0.34) and SRT (p = 0.51). EMPP failed in 4 children because of data loss or unacceptably poor PS whereas GVF failed in 7 children due to unreliable subjective responses. Of the 16 reports, with regard to the central 30-degree VF, 63% of the outputs obtained from both methods were comparable.

Conclusions

EMPP is a reliable method to estimate and characterise the central 30° VF in greater detail in children with IL. EMPP can supplement the conventional method, especially in those children who fail to complete a long duration GVF test.

INTRODUCTION

Children diagnosed with Intracranial Lesions (IL) need a multidisciplinary approach to treatment and monitoring. These children commonly present with Visual Field Defects (VFDs) particularly when the lesions involve the visual pathway and the nature of the lesion dictates its location and extent. Hence perimetry turns out to be an integral component in the ophthalmological management protocol to evaluate the stability or progression of the causative lesion. Perimetry not only contributes to clinical management decisions but also offers essential assistance while rehabilitating these children (Kotecha et al., 2021; Kedar et al., 2011).

Regardless of the development of Standard Automated Perimetry (SAP) for adults, there are still limited possibilities for perimetry in children. Goldmann Visual Field (GVF) technique is a recommended kinetic approach in children that helps to identify the alterations in the Visual Field (VF) shape/area and delineate quadrant/hemifield defects (Wirtschafter et al., 1984; Patel et al., 2019; Agarwal et al., 2000). In GVF, the VF is manually mapped by instructing the participant to remain fixated on the central cue located in the middle of a hemispherical bowl. Meanwhile, a circular light stimulus is gradually moved from the extreme of the projection surface into the field in order to mark the boundaries and establish the isopter. GVF is very efficient in evaluating the periphery beyond 30°, relying on the multiple possible responses from the patient along the entire trajectory and the sequence of kinetic scanning. This aids in identifying sharp-edged scotomas or steep isopter boundaries as seen in classic VFDs associated with neuro-ophthalmic conditions (Agarwal et al., 2000). But the drawback is that there is no consensus or standard protocol to conduct the procedure. Therefore, GVF demands a highly-skilled examiner who can accurately manipulate the stimulus presentation and interact well with the participants for gaining consistent subjective responses. Thus the procedure is prone to substantial outcome variabilities induced by the examiner as well as by the patient. The requirement of prolonged fixation and attention makes it challenging to obtain reliable and

5

repeatable test results in children (Wirtschafter et al., 1984; Patel et al., 2019; Agarwal et al., 2000). Moreover, small sensitivity changes and widespread or diffuse VFDs are difficult to identify using this method. Regardless of its limitations, GVF is still recommended as it permits the evaluation of a wide extent of VF and delivers valuable clinical information in children with neuro-ophthalmic disorders.

In view of the above-mentioned challenges, we evaluated Eye Movement Perimetry (EMP) as an alternative approach of automated perimetry in children with neurological impairment. Previous studies have shown the applicability of EMP among adults in detecting glaucomatous VFD (Meethal et al., 2019; Mazumdar et al., 2020; Murray et al., 2017) as well as in the assessment of visual orienting behaviour in young children, (Pel et al., 2010; Murray et al., 2018) and in infants (Satgunam et al., 2017). EMP relies on natural human reflexes where the detection of static peripheral stimuli is indicated by making prosaccades. From each goal-directed Saccadic Eye Movement (SEM), the system calculates the Saccadic Reaction Time (SRT). A combination of both these outcomes results in a reliable clinical index for VF mapping. Here, we marginally modified the EMP setup used for the adult patients (Meethal et al., 2019; Mazumdar et al., 2020) into an EMPP method (Eye Movement Pediatric Perimetry).

The aim of the current study was to investigate the applicability of EMPP in VF estimation among children with IL for which we included a subset of children diagnosed with IL with and without the genetic mutation of Neurofibromatosis-type 1 (NF-1). The EMPP incorporates a customised VF test protocol integrated with Eye Tracking Technology (ETT) to capture real-time fixation and SEM responses to VF stimuli. The outcome measures from the EMPP testing were the pattern of SEM responses (seen/unseen/invalid), a score calculated from the number of reliable responses, named as Performance Score (PS), and the SRT calculated from 'reliably seen responses. This study addressed the following objectives: (a) to evaluate the feasibility of the EMPP in children, (b) to compare the PS and SRT between a control group and a set

of children diagnosed with IL (c) to describe the applicability of EMPP in predicting the functional deficits associated with the lesions in comparison with the GVF outputs.

MATERIALS AND METHODS

Study participants

To evaluate the feasibility and practicability of the EMPP method in the pediatric population, a set of healthy pediatric participants (n = 35) aged between four to ten years were recruited from a regular primary school in Rotterdam, The Netherlands. This healthy control group was included when the following criteria were met (1) born between 37 to 42 weeks of gestation, (2) no significant history of visual or ocular problems, and (3) no evidence of brain injury/damage.

To explore the clinical value of EMPP, a patient group who was diagnosed with definite IL (with and without genetic mutation of NF-1) with or without clinically evident functional defects on GVF perimetry was included. Patients were recruited from the outpatient clinic of the pediatric ophthalmology department at the Erasmus MC, Rotterdam, The Netherlands. Since the reliable and successful completion of a perimetry test necessitates visual attention and concentration, the patient group specifically included children diagnosed with the genetic mutation of NF-1. Apart from the wide-ranging physical complications, NF-1 is also characterised to cause diverse cognitive dysfunctions including reduced intelligence scores, compromised visuospatial abilities, and attention deficits that might make the perimetry challenging or influence the results (Vogel et al., 2017; Miguel et al., 2015; Garg et al., 2013). Hence the enrollment of this subgroup aided us to explore if the EMPP approach can be successfully applied to children with neurodevelopmental disabilities. Due to the outbreak of COVID-19, only 19 patients were requested to participate in the present study. Parents or legal guardians provided written informed consent before the commencement of the study to access the children's medical registers and to include the video recording of the

5

experimental session. The essential information related to the visual status such as reduced Visual Acuity (VA) and presence of VFDs recorded using GVF perimetry (such as hemianopia or quadrantanopia), evidence of behavioural comorbidities such as Attention Deficit Disorders (ADD), Autism Spectrum Disorder (ASD), developmental delay, and Intellectual disability were extracted from the medical records. Experimental procedures were approved by the Medical Ethical Committee (MEC) of the Erasmus University Medical Centre (EMC), Rotterdam, The Netherlands (MEC-2017-1150) and adhered to the Declaration of Helsinki.

Goldmann Visual Field (GVF) perimetry

GVF perimetry was conducted by a skilled perimetrist who manually mapped the VF by projecting circular light stimuli of six stimulus sizes (ranging from 0.0625 mm^2 to 64 mm^2). The stimulus was moved from the non-seeing area into the seeing area (field of vision) and whenever the patient saw the stimulus, the response buzzer was pressed and the perimetrist marked the corresponding point. At the conclusion of the procedure, the marks were connected by a smooth line to form the isopter. GVF reports were obtained for each of the patients along with the related details such as Pupil Diameter (PD) in mm (measured using a diameter gauge), refractive correction, quality of the subjective responses (good/slow/varying), and reliability of the central fixation (good/moderate/bad).

EMPP: Measurement setup and procedures

The EMP setup and the test paradigm that was developed and evaluated in the adult population were transformed marginally for making it suitable for the pediatric population. The modifications were as follows: (a) the chin rest installed in the EMP used for the adult population was removed while examining the children thereby giving them an unrestricted and naturalistic environment. This was feasible as the Tobii tracker compensates for head motion within some boundaries, (b) the adult EMP test protocol projected white circular visual stimuli (Goldmann size III) at four different stimulus intensity

levels, whereas for the children smiley faces at a single intensity level were used to encourage attention and retain interest, and (c) a webcam recording was added to monitor the child's overall performances, attentiveness, and eye movement behaviour.

Figure 5.1: EMPP set up with a 24-inch display monitor integrated with an infrared eye-tracking device and a height/viewing angle adjustable surface housing. The inset picture shows an illustration of the smiley fixation target (circled with green dotted lines) and a peripheral smiley stimulus (circled with red dotted lines).

The EMPP measurement for the control and patient group differed in certain aspects. For the controls, the EMPP setup comprised of a 24-inch display monitor (test distance ~60 cm) combined with an external and portable re-mote eye tracking bar (Tobii X3-120; Tobii, Sweden). Patients (Figure 5.1) were tested using a 24-inch monitor with an integrated infrared 60 Hertz (Hz) eye-tracking system (Tobii T60 XL; Tobii, Sweden).

For the controls, the customised binocular VF test protocol relied upon a test grid that consisted of 28 locations (Figure 5.2: Left panel, adapted from Meethal NK et al., 2018). The total test duration was ~2 minutes and a maximum of 28 eye movement responses were obtained per individual. Meanwhile, in the patients, a more refined grid was used to detect the VFD that consisted of 56 locations (Figure 5.2: Right panel, adapted from Mazumdar et al., 2014). Each patient was tested under three different conditions: Binocularly (OU) and monocularly (OD and OS) with adequate breaks in between. This approach took ~4 minutes per measurement and a maximum of 168 eye movement responses were recorded per individual. Every measurement series began with a binocular measurement so that the children are familiarised themselves with the testing procedure followed by the monocular measurements, the order of which was randomised. Both the control group and the patient group performed EMPP measurements in a quiet and dim-lit room with no external interruptions. The parents or guardians were instructed to remain quiet during the measurement.
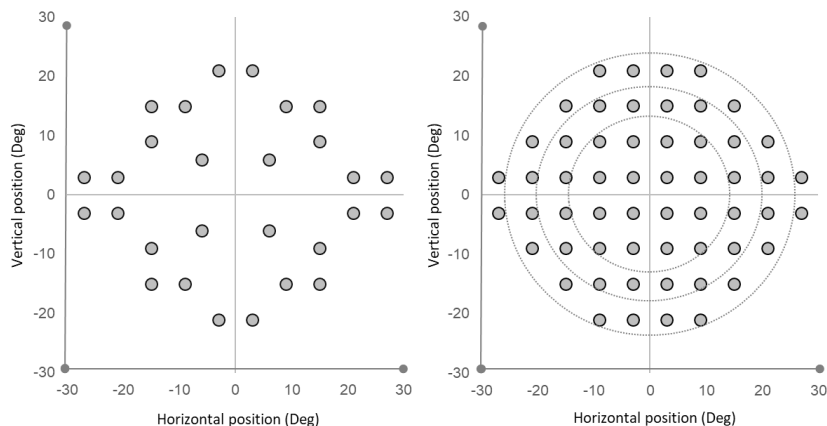

Figure 5.2: Illustration of the screening grid with 28 test locations (Left panel) and of the full-field grid with 56 test locations (Right panel) along with the zonal divisions based on stimulus eccentricity. x and y axis denotes the horizontal and vertical coordinates of the VF test locations in degrees (deg).

The EMPP test protocol was initiated with a tracking status estimation to ensure appropriate eye alignment and uninterrupted gaze tracking. This was

followed by a standardised five-point calibration procedure to obtain optimal gaze accuracy. This step was repeated either for specified locations or for all five locations if a poor calibration was noted due to blink artifacts, poor focusing, or any hardware/software related glitches. Only after a successful calibration, the EMPP test was commenced by projecting a central fixation target (Figure 5.1) and peripheral visual stimuli (at a fixed intensity level) were projected sequentially at random test locations based on an overlap paradigm. The participants were instructed to fixate the central stimulus and look at any detectable stimuli in the periphery and refixate the central stimulus, while the eye tracker was simultaneously recording the eye movements. The natural reflexive eye movement initiated towards a detected peripheral stimulus was considered as a positive response instead of a verbal response or a response buzzer. Participants were instructed not to search for the peripheral stimuli. The peripheral stimuli were projected for a maximum duration of 1.2 seconds (s) on the screen. A random interval of 1 to 2 s was set between stimuli to prevent the predictability of stimulus appearance. For each of the presented stimuli, gaze data was collected and stored for post-analysis.

Eye movement data analysis and creation of VF plots

The trajectory and time course of an SEM initiated towards a peripheral stimulus was analysed using a customised Matlab program (Mathworks Inc., Natick, MA, USA). For each trial, the SEM performance was assessed on the basis of various parameters and was visually inspected and labeled as 'seen', 'unseen', or 'invalid' (Figure 5.3). For each peripheral stimulus, a circular Area Of Interest (AOI) was defined with a radius of 6° and if the gaze trace crossed the border of this area the stimulus was identified as 'seen'. To ensure the reliability of the 'seen' response the following criteria were used: (a) a steady fixation of the central stimulus was followed by a primary SEM directed towards the peripheral stimulus, (b) the angular difference between the direction of the primary SEM and the peripheral stimulus location was ≤ 45°, (c) the amplitude of the primary SEM covered more than half (50%) of the total target distance. Whenever these criteria were not followed, a peripheral stimulus was classified as 'unseen'. An event where inadequate eye movement data was obtained due to blinking or pupil tracking failure was labeled

as 'invalid' and any trial with 'invalid' responses > 25% were excluded from the final analysis.

A measure of the performance called 'Performance Score' (PS) was calculated (ranging from 0 to 100% - least reliable to most reliable) from the number of reliable responses divided by the overall tested locations. The outcome measure for VF responsiveness, the SRT, was calculated from each of the 'seen' responses as the time between the onset of a peripheral stimulus and the initiation of the SEM which was done based on the gaze velocity criterion (the eye velocity ≥ 50°/s).
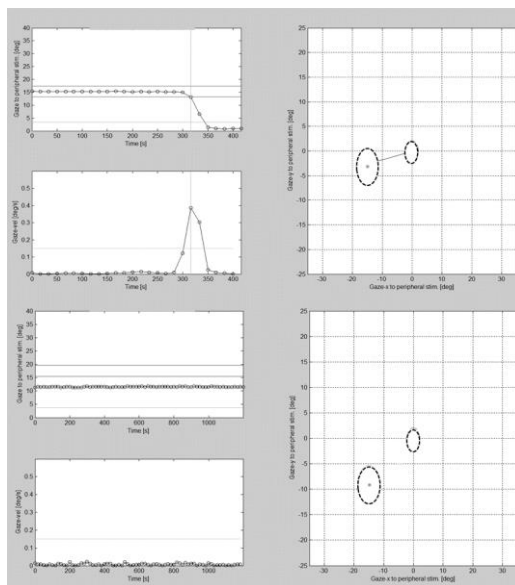

Figure 5.3: Top panel - Illustration of the Matlab window displaying an eye movement initiated from the central fixation to a peripheral stimulus (Right Panel) and the gaze position map used to estimate the Saccadic Reaction Time (Left panel - top), and the corresponding gaze velocity (Left panel - bottom). Bottom Panel - Illustration of the Matlab window displaying no eye movement initiated from the central fixation to a peripheral stimulus (Right Panel) and the corresponding gaze position map (Left panel).

Furthermore, a clinically utilisable index seemed necessary that can be grossly compared with the Visual Field Index (VFI) displayed in the standard

VF reports of the Humphrey Field Analyser (HFA). Here, we introduced an EMP Index (EMPI) as an aggregate percentage of visual function for a given VF including the test locations where a visual response is estimated (Bengtsson et al., 2008). EMPI was calculated from responses with reliable SRT divided by the total reliable responses (excluding invalids). As in the VFI, the central VF locations were given relatively higher weightage compared to the mid-perioral and peripheral VF areas for which a weightage factor was introduced depending upon the eccentricity (degrees) of the stimulus locations (Figure 5.2: Right panel). The weightage factors were 0.5, 0.3, and 0.2 for central, mid-peripheral, and peripheral zones respectively, hence ranging the EMPI on a percentage scale of 0 to 100% (perimetrically blind to normal).

To demonstrate the integrity of the VF we generated two customised EMP plots per patient. The first plot, the Performance Score (PS) plot, displayed the eye movement response at each tested location as 'seen', 'unseen', or 'invalid' (small empty circles). 'Seen' and 'unseen' test locations were denoted using filled-in circles with RGB shades of Grey (217-217-217) and black (0-0-0) respectively. The second plot named the Saccadic Reaction Time (SRT) plot displayed the SRT values corresponding to the 'seen' locations. SRT values from 200 to 1200 ms were illustrated using an RGB scale ranging from 230 to 25. The maximum duration window provided for a participant to respond reliably to a projected stimulus was 1.2 seconds (1200 ms), hence the maximum SRT on the scale was 1200 ms.

Statistical Analysis

In order to address the first research question that focused on evaluating the feasibility of the EMPP method in the pediatric population, EMPP performance (seen, unseen, and invalid) and SRT values of the control group was described and compared by subdividing them into two age groups i.e. < 7 and ≥ 7 years (Independent t-test). In addition, for each age group, the effect of stimulus eccentricity on SRTs was tested for significance by using one-way ANOVA. To explore the applicability of EMPP in predicting the functional deficits concomitant with IL, EMPI and SRT values were compared between the

patients (Non-NF-1 and NF-1) and the age-matched controls (Independent t-test). Since the test grid used for both the groups was different, this comparison was done by considering only those common test locations (n = 24) that are shared between the 28-point (controls) and 56-point (cases) test grids. A subgroup of healthy controls was assessed for age-matched comparison with the patient group. In the patient group EMPI and SRT values were descriptively compared between monocular (OD and OS) and binocular viewing (OU) conditions for both Non NF-1 and NF-1. To evaluate the clinical usefulness of EMPP a two-by-two contingency table was used to compare the gross agreement of 'normal' and 'abnormal' VF status shown by the GVF and the EMPP plots.

RESULTS

A total of 54 pediatric participants were recruited that included 35 healthy controls (n = 20 females) and 19 cases (n = 8 females) with IL. In 2 controls (6%) and in 2 cases (11%), the EMPP measurement failed because of eye tracking data loss due to blinking or poor eye-tracking quality. The mean age of the resulting 33 controls was 7.3 (SD: 1.5) years and that of the 17 cases was 9.4 (SD: 2.4) years. The latter group consisted of lesions associated with (n = 8) and without (n = 9) the genetic mutation of NF-1.

Table 5.1: Binocular PS and SRT value comparison between the older and younger children in the healthy control group.

Healthy controls (n = 30)	< 7 years (n = 11)	≥ 7 years (n = 19)	p-values*
Age range (years)	4 - 6	7 - 10	
Mean age (SD) in years	6.0 (0.9)	8.1 (1.1)	
Male: Female	3:8	7:12	NA
No: of reliable SEM responses obtained (n)	240	477	
Mean PS (SD) in %	98 (3)	98 (2)	1.00
Mean SRT (SD) in ms	344 (106)	311 (91)	0.008

*Independent t-test

Feasibility of EMPP in the control group

In the control group, 3 children had an unacceptably low EMPP Performance (PS ≤ 10%), hence they were excluded from the analysis. A total of 717 reliable SEM responses were obtained from the control group that were used to calculate the mean SRTs. The older children (≥ 7 years) showed an equal PS but a statistically significantly faster SRT values (p = 0.008, Independent t-test) when compared to the younger group (Table 5.1). Next, in both the groups of children (older children and younger), stimulus eccentricity had a significant effect on SRT (One-way ANOVA) with p-values < 0.001 and 0.03 respectively (Figure 5.4).
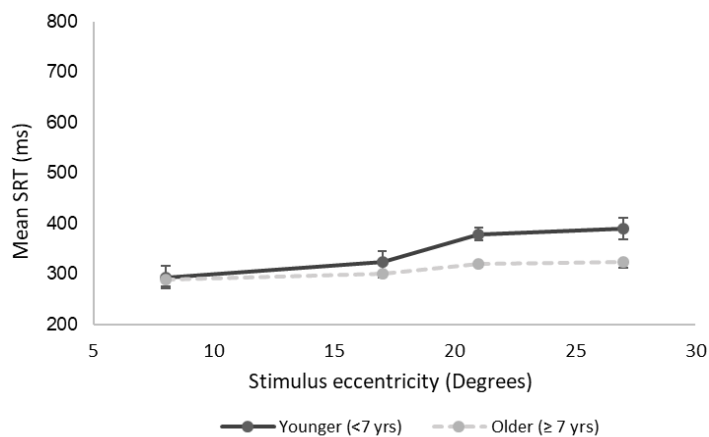

Figure 5.4: The Saccadic Reaction Time (SRT) plotted against stimulus eccentricity for younger and older children illustrating the delay in SRT with increasing eccentricity. The error bars represent Standard Error (SE).

EMPP applicability in the patient group

The binocular EMP measurements (Independent t-test) compared between the age-matched controls (n = 17) and the cases (n = 17) on the basis of 24 common tested locations revealed no statistically significant difference in PS (p = 0.67) and SRT (p = 0.51) between the groups. The patient group comprised of children diagnosed with IL associated with Non NF-1 and NF-1 mutations.

There was no statistically significant difference between the mean age of both the subgroups (p = 0.67). Table 5.2 describes the demographics and the clinical diagnosis of the Non NF-1 sub group and the type of neuro-developmental disabilities detected in the NF-1 group.

Table 5.2: Description of the cases/patient category including the Non NF-1 and NF-1 subgroups and their clinical diagnosis. *ADHD – Attention Deficit Hyperactivity Disorder, ASD – Autistic Spectrum Disorder.

Patient category (n = 17)	Gender ratio (male: female)	Mean age (SD) in years	Clinical diagnosis
Non NF-1 (n = 9)	3:6	9.3 (2.7)	1. Craniopharyngioma (n = 4) 2. Pilocytic astrocytoma (n = 3) 3. Chiasmal neuritis (n = 1) 4. Low-grade thalamic glioma (n =1)
NF-1 (n = 8)	6:2	9.1 (2.1)	1. Neurofibroma (n = 4) 2. Optic nerve Glioma (n = 3) 3. Astrocytoma (n = 1) **Neurodevelopmental disabilities** 1. ADHD* (n = 1) 2. ASD* (n = 1) 3. ASD suspect (n = 1) 4. Developmental delay (n = 2) 5. Attention deficits (n = 1) 6. Mild intellectual disability (n =2)

Three of the 17 patients who exhibited unacceptably poor performance on EMP (PS ≤ 10%) during either monocular or binocular testing conditions were excluded from the analysis which compared the performance between the two subgroups (Non NF-1 and NF-1) under monocular and binocular conditions. In total 1738 and 1859 reliable SEM responses obtained from the Non NF-1 and the NF-1 groups respectively were used to calculate the EMPI and the mean SRT values. At a sub group level, the mean monocular and binocular EMPI (Figure 5.5: Top panel) and SRT (Figure 5.5: Bottom panel) were comparable between the Non NF-1 (patient number 1 to 7) and NF-1 subgroups (patient number 8 to 14). Overall, the patient group showed a relatively

improved EMPI ranging from 0% to 60% (Figure 5.5: Top panel) and faster SRTs (Figure 5.5: Bottom panel) in binocular viewing conditions when compared to monocular responses.
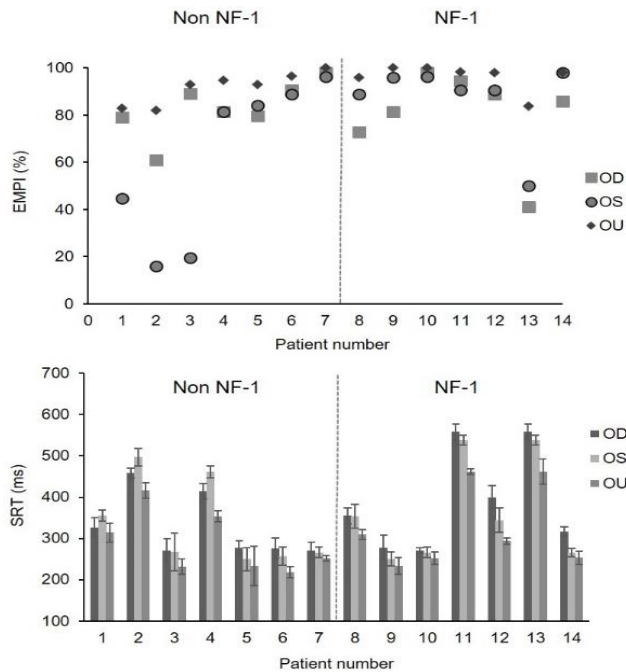

Figure 5.5: Scatter plot (Top panel) illustrating the improvement in Eye Movement Perimetry Index (EMPI) and fastening of Saccadic Reaction Time (SRT) values during monocular and binocular viewing conditions among the patient group (Bottom panel). Patient number 1 to 7 belongs to the non NF-1 and 2 to 14 to NF-1 subgroup and the dotted line separates the subgroups for a visual comparison.

Evaluation of the clinical usefulness of EMPP

Among the 14 cases, 64% (n = 9) children showed VA status in accordance with the EMPI i.e. poor VA (< 0.7) was presented with a poor level of EMPI (< 80%) whereas good VA was presented with a good level of EMPI. The rest of the children had either a good VA with a poor EMPI or vice versa. Overall 8 children were capable of to reliably perform both the EMPP and GVF procedures and among those 16 reports, a moderate agreement was found between the two perimetry methods (kappa: 0.52, p = 0.02). 11 outputs were

agreeing with each other on the basis of the presence and extent of VFD (An example is displayed in figure 5.6).
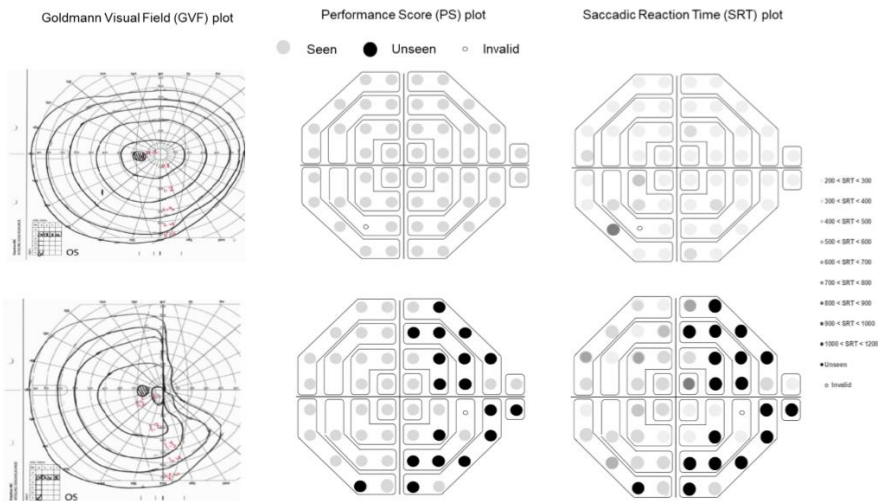

Figure 5.6: Top panel - A comparison of GVF and EMPP plots illustrating a normal visual field on GVF as well as on the EMP. Bottom panel – A comparison of GVF and EMPP plots (PS plot and SRT plot) illustrating an abnormal visual field with the presence of nasal field loss with a residual temporal field. The scaling used for the PS and SRT plot are provided.

DISCUSSION

This study evaluated the feasibility of EMPP in healthy children and its clinical applicability in children diagnosed with IL. The customised method could be successfully performed by 94% of the controls and 89% of the cases, which included even children under four years of age. The testing method seemed sound among children as they were not required to maintain a constant fixation instead were encouraged to perform a natural reflexive reaction in response to randomly appearing visual stimuli. In contrast from the EMP test set up implemented among the adults, EMPP was modified in such a way that the children were not required to place their heads in a fixed position because the data provided by the eye tracking system was compensated for limited head rotation. This gave a similar ambience as that of an electronic gaming with which most children were familiar.

Our cases included children with NF-1 gene mutation who presented with diverse cognitive/developmental dysfunctions including ADHD, ASD, and intellectual disability. Since the preparation of eye movement requires processes including the shift of visual attention to the new stimuli and disengagement of oculomotor fixation we evaluated the subgroup with NF-1 mutation in specific (Vogel et al., 2017; Miguel et al., 2015; Garg et al., 2013). Irrespective of the neuro-developmental disabilities, we found the NF-1 group to complete EMPP measurements with a promising and equal success rate in comparison with the Non NF-1 subgroup. The test failure that occurred in two controls and two cases was due to poor eye tracking quality and the measurements were not considered for the final analysis.

This study included a control group to essentially evaluate the feasibility and practicability of the proposed EMPP method in the pediatric population. Since these control children were enrolled in a regular primary school, we needed a portable eye-tracking test setup with a rapid and accurate VF evaluation protocol (binocular screening grid with 28 test locations). As a next step, cases were recruited for comprehensively evaluating the clinical applicability, and here we conducted monocular and binocular testing protocols (full-field with 56 test locations). The usage of a full-field grid (comparable to that of the HFA 24-2 protocol) made it possible to obtain extensive and relevant clinical information on the central VF. The screening grid locations were a subset selected from the full-field grid and the testing environment, decision algorithm, and analysis strategies were kept uniform to ensure comparability between the groups. In spite of the increased number of test points, we didn't anticipate a fatigability component to influence the EMPP performance as the test was rapid with a maximum test Darion of ~4 minutes. Still, the adequate breaks (minimum of 5 minutes) provided between the measurements ensured the elimination of the factor of fatigability. Moreover, the PS (%) reflected the level of EMPP performance and the calculated values didn't show any effect of fatigability in both the test cohorts.

5

Among the controls, the older children (≥ 7 years) showed a comparable PS (%) but significantly faster SRT values when compared to that of the younger group. SRTs also showed a dependency on the stimulus eccentricity which was more pronounced in the younger group of children. This response pattern was on par with the literature that described the nature of saccade development throughout childhood (Salman et al., 2006; Luna et al., 2008) and also the dependency of SRT on stimulus eccentricity though it was evaluated in a group of adults (Mazumdar et al., 2019). Among the cases, the improved eye movement responses during binocular measurement when compared to the monocular condition were similar to the eye movement behaviour observed among adults with glaucoma (unpublished data from the current study group) and also with contrast sensitivity thresholds on Humphrey Field Analyser (Asaoka et al., 2011). SRT values were statistically comparable between the controls and cases probably due to the inclusion of only binocular responses on the basis of common tested locations.

This study showed that EMPP can detect the presence and extent of expected VFD associated with the brain lesions with a moderate inter-method agreement in comparison with GVF. A previous study with a comparable methodology to the current study evaluated the clinical applicability of a novel technique called Saccadic Vector Optokinetic Perimetry (SVOP) in detecting VFD associated with brain tumors in children [10]. Similar to EMPP, the SVOP system also integrates eye-tracking technology with a customised test paradigm. But instead of their gap paradigm, the current study used an overlap paradigm as SRT is reported to be influenced by the fixation task (Bucci et al., 2005). Similar to SVOP, EMPP is also a viable method for VF testing in children to detect the presence and extent of VFD, with a possibility for monocular as well as binocular measurements. In addition to a binary response plot (seen/unseen), EMPP has an SRT plot for displaying the VF responsiveness, thereby offering supplemental clinical information. In EMPP, each test location was tested once. In our previous papers, we have reported the benefits of an interactive protocol, which we applied to patients with glaucoma [6, 7]. This approach not only makes the test faster but also allows for an ongoing

check for SEM responses from the fixation target to the peripheral visual stimuli. Here in EMPP, each test location was tested once, but the customisable protocol offers the possibility to repeat testing/crosschecks for preselected test locations. Hence in the future, we recommend further refinement of the protocol by incorporating this interactive approach between the participant and the test paradigm.

The stimulus grid used in EMPP is extended to a total visual angle of 54° horizontally and 42° vertically, hence could characterise the central VF area in greater detail. (≤ 30° VF). GVF and EMPP outputs showed only a moderate agreement, and the maximum proportion of disagreement (25%) occurred due to the presence of VFD detected in the SRT plot of EMPP (generalised/localised delays in SRT) whereas GVF showed a relatively normal VF. This mandates a further comparison of EMPP outputs with the VF outcome predicted in correspondence to the structural abnormalities detected using Optical Coherence Tomography (OCT) and Magnetic Resonance Imaging (MRI). A single report which presented with a peripheral field loss beyond the central 30° was categorised as normal by EMPP whereas GVF identified a functional loss. Similarly, only 64% of the cases had a decline in central VA in combination with poor EMPI, hence it is evident that alternative approaches to VF testing are not a replacement for the current clinical standards. Instead, it is an additional source of supplementary information. A calculation of EMPI for the central test locations (within 10°) would be worthwhile to compare this functional index with central VA. A follow-up study would be beneficial to evaluate the scope of using eye movement based parameters as prognostic indices among patients diagnosed with IL.

CONCLUSIONS

EMPP is a feasible method for estimating the VF among children with IL. The empirical plots of EMPP could detect and characterise the central 30° VF in greater detail thereby complementing GVF perimetry. In the future, a formal evaluation of its diagnostic ability in comparison with structural defects detected using imaging modalities might be beneficial.

CHAPTER 6

Eye Movement Perimetry to evaluate visual field responsiveness in optic nerve demyelination: An exploratory case report

Appendix chapter

ABSTRACT

Background

Optic neuritis often leads to the disruption of Saccadic Eye Movement (SEM), particularly in the Saccadic Reaction Time (SRT). To date, there are very few standardised tests to assess SEM parameters for clinical diagnosis and disease monitoring in optic neuritis. Hence, the aim of this case report was to explore the clinical value of an SEM-based perimetry to quantify afferent conduction defects associated with Optic Nerve (ON) demyelination.

Case description

This case report describes the clinical course of a 26-year-old female who presented with a complaint of gradually worsening vision in the right eye and bilateral pain during eye movements that she experienced over the preceding week. Clinical evaluation revealed severely reduced visual acuity in the right eye, Relative Afferent Pupillary Defect (RAPD), bilateral disc edema, and constricted Visual Fields (VF) on Standard Automated Perimetry (SAP). The patient underwent Eye Movement Perimetry (EMP) using monocular as well as binocular protocols to obtain SRTs to 'seen' peripheral locations. The patient was advised to undergo the intravenous administration of corticosteroid and oral immunotherapy. Post-treatment course, the patient was re-evaluated for the structural and functional components of vision including EMP. A significantly positive enhancement was recorded in both structural and functional aspects of vision. These improvements corresponded with the results of VF responsiveness maps generated with SRTs.

Conclusions

This preliminary report demonstrated that the VF responsiveness of the patient predicted on the basis of EMP correlated well with the structural and functional diagnostic outcomes during the active stage of the disease as well as during its recovery phase. This finding suggests that the assessment of SEM-based parameters with a rapid and standardised EMP test has clinical implication as a diagnostic and prognostic mode in neuro-ophthalmic diseases. In addition, we suggest future modification of the eye tracking system to incorporate pupil evaluation along with EMP for a better comprehensive evaluation of the visual system integrity

6

6

6

6

6

6

CHAPTER 7

A haploscope based binocular pupillometer system to quantify the
dynamics of direct and consensual Pupillary Light Reflex

Najiya Sundus K. Meethal[1,2], Deepmala Mazumdar[1,2], Sergii Morshchavka[3],
Jasper Robben[1], J. van der Steen[1,4], Ronnie George[2], Johan J.M. Pel[1]

1. Dept. of Neuroscience, Vestibular and Ocular Motor Research group,
   Erasmus MC, Rotterdam, The Netherlands
2. Medical Research Foundation, Chennai, India
3. Zaporizhzhia Polytechnic National University, Zaporizhzhia, Ukraine
4. Royal Dutch Visio, Huizen, The Netherlands

ABSTRACT

Background

This study described the development of a haploscope-based pupillometer for the parametrisation of the Pupillary Light Reflex (PLR), and its feasibility in a set of 30 healthy participants (light or dark-coloured irides) and five patients diagnosed with Relative Afferent Pupillary Defect (RAPD). Our supplementary aim focused on evaluating the influence of iris colour on the PLR to decide whether a difference in PLR parameters should be anticipated when this system is used across ethnicities.

Materials and Methods

All the participants underwent a customised pupillometry protocol and the generated pupil traces, captured by an eye tracker, were analysed using exponential fits to derive PLR parameters. A Pupil Response Symmetry (PRS) coefficient was calculated to predict the presence of RAPD.

Results

The mean (SD) Initial PD during dilation (3.2 (0.5) mm) and the minimum PD during constriction (2.9 (0.4) mm) in the light iris group had a statistically significant ($p < 0.001$) higher magnitude compared to the dark iris group. The normal limits of the PRS coefficient ranged from -0.20 to $+1.07$ and all RAPD patients were outside the calculated normal limits.

Conclusions

This proposed system, analysis strategies, and the tested metrics showed good short-term repeatability and the potential in detecting pupil abnormalities in neuro-ophthalmic diseases.

INTRODUCTION

The photosensitive cells in the human retina are uniformly adapted to function over a wide range of ambient light conditions. When transitioning from various light intensity levels, Pupil Diameter (PD) undergo dynamic alterations elicited by Pupillary Light Reflex (PLR), thereby assisting in the process of visual adaptation. In addition, PLR also acts as a protective mechanism to safeguard the retinal cells from phototoxic damage caused by any exposure to intense visible light. In such instances, PLR results in a rapid change in PD, thereby optimising the influx of light that strikes the retina (McDougal et al., 2015 and Mathôt, 2018). The PLR pathway is controlled by the integration of signals from the photoreceptors as well as the intrinsically photosensitive Retinal Ganglion Cells (ipRGCs), a subpopulation of Melanopsin containing RGCs that are sensitive to blue light. This reflexive process is directed by the antagonistic action of sphincter and dilator pupillae muscles subserved by the parasympathetic and sympathetic nerves, respectively. Hence, the analysis of PLR provides essential information regarding the integrity of these neural pathways (McDougal et al., 2015; Mathôt, 2018; Bremner, 2004 and Woodhouse, et al., 1994). Even though the key determinant of PLR is the level of retinal illuminance, additional factors such as age, gender, iris colour, clarity of optical media of eye, the integrity of optic nerve, etc. are also found to have an effect (Winn et al., 1994).

Conventionally, the PLR is evaluated using a Swinging Flashlight Test (SFT), which is a qualitative assessment of the direct and consensual pupillary reflexes ((McDougal et al., 2015; Mathôt, 2018; Bremner, 2004). This deceptively simple approach is crucial and beneficial in routine clinical practice for defect detection and monitoring. However, it is prone to substantial inconsistency and inter-examiner variability due to its dependence on the examiner's judgment and clinical expertise. Moreover, this method does not provide information regarding the delay, the speed, the extent, and the sustainability of pupil response. Thus, well-controlled systems are required to precisely quantify the parameters of both pupils (Levatin, 1959; Litvan et al., 2000; Meeker et al., 2005).

7

The technological advancements have led to multiple attempts to improve the objectivity of pupil response analysis by introducing pupillometer systems that aid in quantifying not just pupil diameters but also additional parameters that can be documented and monitored over time (Hall et al., 2018; Radzius et al., 1989; Chen et al., 2014; Shin et al., 2016; Martin et al., 2021; Nowak et al., 2014; Szczepanowska et al., 2004; Bos et al., 1988; Tekin et al., 2018; Bremner et al., 2012; Shwe-Tin et al., 2012; Cohen et al., 2015; Kurz et al., 2004). Currently, pupillometers are either commercially available and accessible pupillometers or laboratory-based prototypes. These are often designed for a specific clinical application or configured for a particular scientific study and differ from each other in their design, geometry, system characteristics, technical specifications, and range of applications. The proposed designs include monocular (Hall et al., 2018; Radzius et al., 1989; Chen et al., 2014; Shin et al., 2016; Martin et al., 2021) and binocular pupillometer systems (Nowak et al., 2014; Szczepanowska et al., 2004; Bos et al., 1988; Tekin et al., 2018; Bremner et al., 2012; Shwe-Tin et al., 2012; Cohen et al., 2015; Kurz et al., 2004), that offer non-invasive, precise quantification of pupil parameters by relying on techniques such as CCD camera (Charge Coupled Device) detectors, firmware camera, video-based eye tracking technology, etc.

While intending to use such systems in a clinical or research arena, a binocular registration of pupil response is advised for various reasons. First, it is a diagnostically important information to quantify not only the direct PLR but also the consensual one. Next, the pupil responses are markedly variable over time; therefore, a simultaneous recording and comparison of inter-pupil activities are always reliable/preferred. Moreover, binocular assessment is considered to be a realistic imitation of a person's life situations (Kurz et al., 2004). Though the literature has described various binocular pupillometers they are either inaccessible, expensive, inflexible, or less versatile to exclusively use for comprehensive pupil research (Nowak et al., 2014; Szczepanowska et al., 2004; Bos et al., 1988; Tekin et al., 2018; Bremner et al., 2012; Shwe-Tin et al., 2012; Cohen et al., 2015; Kurz et al., 2004). Hence, we decided to customise a binocular pupillometer setup by integrating an infrared

eye tracking device with a computer system for administering light stimulation. A previous study that evaluated pupillary reflex during perceptual rivalry used a binocular stimulus presented dichoptically on two monitors by projecting them with a mirror stereoscope to each eye separately. They could successfully quantify the pupil size and gaze direction using an infrared based eye tracking device placed behind the dissociating mirrors (Naber et al., 2011). Yet another study described a detailed practical guide to build a specific eye tracker based set up integrated into a system with the possibility of an independent (dichoptic) visual stimuli presentation to each of the two eyes. Relying on a similar concept, we developed a haploscopic system to control the laterality and the spatial extent of retinal stimulation and to further extend the possibility of the intended system to display three-dimensional simulation. The haploscope is an optical device that enables the dissociation of two eyes and the projection of two separate images to each of the observer's eyes (Naber at al., 2011; Brascamp et al., 2017 and Ramey et al., 2008). It offers the option for simultaneous, unilateral, and alternating pupillary light stimulation (named as stimulation phases) whereas the real-time monitoring and recording of pupillary responses can be done using the eye tracking device. Most (commercial) pupillometers report parameters such as minimum and maximum PD and average contraction speed. Here, we analysed the pupil response signals obtained during each phase using exponential fitting procedures to extend the list of parameters with time-related pupil parameters, such as latencies and time constants, during dilation, constriction, and even redilation (pupil recovery/escape).

The aim of this study was to describe (i) the design and development of a haploscope-based binocular pupillometer system, (ii) the description of a double exponential fit function in the parametrisation of the PLR, (iii) and the first-line evaluation of the system's feasibility and applicability in a set of healthy controls and patients diagnosed with Relative Afferent Pupillary defect (RAPD). Following this, we present two sample applications of the system as a proof of concept: (i) quantification of pupil dynamics during redilation responses (ii) the establishment of an asymmetry limit to predict the presence of RAPD. Even though the previous literature has reported the effect of

7

factors such as iris colour on pupil dynamics, the reported findings are contradictory (Winn et al., 1994; Vaswani et al., 2002; Dain et al., 2004; Bergamin et al., 1998; Bradley et al., 2010). Our supplementary aim focused on evaluating the effect of iris colour on PLR characteristics. This comparison was expected to help us in deciding whether a difference in pupil parameters should be anticipated when our customised system is used across ethnicities.

MATERIALS AND METHODS

Study participants

Study participants included a total of 30 healthy controls and five patients diagnosed with RAPD. The group of healthy controls constituted volunteers aged between 20 to 29 years, recruited at two institutes: 1) the Erasmus Medical Centre, Rotterdam, The Netherlands, (source of participants with light coloured irides, n = 15) and 2) at a tertiary eye care centre, Sankara Nethralaya, Chennai, India, (source of participants with dark coloured irides, n = 15). Healthy control group was defined as those with Best Corrected Visual Acuity (BCVA) of 20/20 for distance and N6 for near, ≤ 3.00 DS and < − 2.00 DCyl of spherical and cylindrical ametropia respectively, normal pupil morphology and reactivity with no RAPD, and a healthy anterior and posterior segment. A detailed clinical history was obtained to rule out any systemic conditions/surgery/trauma or intake of pharmacological elements that would have a potential effect on pupil reactivity. The latter group had 5 patients diagnosed with neuro-ophthalmic diseases and an associated RAPD, recruited from the neuro-ophthalmology Department, Sankara Nethralaya, Chennai, India.

Written informed consent was obtained from all the participants before enrolment. The study adhered to the Declaration of Helsinki for research involving human participants and the clinical procedures were reviewed and approved by the Medical Ethics Committee (MEC) of Erasmus University Medical Centre (EMC), Rotterdam, The Netherlands, and the Institutional Review Board (IRB) of Vision Research Foundation (VRF), Chennai, India.

After the preliminary clinical history, all the healthy controls underwent pupillary evaluation using SFT by an experienced examiner performed to assess the direct and consensual PLR. A flashlight was shone onto the right eye followed by the left eye pupils from the inferotemporal quadrant from an approximate distance of 10 cm. Extent and rapidness of pupil constriction and dilation were evaluated and this was used as a screening process to rule out the presence of RAPD. Meanwhile, for the five neuro-ophthalmic patients, a comprehensive ophthalmic evaluation was performed (according to the routine clinical protocol), followed by SFT and quantification of the severity of RAPD using a Neutral Density Filter (NDF). Next, an external photograph of the iris was taken by a single examiner using a 12-megapixel camera equipped with the six-element lens under standardised illumination conditions and camera settings. If necessary, the eyelids were lifted to eliminate shadowing. A previously published iris colour classification system was used as a reference set to grade iris pigmentation (Bergamin et al., 1998). The photographs were subjectively ranked into five categories from grade 1 to grade 5 (blue, blue-green, green–brown, light brown, and dark brown) independently by two observers with no colour deficiencies (assessed using Ishihara pseudo-isochromatic plates). The final iris colour grade was determined by calculating the median scores of these two observers.

The haploscope-based pupillometer

All the study participants underwent pupillometry using the customised test protocols incorporated in the haploscope. We had two identical setups with respect to their geometry, optical aspects, hardware, and software, one available in each lab (Figure 7.1A). The system is comprised of an image acquisition module integrated with a customised test paradigm. The image capture unit consisted of an infrared-based eye tracker (Tobii Pro X3-120: sampling rate of 120 Hertz (Hz) for gaze and 40 Hz for pupil size) and two Light Emitting Diode (LED) displays for stimulus presentation. Two identical dichroic/cold mirrors (dimension: 101.0 mm × 127.0 mm) inclined at an angle of 45° were placed in front of the right and the left eye, which had a dual purpose. Firstly, the multi-layered dielectric coating of these mirrors reflected 90% of the visible light while transmitting 80% of infrared radiations

thereby ideally reducing the undesirable heat emitted by the IR based camera. Secondly, they acted as a beam splitter to dissociate the eyes to create a haploscopic stimulus presentation (Schematic illustration in Figure 7.1B).
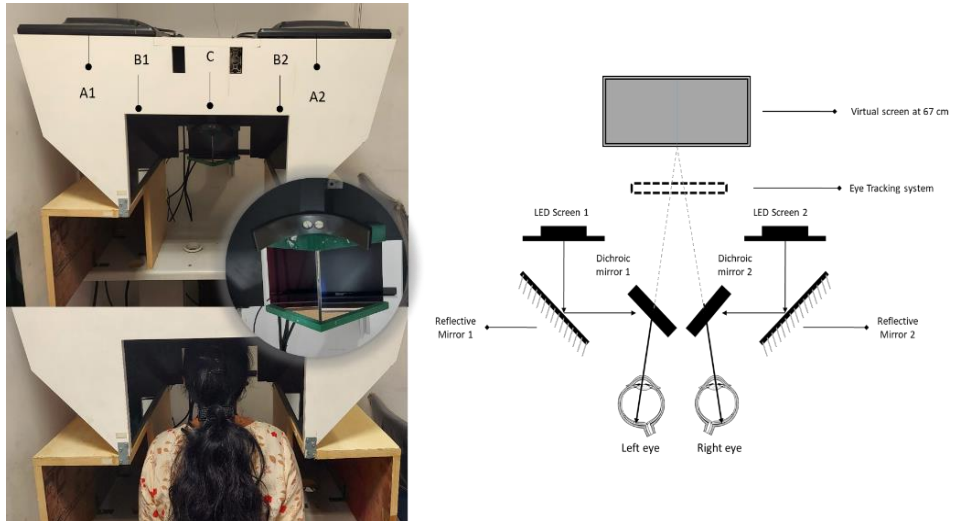

Figure 7.1. (**A**) Top panel: Image of the lab-based prototype of the binocular pupillometer. A1 and A2—LED screens 1 and 2, B1 and B2—the reflective mirrors, C—the cold mirrors inclined at an angle of 45°. Middle panel: The zoomed in picture of the cold mirror and headrest. Bottom panel: Healthy volunteer with the head positioned at the device's headrest. (**B**) The Schematic illustration of Haploscope-based pupillometer system that shows the image acquisition module with an infrared-based eye tracker and two Light Emitting Diode display monitors with two identical dichroic/cold mirrors in the optical path.

The Psychtoolbox-3 package was used to create stimulation and to provide a mechanism for accurate timestamps and synchronous changes in stimuli on screens. Synchronisation was carried out both between the right and left screens and with timestamps, provided using the Tobii Pro X3-120 device. An auxiliary PC unit with an inbuilt video card (NVIDIA—ION graphics processor) was used to control the test paradigm and store the acquired data. The high-definition video card supported a superior quality visual display, rapid graphics processing, and image rasterisation. The participant's head was positioned at the device's headrest where they had to remain in a stable viewing position and orientation with respect to the eye tracker. Each participant

was instructed to rest his/her forehead on the mount and to look into the virtual screens through the two dichroic/cold mirrors.

Customised pupillometry test paradigm

The testing took place in a dark room and the light from the LED display was the only source of illumination. Each measurement began with an inbuilt five-point calibration procedure. After a successful calibration, each participant was instructed to look straight by fixating steadily at a Maltese cross target that was presented at the middle of an elliptical-shaped patch of light that appeared at the centre of the screen. Next, a computerised pupil stimulation protocol was introduced (Figure 7.2: Top panel). This customised protocol was divided into three sections, denoted as stimulation phases namely, (a) Simultaneous stimulation phase (Sim OU), (b) Unilateral stimulation phase (Uni OD and Uni OS), and (c) Alternating stimulation phase (Alt OD and Alt OS). During the first phase (Sim OU), both the eyes received light stimulation simultaneously, whereas, in the second phase (Uni OD and Uni OS), only one eye received light stimulation at a time. During the third stimulation phase, both the eyes received light stimulation in alternative turns. Light stimulation was made possible by projecting a white screen (RGB: 255:255:255), referred to as the white panel (illuminance at the eye level ranging from 109–115 Lux), and the removal of the light stimulation was made possible by projecting a black screen (RGB: 0–0–0), referred to as the black panel (illuminance at the eye level ranging from 0–2 Lux).

So in brief, each of the stimulation phases consisted of four stimulation panels either white or black for light stimulation and withdrawal of light stimulation respectively. Each stimulation panel lasted for 2.7 s. In between each of the phases, a resting panel of 2.7 s (RGB: 169:169:169) was shown to minimise the effect of one cycle on the other. During the stimulation phases, participants were instructed to refrain from blinking, but during the resting panel (grey), they were allowed to blink if necessary. The entire stimulation protocol consisted of 19 stimulation panels that lasted for a total duration of 51 s. Participants underwent two measurement series for PLR within an interval

7

of ~ 5–10 min in which the initial one was considered as a baseline measurement (test 1) to evaluate the inter-test repeatability.
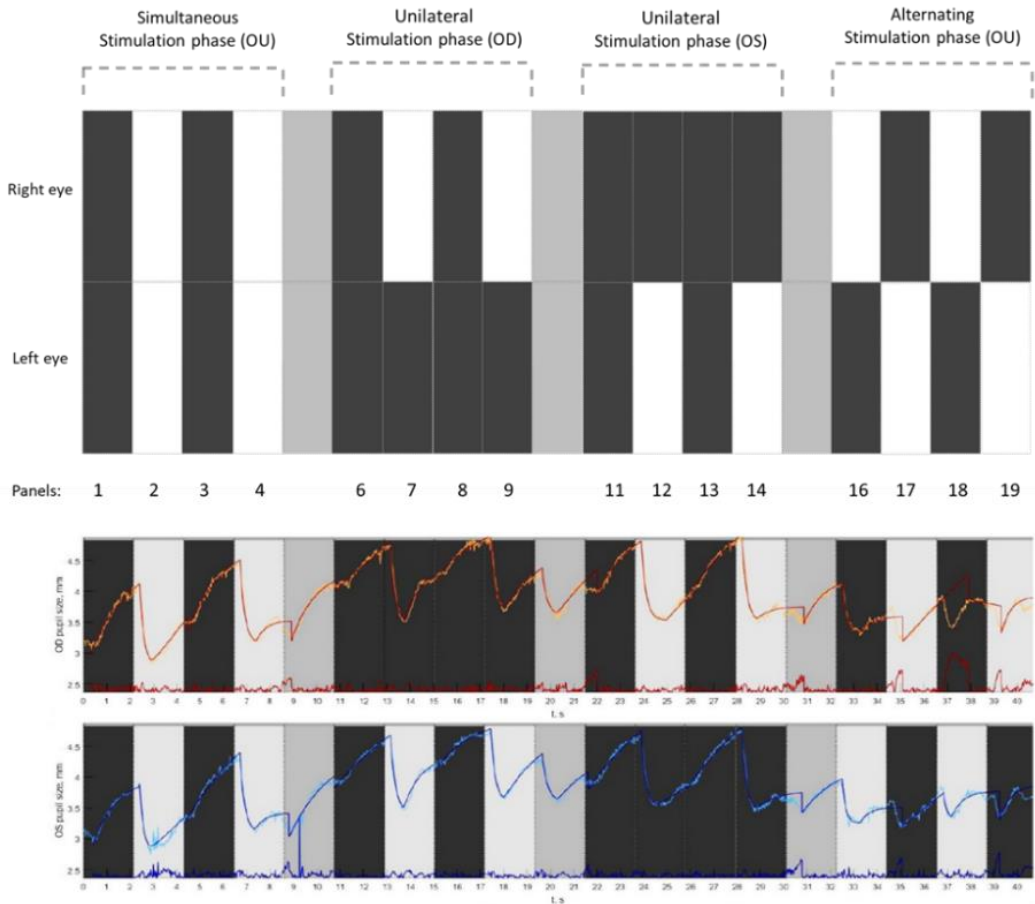

Figure 7.2: Top panel: A graphical illustration of the pupil stimulation protocol consisting of three stimulation phases. Simultaneous stimulation phase where both the eyes were stimulated; the unilateral stimulation phase where only one eye was stimulated followed by the other; and an alternating stimulation phase where both the eyes got alternatively stimulated. Bottom panel: Example of a pupillogram generated from the recordings of a healthy control displaying the raw pupil traces from the right eye (in orange) and left eye (in blue). The superimposed red and blue traces are the best fit lines based on the double exponential fitting procedure along with the residual errors (red and blue traces displayed at the bottom).

Data processing and response analysis

The data that was collected using the eye-tracker consisted of gaze positions and PD traces. The data on pupil dynamics were imported into a custom-made MATLAB program and processed to yield a pupillogram. It consisted of raw PLR response curves for each eye with PD plotted (y-axis) as a function of time in seconds (Figure 7.2: Bottom panel). The raw traces were superimposed with the best fit lines obtained through the exponential fitting procedures (Figure 6.2: Bottom panel). The pupillogram also displayed the amount of residual error of each exponential fit, by calculating the Root Mean Square Error RMSE) values. This exponential fit function was used to analyse the time course of the pupil trajectory and the quantify PLR parameters from the double exponential equations (Appendix 7.1).

From the Eq. 1 to 5 (Appendix 7.1) we calculated 'dpup' the PD varying from minimum (min) to maximum (max) diameter, 'Δd' the change in diameter during a stimulation phase (the direction of change was taken into account), 't' the duration of a response, 'Δt' the latency for the PD change and 'T' the time constant (time for the pupil to reach ~ 60% of its end value) related to the speed of PD change (Figure 7.3). Finally, the PRS coefficient (Appendix 7.1—Eq. 6) was calculated to characterise the inter-pupillary symmetry during constriction on the basis of constriction latency, speed, and amplitude. Here, the normative limits (mean ± SD) of PRS were calculated for each of the constriction panels from the group of healthy controls and was compared with that of five patients with clinically diagnosed RAPD.

Statistical analysis

Descriptive analysis of the demographic data was followed by the inspection of those parts of the obtained signal that resulted in a fit error > 0.2. A descriptive analysis of the error scores calculated for the exponentially fitted function revealed a definite cluster of 91.6% of the residual errors within 0.2 × 0.2 interval for the dilation and constriction panels ensuring an optimal quality of the data. Kappa-statistics was used for assessing the inter-observer agreement for iris colour grading. Participants with iris colour grades 1 to 3

7

were labelled as 'light iris group' whereas grades 4 and 5 were labelled as 'dark iris group'. Pearson's correlation was done for the inter-ocular comparison of the PLR parameters during dilation and for constriction. Intraclass Correlation Coefficient (ICC) was used as an index for repeatability that reflected both the degree of correlation and agreement between baseline and repeated measurements.
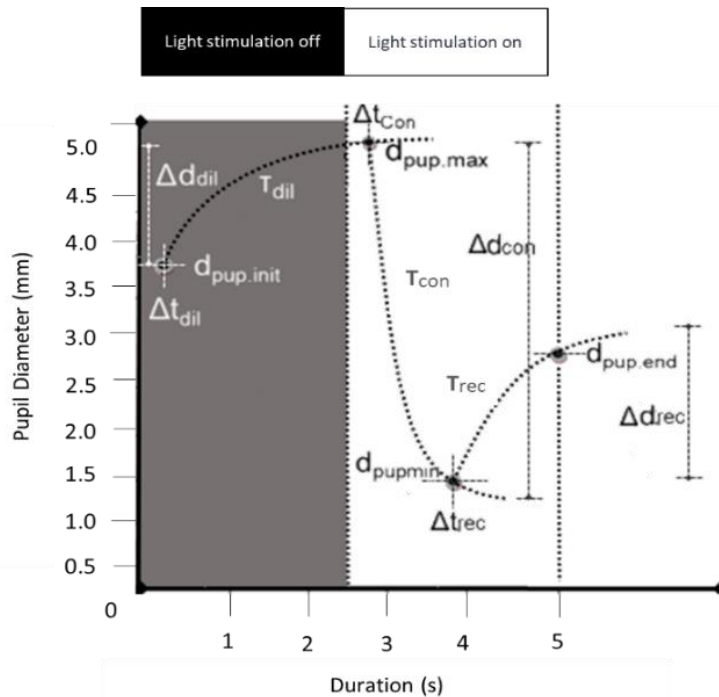

Figure 7.3: Shows the schematic diagram of a PLR curve and illustrates each of the measured parameters. PLR parameters derived were: $d_{pup.init (c)}$ - The initial pupil diameter in a panel , $d_{pup.max (c)}$ - The maximum pupil diameter in a dilation panel, $d_{pup.min (c)}$ - The minimum pupil diameter in a constriction panel, $d_{pup.end (c)}$ - The pupil diameter at the end of a redilation period in a constriction panel, Δd (amplitude i.e. absolute values of changes) -difference between $d_{pup.max}$ or $d_{pup.min}$ and the $d_{pup.init.,}$ Δt_{dil} - The time delay/latency for the initiation of dilation after light stimulation is off, Δt_{con} - The time delay/latency for the initiation of constriction after light stimulation is on, Δt_{rec} - The time delay/latency for the initiation of pupil redilation after the maximum constriction. T_{dil}, T_{con}, T_{rec} - the time constants (tau) representing the elapsed time required for the pupil to reach ~60% of its end value during dilation, constriction, and redilation.

An independent t-test was carried out to compare the diameter-related and time-related pupil dilation and constriction parameters between light and dark iris groups. One-way ANOVA was carried out to compare the diameter and time-related pupil constriction parameters to evaluate the constriction and redilation characteristics during bilateral and unilateral light stimulation and the posthoc evaluation was carried out by applying the conservative p-value. An independent t-test was carried out to compare the temporal characteristics of redilation with dilation responses. For each healthy control, the PRS coefficient was calculated for OD and OS based on Eq. 6 (Appendix 7.1) and the inter-pupillary difference was obtained (OD–OS) from which the mean PRS and SD were calculated. The inter-pupillary difference in PRS coefficient was calculated for five RAPD patients and descriptively compared with the expected normal limits.

RESULTS

A total of 29 healthy controls with a mean age of 24 years (SD: 3) were enrolled which consisted of 21 females (72%) and 8 males (28%). The iris colour group classification comprised of 15 (52%) light iris (blue-green and green–brown) and 14 (48%) dark iris participants (Light brown and dark brown). One participant from the dark iris group was excluded due to a pupillogram with a residual fit error > 0.2. The inter-observer agreement for iris colour grading was excellent with a kappa coefficient of 1.0.

PLR parameters during dilation response as a function of Iris colour and inter-ocular comparison

Two panels in the simultaneous stimulation phase i.e. Panel 1 and 3 (bilateral stimulation with black panels) were considered for comparing the PLR parameters during dilation. Table 7.1 summarises the five different dilation parameters for the right and left eye and their statistical comparison between light and dark iris groups. A strong positive correlation (r = 0.7 to 0.9, p < 0.05, Pearson's correlation) of all the dilation parameters between the right eye and left eye suggested no inter-ocular asymmetry. ICC coefficient values ranged from 0.81 to 0.92 for the dilation parameters, which showed a good

agreement between baseline and repeated measurements with respect to dilation responses.

Table 7.1. Displays the statistical comparison of dilation parameters obtained from stimulation panel 1 and panel 3 between light and dark iris participants. Diameter-related pupil parameters expressed in millimetres (mm). Time-related pupil parameters expressed in milliseconds (ms).

Mean Dilation parameters (SD)		Right eye			Left eye		
		Light Iris (n = 15)	Dark Iris (n = 14)	p values	Light Iris (n = 15)	Dark Iris (n = 14)	p values
Panel 1	$d_{pup.init}$ (mm)	3.5 (0.7)	3.2 (0.6)	0.25	3.4 (0.6)	3.3 (0.5)	0.57
	$d_{pup.max}$ (mm)	4.7 (0.8)	4.3 (0.4)	0.07	4.6 (0.7)	4.3 (0.4)	0.11
	Δd (mm)	1.2 (0.3)	1.2 (0.3)	0.57	1.2 (0.3)	1.1 (0.2)	0.65
	Δt (ms)	310 (170)	290 (160)	0.41	320 (165)	280 (160)	0.30
	T(ms)	1420 (495)	1285 (400)	0.60	1425 (420)	1200 (450)	0.80
Panel 3	$d_{pup.init}$ (mm)	3.2 (0.5)	2.7 (0.3)	**<0.01**	3.2 (0.5)	2.7 (0.4)	**<0.01**
	$d_{pup.max}$ (mm)	4.5 (0.7)	4.2 (0.3)	0.17	4.5 (0.8)	4.2 (0.4)	0.21
	Δd (mm)	1.3 (0.3)	1.5 (0.3)	0.08	1.4 (0.4)	1.6 (0.3)	0.15
	Δt (ms)	285 (130)	310 (110)	0.67	275 (140)	310 (100)	0.69
	T(ms)	1600 (445)	1260 (450)	0.08	1580 (375)	1320 (440)	0.14

*p-values - Independent t-test

PLR parameters during constriction response as a function of Iris colour and inter-ocular comparison

For panel 3, a significantly (p < 0.01) higher magnitude of Initial PD (dpup.ini (dil)) was found in the light iris group when compared to the dark iris one. Other dilation parameters including Time constant and latency were closely comparable irrespective of the stimulation panels (Panel 1 and 3). Panel 2 and 4 (bilateral stimulation with white panels) were used to compare the PLR parameters during constriction. Table 7.2 summarizes the six different constriction parameters for the right and left eye and their statistical comparison

between light and dark iris groups. A strong positive correlation (r = 0.7 to 0.9, p < 0.05, Pearson's correlation) of all the dilation parameters between the right eye and left eye suggested no inter-ocular asymmetry. The calculated ICC coefficient values were found to be ranging from 0.86 to 0.96 for the constriction parameters, which showed a good agreement between baseline and repeated measurements with respect to constriction responses. For both the panels, a significantly (p < 0.01) higher magnitude of minimum PD (dpup.min (con)) was found in the light iris group when compared to the dark iris group. Other constriction parameters including latency, duration, and time constant were statistically comparable irrespective of the stimulation panels (Panel 2 and 4).

Table 7.2: Displays the statistical comparison of constriction parameters obtained from stimulation panel 2 and panel 4 between light and dark iris participants

Mean Constriction parameters (SD)		Right eye			Left eye		
		Light Iris (n = 15)	Dark Iris (n = 14)	p-value	Light Iris (n = 15)	Dark Iris (n = 14)	p-value
Panel 2	$d_{pup.init}$ (mm)	4.7 (0.7)	4.3 (0.4)	0.07	4.8 (0.8)	4.3 (0.4)	0.12
	$d_{pup.min}$ (mm)	2.7 (0.4)	2.4 (0.3)	**<0.01**	2.8 (0.4)	2.4 (0.2)	**<0.01**
	Δd (mm)	1.9 (0.4)	1.8 (0.3)	0.60	1.8 (0.3)	1.9 (0.4)	0.46
	t (ms)	949 (274)	971 (237)	0.25	934 (239)	966 (271)	0.10
	Δt (ms)	255 (30)	260 (30)	0.47	250 (50)	240 (40)	0.68
	T (ms)	250 (40)	260 (50)	0.67	250 (50)	260 (60)	0.23
Panel 4	$d_{pup.init}$ (mm)	4.7 (0.8)	4.3 (0.3)	0.08	4.7 (0.9)	4.3 (0.4)	0.10
	$d_{pup.min}$ (mm)	2.9 (0.4)	2.3 (0.3)	**<0.01**	2.7 (0.4)	2.3 (0.3)	**<0.01**
	Δd (mm)	1.9 (0.4)	2.1 (0.3)	0.27	1.9 (0.5)	2.0 (0.4)	0.61
	t (ms)	795 (197)	784 (203)	0.39	788 (252)	814 (258)	0.34
	Δt (ms)	225 (40)	250 (30)	0.16	235 (50)	250 (35)	0.62
	T (ms)	250 (40)	260 (35)	0.67	245 (45)	260 (35)	0.21

*p-values - Independent t-test

7

Temporal characteristics of pupil dynamics: Comparison between dilation and constriction responses

Two dilation and two constriction panels in the simultaneous stimulation phase were used for comparing the time-related pupil parameters during dilation and constriction.

Time constant values: The mean time constant value for dilation was 1260 (SD: 420) ms whereas it was 250 (SD: 50) ms for constriction. Figure 7.4 illustrates an evidently higher Time constant values for dilation responses when compared to that of constriction which was statistically significant (One-way ANOVA, $p < 0.001$). The posthoc (Bonferroni) tests showed a significant difference between the two dilation panels in comparison with the two constriction panels.
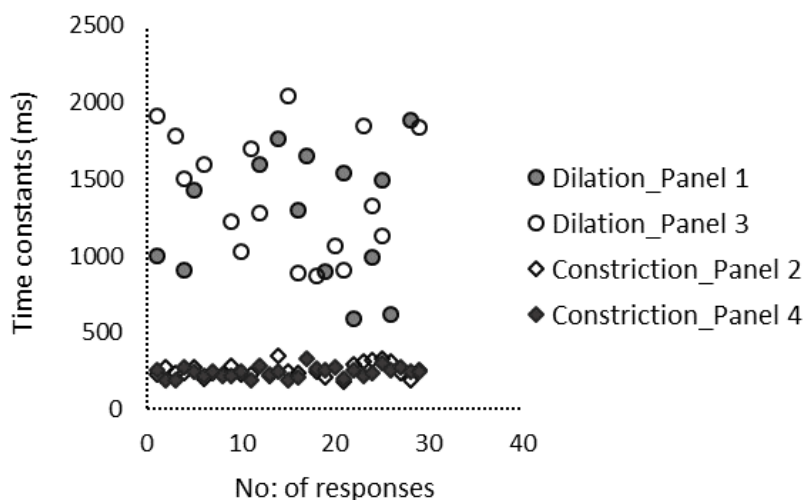
Figure 7.4: The scatter plot generated using number of participants and Time constant values in the X and Y-axes respectively displaying higher Time constants for dilation in comparison with the constriction panels.

Latency values: Figure 7.5 illustrates markedly delayed latencies during the dilation when compared to the constriction responses which was statistically

significant (Mean difference: 35 ms, Independent t-test, p = 0.01) irrespective of their iris colour.

Constriction characteristics: Comparison between bilateral and unilateral photic stimulation.

This analysis focused on constriction panels in the simultaneous stimulation phase (Sim OU) and unilateral stimulation phase (Uni OD and Uni OS).

Diameter-related parameters: The comparison of minimum PD (dpup.min (con)) between the stimulation panels was found to be statistically significantly higher (Mean difference: – 0.3 mm, Independent t-test, p-value: 0.02) during simultaneous stimulation phase in contrast to the unilateral stimulation phase. Rest of the diameter related constriction parameters such as initial PD ($d_{pup.init}$ (con)) and PD amplitude (Δd (con)) were statistically not significantly different.
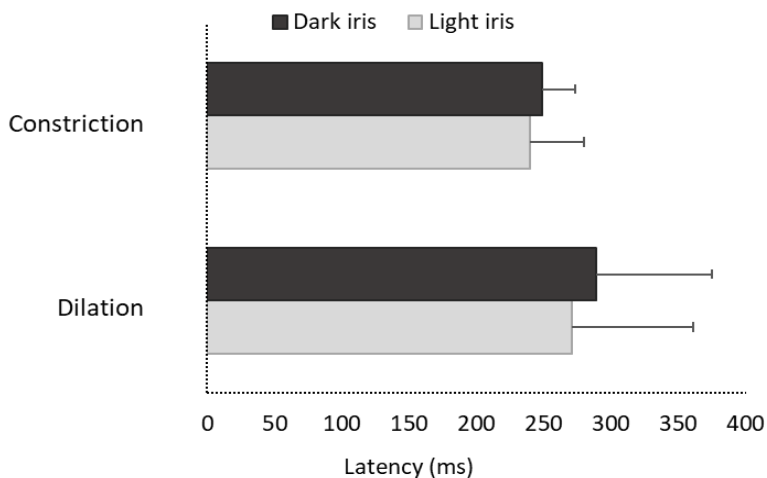
Figure 7.5: A cluster bar graph illustrating the delayed latency (milliseconds) during dilation in comparison with that of constriction among dark and light iris groups. Error bars represent the Standard Deviation (SD).

Time-related parameters: No statistically significant difference was found between the six panels (Supplementary Figure 7.1) with respect to the Time

constants (One-way ANOVA, p = 0.41) as well as the latencies (One-way ANOVA p = 0.62).

Redilation characteristics: Comparison with dilation and between bilateral and unilateral photic stimulation

A statistically significant difference (Independent t-test, p-value: < 0.001) in Time constant values was found between redilation (mean ± SD: 620 ± 320 ms) and dilation responses (mean ± SD: 1360 ± 455 ms), revealing a faster redilation compared to the usual dilation process (Figure 7.6). The mean Time constants between the six panels ranged from 630 to 675 ms (mean ± SD: 650 ± 335 ms) where there was no statistically significant difference between the panels (One-way ANOVA p = 0.73), hence revealing no difference in redilation behavior during bilateral or unilateral photic stimulation.
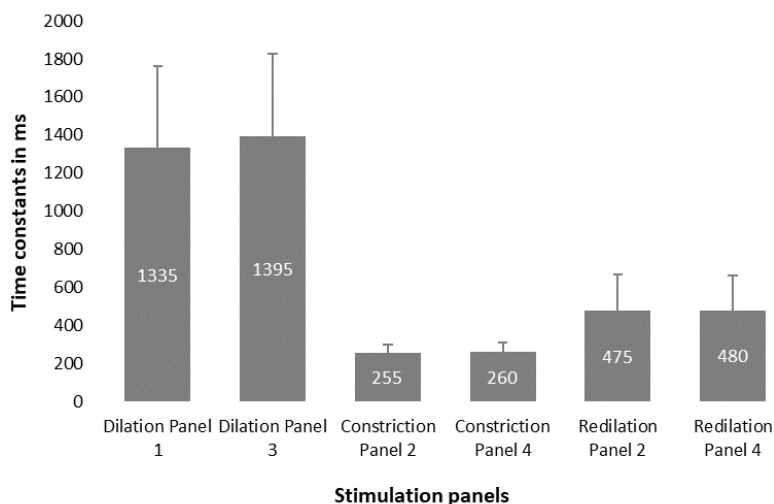
Figure 7.6: Bar graphs displaying the comparison of the Time constant values of constriction, dilation and redilation between the six stimulation panels. The error bars represent the Standard Deviation (SD).

Pupil Response Symmetry (PRS) coefficient

The diameter and time-related constriction parameters obtained from all the six light stimulation panels were used to calculate the PRS coefficients for

both healthy controls and patients with RAPD. The descriptive summary of those parameters are enumerated in Table 7.3. The mean (SD) inter-pupillary difference in PRS coefficient values for the healthy controls (irrespective of their iris colour grades) obtained from the six constriction panels that ranged from -0.20 to +1.07 (SD ~ ±4.0). Figure 7.6 illustrates distinctly higher inter-pupillary difference in PRS coefficients for the three RAPD patients across all the stimulation panels that are noticeably outside the expected normative limits. The laterality of the afferent defect was evident from the direction of the PRS difference, for example, Patient 1 was clinically diagnosed with grade 3 RAPD in the left eye whereas patient 2 and 3 were presented with grade 3 and 2 RAPD respectively in right eye (Figure 7.7).

Table 7.3: Displays the descriptive summary of the constriction parameters obtained for healthy controls and RAPD patients from all the six light stimulation panels

Mean Constriction parameters		Panel 2	Panel 4	Panel 7	Panel 9	Panel 12	Panel 14
Healthy Controls (n = 29)	$d_{pup.init}$ (mm)	4.6 (0.7)	4.4 (0.3)	4.5 (0.4)	4.6 (0.4)	4.3 (0.4)	4.5 (0.3)
	$d_{pup.min}$ (mm)	2.7 (0.4)	2.6 (0.3)	2.7 (0.3)	2.8 (0.4)	2.4 (0.3)	2.6 (0.3)
	Δd (mm)	1.9 (0.4)	1.8 (0.3)	1.8 (0.3)	1.8 (0.3)	1.9 (0.4)	1.9 (0.4)
	Δt (ms)	255 (30)	260 (30)	251 (35)	250 (50)	240 (40)	245 (35)
	T(ms)	250 (40)	260 (50)	250 (40)	250 (50)	260 (60)	255 (40)
	RMSE	0.04 (0.1)	0.05 (0.1)	0.08 (0.1)	0.10 (0.1)	0.12 (0.1)	0.07 (0.1)
RAPD patients (n = 5)	$d_{pup.init}$ (mm)	4.4 (0.3)	4.4 (0.3)	4.4 (0.3)	4.2 (0.4)	4.2 (0.4)	4.1 (0.4)
	$d_{pup.min}$ (mm)	2.9 (0.3)	2.8 (0.4)	3.5 (0.3)	3.3 (0.4)	3.2 (0.3)	3.1 (0.4)
	Δd (mm)	1.5 (0.3)	1.6 (0.4)	0.9 (0.3)	0.9 (0.4)	1.0 (0.4)	1.0 (0.3)
	Δt (ms)	240 (40)	230 (40)	230 (30)	235 (30)	240 (45)	235 (30)
	T (ms)	240 (35)	245 (35)	220 (30)	225 (35)	235 (35)	230 (35)
	RMSE	0.04 (0.1)	0.04 (0.0)	0.11 (0.1)	0.07 (0.1)	0.06 (0.1)	0.07 (0.1)

DISCUSSION

The current study described the design and development of a haploscope-based binocular pupillometer. The proposed system incorporated a stimulus presentation paradigm that replicated the SFT. The double exponential fit function aided in the

comprehensive parametrisation of the PLR and good repeatability of diameter and time-related values were found. The suggested method was found to be feasible and applicable in describing the pupillary dynamics among healthy controls as well as patients diagnosed with RAPD.
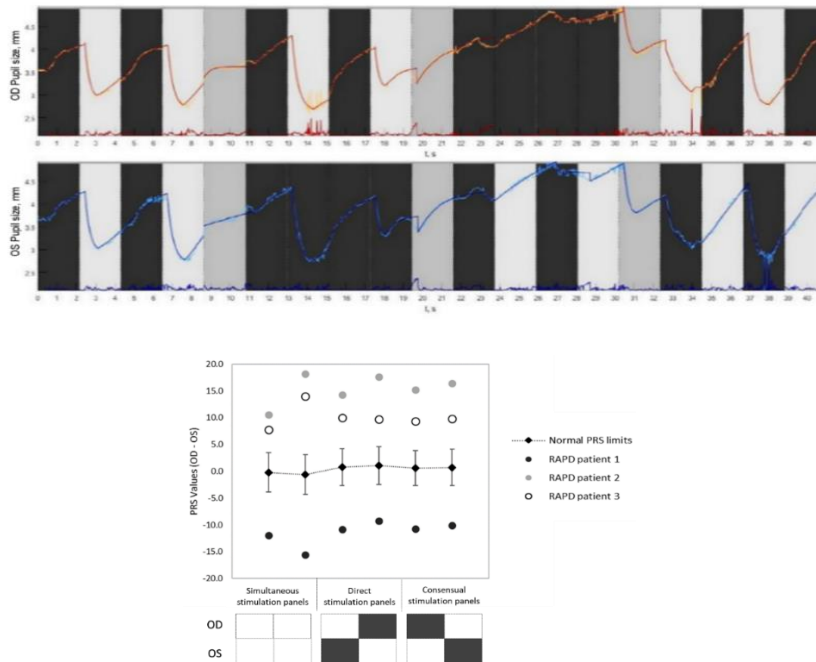

Figure 7.7: The top panel: The generated pupil traces from a patient with clinically detected RAPD. Pupillogram showed normal pupil traces during the simultaneous stimulation phase (Sim OU) and unilateral stimulation phase OD (Uni OD), but during the unilateral stimulation phase OD showed no constriction responses from the pupil on light stimulation which was persistent during the Alternating stimulation phase (Alt OD and Alt OS) as well. The bottom panel: The scatter plot generated using the mean inter-pupillary difference in PRS coefficient values for the healthy controls (Error bar represents the SD) and the five patients with clinically diagnosed RAPD. The X axis represents the stimulation panels whereas the Y axis displays the inter-pupillary difference in PRS.

The evaluation of the effect of iris colour on pupillary dynamics showed that the initial PD (dilation phase) and minimum PD (constriction phase) depended on iris colour whereas no statistically significant differences were

found with respect to other parameters. The results showed that the constriction response had a faster course than the dilation and also demonstrated the temporal dynamics of the redilation phase. In SFT, the pupil reactivity is described with terminologies that relate to the laterality (unilateral/bilateral), pupil size (miotic/mid-dilated/dilated), and reactivity (brisk/sluggish/non-reactive) that is often applied in the absence of any standardised clinical protocol or consistent definition (McDougal et al., 2015; Mathôt, 2018; Bremner, 2004; Woodhouse, et al., 1994; Winn et al., 1994; Levatin, 1959; Litvan et al., 2000). Similar to other automated pupillometry devices, our binocular system, generated the quantifiable outcome measures for PLR under well-controlled lighting conditions including the amount, angulation/direction, and duration of photic stimulation. Hence, this system showed good repeatability of the measurements, resolved the issue of variability resulting from the examiner-dependent errors, and reduced the false-negative responses.

Pupil dynamics during dilation, constriction, and redilation responses

The current study showed the comparative analysis of time-related pupil parameters during dilation, constriction, and redilation where the dilation phase had higher time constants (Figure 7.4 & 7.6) and latency values (Figure 7.5) when compared to constriction phases. That means constriction due to light onset happened significantly faster i.e. approximately 5 times (5.3x times) than the dilation due to light offset. These findings are in par with the literature concerning the description of the physiological trait of pupil constriction as an involuntary reflex mechanism to safeguard retinal cells from phototoxic damage whereas the less well understood neural pathway of dilation in this setting is a passive process when adapting to low levels of illumination (McDougal et al., 2015; Mathôt, 2018).

The pupil tends to constrict muscularly and briskly until it reaches its minimum size, and remains in the fully constricted state for a while and slowly dilates which is termed as the redilation here. The time constant for this redilation response was found to be approximately two-times (1.9x times)

7

higher than constriction but lower than dilation, a rapid pupil recovery process after reaching the maximum constriction plateau of sphincter muscle whereas the dilation process is rather a passive visual adaptation process to dark/low levels of illumination. The nature of these temporal characteristics in accordance with the reported pupil physiology acts as a considerable evidence for the rightness of the analysis method we have adopted. The precise quantification of the time courses of pupil response would aid in an improved description of the brisk/sluggish/ill-sustained pupillary reaction in a quantifiable manner unlike the qualitative documentation during the routine clinical practice. The temporal parameters of dilation quantified in this study is probably unique to this experimental set up. The values can be anticipated to be altered if conditions of increased intellectual activity, levels of arousal, wakefulness, and the fight-or-flight response termed as the psychosensory pupil response are applied (McDougal et al., 2015; Mathôt, 2018; Bremner, 2004; Woodhouse, et al., 1994; Winn et al., 1994; Levatin, 1959; Litvan et al., 2000).

PLR parameters as a function of iris colour

In addition to the level of retinal illumination, accommodative status, and various emotional conditions, iris colour is also reported to have an influence on PD (Winn et al., 1994; Vaswani et al., 2002; Dain et al., 2004; Bergamin et al., 1998; Bradley et al., 2010; Kleiner et al., 2007; Said et al., 1972). The difference in iris colour among healthy individuals occurs as a result of variable quantities of melanin pigment granules in the superficial stroma of the iris. A previous study quantified PD during a steady light adaptation using an objective infrared-based continuous recording technique and investigated the effect of various factors on pupil size. They reported a dependency of PD on chronologic age whereas it was independent of the gender, refractive error, or iris colour among healthy humans (Winn et al.,1994).

A previous study that evaluated the effect of iris colour on the Dark-Adapted Pupil Diameter (DAPD), showed no difference in PD between light and dark coloured iris groups and concluded that iris colour does not seem to have a significant role in determining pupil size (Bradley et al., 2010; Said et al., 1972).

In contrast, a few other studies found a significant difference in PD between different iris colour grades under various lighting conditions (Vaswani et al., 2002; Dain et al., 2004; Schintzler et al., 2000). These contradictory findings in the literature were our basis for aiming at an evaluation of the quantified PLR parameters between the dark and light iris groups. We found that other than the initial PD during dilation (Table 7.1) and minimum PD during constriction (Table 7.2), the rest of the parameters were comparable between the two iris groups. This confirmed that the amplitudes and time-related parameters (constriction and dilation) can be clinically used and relied upon irrespective of the iris colour grades. Since the difference in the diameter-related parameters can possibly be attributed to the variation in the density of melanin pigments/number or sensitivity of autonomic receptors (Dain et al., 2004), a significant change in the current findings is not expected, even if we apply a baseline correction for standardisation. Bergamin et al. also demonstrated the dependency of contraction amplitude and velocity on iris colour and suggested that iris colour to be considered as a factor (Bergamin et al., 1998) while evaluating pupil movements which was not confirmed in our study.

Binocular pupillometer system - stimulation and image processing module

Literature has described various binocular pupilometers with unique stimulus projection and image capturing modules to estimate the PLR characteristics by quantifying reliable pupil parameters and evaluating their mutual interactions (Nowak et al., 2014; Szczepanowska et al., 2004; Bos et al., 1988; Tekin et al., 2018; Bremner et al., 2012; Shwe-Tin et al., 2012). Meanwhile, certain other studies further explored the possibility of such pupillometer systems (commercially available or lab-based prototypes) to detect and quantify Relative Afferent Pupillary Defects (RAPDs) that showed promising results with a high positive correlation with conventional methods i.e. SFT and NDF (Shwe-Tin et al., 2012; Cohen et al., 2015; Takizawa et al., 2018; Pillai et al., 2019). In contrast, in this study, we adopted a haploscopic principle (Naber et al., 02011; Brascamp et al., 2017; Ramey et al., 2008) to design a pupillometer system that can offer a more extensive evaluation of pupil dynamics during bilateral, unilateral, and alternating light and dark stimulation

7

thereby acquiring direct and consensual reflexes concurrently. The captured pupil signals were further processed using a custom-written algorithm to generate PLR curves.

Since the changes in pupil size were non-linear (Figure 7.3) the PLR traces were fitted with double-exponential growth or decay curves for dilation and constriction respectively, aiding in the quantification of a substantial list of pupil parameters including latency and time constants. Double exponential equations were chosen as it is a promising empirical method to characterise the temporal aspects of the spontaneous fluctuations of biological signals (Sarracino et al., 2020). In the present study, the use of exponential function adds value for the accurate calculation of the PRS coefficients. Generally, the functional evaluation using electrophysiological methods emphasise the speed of afferent conduction, so likewise even in pupillometry techniques, the pupil latency and time constants describe the abstract summation of afferent and efferent times of the pupillary pathway until the pupil initiates a response (Bos, 1988; Begramin et al., 2003).

Literature has put forward evidence that pupil latency is delayed in patients with afferent diseases, such as demyelinating disease, optic atrophy, and disorders such as diabetes that affect the efferent autonomic innervation to the iris. Latency, when compared with diameter-related parameters, is reported to be less variable and influenced by the muscular properties of the iris that are known to restrain the drive of the pupil that occurs after the onset of contraction. The exponential fitting procedures aided us in reliable quantification of these temporal aspects of the pupillary dynamics (latencies and time constants) hereby promising objective indices for disease diagnosis and progression assessment (Bos, 1988; Sarracino et al., 2020; Bergamin, 2003).

Clinical applicability of haploscope based binocular pupillometer

We observed that the method demands no expert skill from the examiner because the system is relatively simple to use and the procedure was reported to be convenient by the participants due to its quick and non-invasive nature. That means the features of the prototype and the procedure is well

placed for the inclusion of the system in screening assessments and could complement other clinical evaluations to identify individuals at risk who warrant further investigations. However, this prototype requires further considerations and research to enable translation into clinical/community settings. For instance, neurological/neuro-ophthalmic conditions that influence the integration of parasympathetic and sympathetic stimulation and inhibition may affect the dynamics of the PLR. Among various such pupil abnormalities, RAPD is a key clinical sign detected using SFT, which displays an unequal inter-pupillary reaction corresponding to underlying asymmetric damage in the afferent pathways. Here is the relevance of introducing the PRS coefficient considering not only the diameter-related features of the pupil (amplitude) but also the constriction latency (Figure 7.5) and time constant (Figure 7.4). The descriptive comparison of the diameter and time-related parameters obtained during the constriction panels (Table 7.3) for the healthy controls and RAPD patients showed markedly smaller pupillary amplitudes (change in PD) among the patients.

Though not statistically significant, the Tcon values (Time constants in ms) were numerically faster for the RAPD patients when compared to the controls. This might be linked to the faster but weak initial constriction response followed by a greater redilation that is clinically observed during SFT while examining grade 1 RAPD patients. In the present study, in addition to visual observation, we have quantified this characteristic behaviour in grade 1 RAPD patients. Still, this would require further inclusion of patients for confirming these findings. A combination of the parameters obtained during constriction responses served as a basis for the calculation of PRS coefficients in which distinctive limits were found between healthy and patients with RAPD. The PRS related assessment could function as a preliminary evaluation towards the establishment of an asymmetry limit to predict the presence of RAPD. But then again in cases of severe grades of RAPD, we speculate there might be no attempt for pupil constriction, rather an instant dilation on light stimulation, then we might have to assume tcon close to zero in order to avoid a PRS coefficient of infinity (∞). Hence, the limits of this coefficient

should be further explored in patients with different grades of RAPD to evaluate its clinical applicability. Additional research is also necessary to establish whether the extracted PLR parameters are satisfactory in terms of specificity and sensitivity to be used diagnostically.

Since the pupilometer system we used has haploscopic optics for stimulus presentation, it offers the possibility of evaluating the Pupillary Near Reflex dynamics thereby expanding the applicability to detect Light-near dissociation signs. This could aid in the detection of clinical conditions such as Adie's tonic Pupil, and Argyll Robinson's pupil. The customisable protocol offers the opportunity to explore the possibility of chromatic pupillometry and acquire knowledge regarding the Post Illumination Pupillary Response (PIPR) to detect abnormalities in the function of ipRGCs (Ellis et al., 1981; Rukmini et al., 2019; Lei et al., 2014). This can aid as a promising diagnostic and therapeutic outcome measurement tool to assess the functional integrity of the inner retina independent of visual photoreceptor input.

Further enhancement in the design of this current lab-based prototype can promote it into a portable device and finer modifications in its interface might even open up possibilities for a tele-ophthalmic evaluation of clinically relevant pupil signs. Even though, the current study has attempted to take care of various factors influencing PLR measurements, a variety of emotional and cognitive elements should be considered as covariates. Moreover, there was no availability of other pupillometer systems for a preliminary comparative analysis.

CONCLUSIONS

The current study proposed an automated haploscope-based binocular pupillometer system. This provides insights into analysis strategies that could be successfully applied to optimise the quantification of PLR parameters. The clinical relevance of this protocol can be further explored in detecting the pupil abnormalities in various neuro-ophthalmic diseases, and in utilising the

characteristics of pupil redilation in disease detection. Further steps can focus on optimising the PRS coefficient for quantifying afferent pupillary defects.

7

APPENDIX – Chapter 7

The double exponential equations used to analyse the time course of the pupil trajectory and the quantify PLR parameters:

$d_{pup.init (c)}$ - The initial pupil diameter in a panel, $d_{pup.max (c)}$ - The maximum pupil diameter in a dilation panel, $d_{pup.min (c)}$ - The minimum pupil diameter in a constriction panel, $d_{pup.end (c)}$ - The pupil diameter at the end of redilation period in a constriction panel, Δd - difference between $d_{pup.max}$ or $d_{pup.min}$ and the $d_{pup.init.}$, Δt_{dil} - The latency for the initiation of dilation after light stimulation is of, Δt_{con} - The time delay/latency for the initiation of constriction after light stimulation is on, Δt_{rec} - The time delay/latency for the initiation of pupil redilation after the maximum constriction, $T_{dil,} T_{con}, T_{rec}$ - the time constants.

$$d_{pup.max} = d_{pup.init} + \Delta d_{dil} \left(1 - \exp\left[-\frac{t-\Delta t_{dil}}{T_{dil}} \right] \right) \qquad \text{(eq. 1)}$$

$$d_{pup.min} = d_{pup.max} - \Delta d_{con} \left(1 - \exp\left[-\frac{t-\Delta t_{con}}{T_{con}} \right] \right) \qquad \text{(eq. 2)}$$

$$d_{pup.end} = d_{pup.min} + \Delta d_{red} \left(1 - \exp\left[-\frac{t-\Delta t_{red}}{T_{red}} \right] \right) \qquad \text{(eq. 3)}$$

$$t_{con} = \Delta t_{red} - \Delta t_{con} \qquad \text{(eq. 4)}$$

$$RMSE = \sqrt{\frac{\sum_{i=1}^{N}(predicted(i)-actual(i))^2}{N}} \qquad \text{(eq. 5)}$$

$$PRS = \frac{T_{con}/t_{con} \times 100}{\Delta d_{con}} \qquad \text{(eq. 6)}$$

Supplementary Figure 7.1: Bar graphs displaying the comparable Time constant values (top panel) and latencies (bottom panel) between the six constriction panels. The error bars represent the Standard Deviation (SD).
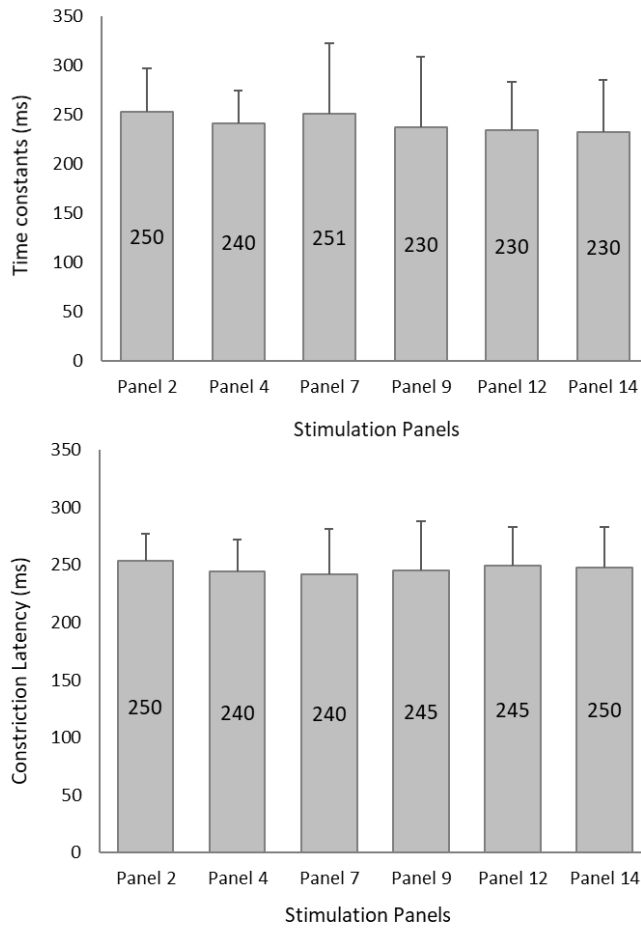
CHAPTER 8

General Discussion

8.1 Highlights of the thesis: Research questions and key findings

Over the past decade, considerable expansions in eye-tracking technology have opened up new possibilities for innovative diagnostic approaches in eye care. The aim of this thesis was to determine potential biomarkers to assess the functional integrity of the visual system on the basis of Eye Tracking Technology (ETT). The central element of this thesis was the application of ETT to design, develop, and evaluate prototype(s) integrated with Eye Movement Perimetry (EMP) and pupillometry protocols. The customised protocols facilitated the study of eye movement behaviour and Pupillary Light Reflex (PLR) dynamics to detect visual system defects associated with glaucoma and neuro-ophthalmic conditions. This thesis addressed two main topics (Figure 8.1).
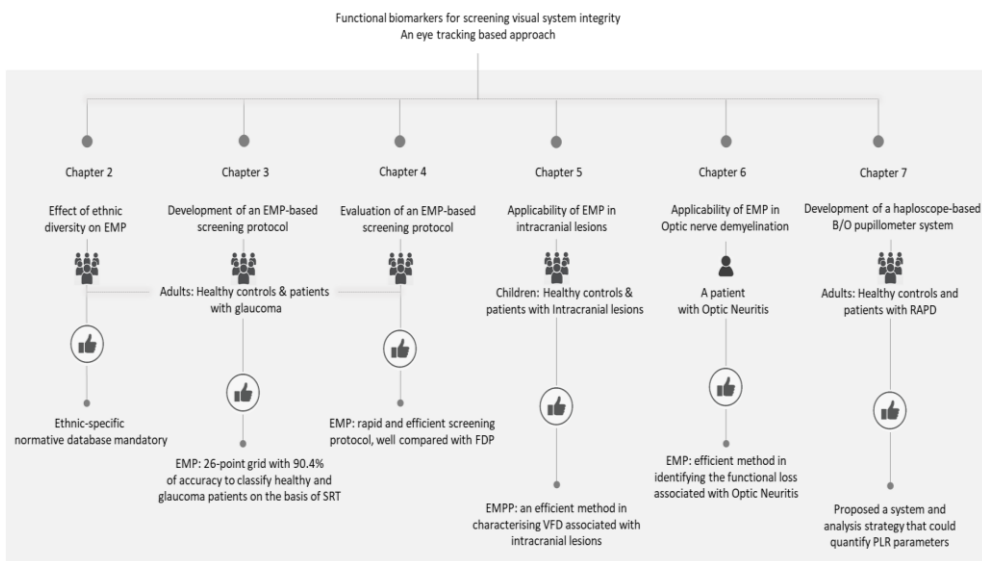
Figure 8.1: A summary of the thesis chapters 2 to 7 with the specific research questions addressed under each of them, the sample population included, and the key findings.

Firstly, the successful development and validation of an EMP protocol (Chapters 2 to 6) that allowed the generation of Visual Field (VF) responsiveness plots, created on the basis of Saccadic Eye Movement (SEM).

Chapters 2 to 6 provide evidence that this approach can be used as a clinical tool to identify Visual Field Defects (VFDs) associated with glaucoma and neuro-ophthalmic diseases. Secondly, the development and evaluation of a binocular (B/O) pupillometry protocol (Chapters 6 and 7) that well quantified the defects pertaining to the pupillary pathway on the basis of pupil parameters and an inter-pupillary comparison index.

In addition, I examined the methodological aspects of the EMP technique to ensure its feasibility, reliability, and validity among younger and older adults (Chapters 2 to 4, 6) as well as the pediatric population (Chapter 5). The EMP plots displayed the extent, and integrity of the monocular VF (MVF), via the full-field and screening modes. The results were in good agreement with conventional perimetry methods, Standard Automated Perimetry (SAP), and Frequency Doubling Perimetry (FDP). Apart from the MVF testing, EMP also provides the possibilities to evaluate the Binocular VF (BVF). To extend the applicability of ETT, a dual screen-based (haploscopic view) prototype was conceptualised and established into which the validated EMP protocol was integrated. Furthermore the haploscopic prototype enabled the combination of a pupillometry procedure. Consequently, the second focus was on the development and evaluation of a pupillometry protocol that efficiently generated pupillary traces in response to photic stimulation. The pupillary traces computed comprehensive pupil parameters and the introduction of a Pupil Response Symmetry (PRS) co-efficient predicted the presence of Relative Afferent Pupillary Defect (RAPD). Overall, Saccadic Reaction Time (SRT) and PLR-based ocular biomarkers were extracted to evaluate the functional integrity of the visual system. These objective indices detected the presence of the disease and aided in monitoring the disease course and prognosis. These results paved the way to find supplementary/surrogate means to study oculomotor and pupil behaviour to diagnose visual system defects that can be possibly translated in the future into population-based screening strategies.

This 'general discussion' is sub-sectioned into ETT-based perimetry (EMP) and pupillometry. In the following paragraphs, I will first discuss the

consolidated review of the prototypes described in the literature that are to some extent comparable to the approaches described in this thesis (Table 8.1). Subsequently, the highlights of the current approach by refocusing on the prototypes (design and assembly) and the measurement protocols are detailed. This is followed by the description of the analysis algorithms that facilitated the extraction of potential functional biomarkers and their translation to generate perimetry and pupillometry outputs. Next, the characteristics of the study sample and the pathophysiological aspects of SRT delays and pupillary abnormalities (diameter and time-related) in the selected ophthalmic conditions are discussed. Finally, the future directions toward the clinical implementation of the proposed methods, applicability in remote ophthalmic care, gaze re-training strategies, and ophthalmic/optometry education are discussed.
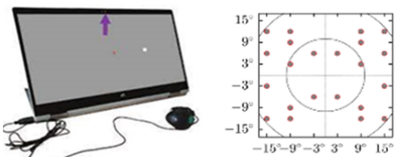
8.2 Eye tracking as a tool for perimetry
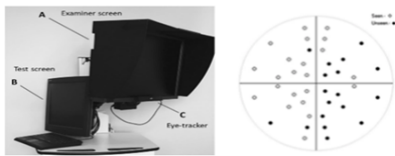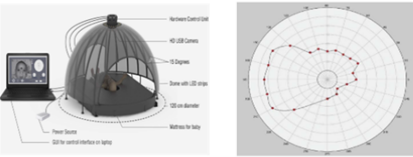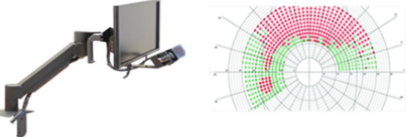
In conventional approaches of perimetry (SAP), the measurement of human perceptual performance relies on subjective responses. This process is often complicated due to the demands for prolonged attention, stable fixation, and the necessity for motor responses (e.g. pressing the response button). These aspects restrict the application of SAP in a certain set of patient cohorts such as elderly people, those individuals with fixation disorders, those with shorter attention spans, children, etc.

8.2.1 State-of-the-art EMP systems and strategies

Since the technological developments are entirely aspiring to expand the performance and quality of medical diagnostics, complementary techniques to SAP were and are being introduced (Jernigan, 1980; Trope et al., 1989; Kim et al., 1995; Murray et al., 2009; Pel at al., 2013; Mazumdar et al., 2014; Jones et al., 2021). EMP is one of those alternative techniques that rely upon ETT, a non-invasive technique to measure an individual's eye movement behaviour. EMP opens up a naturalistic ambiance to test human perceptual performance, a relatively objective approach, wherein the adaptation artifacts and

the task difficulty levels are relatively minimal (Jernigan, 1980; Trope et al., 1989; Kim et al., 1995; Murray et al., 2009; Pel at al., 2013; Mazumdar et al., 2014; Jones et al., 2021).

Table 8.1: The consolidation of the recently proposed EMP systems in the literature with their key specifications

Proposed EMP systems and test grids	Key specifications
Saccadic vector Optokinetic Perimetry (SVOP): *Murray et al., 2009*	1. Liquid Crystal Display (LCD) screen presented Goldmann III stimuli of variable intensity, at 24-2/C-40 perimetric grids 2. Detection thresholds were determined on the basis of eye movements (seen/unseen) using a remote eye-tracker
Pediatric Perimeter: *Satgunam et al., 2017*	1. A hemispherical dome, with Light Emitting Diodes (LEDs), placed along the meridians displayed sequentially using a hybrid mode (kinetic & static) 2. VF isopter and RT are used to quantitatively estimate the VF using an Infrared camera
Eye-tracking-based visual Field Analysis (EFA): *Leitner et al., 2021*	1. LCD screen presented Goldmann IV stimuli of variable intensity, at 30-2 perimetric grid 2. Detection thresholds were determined on the basis of eye movements (seen/unseen) using a remote eye-tracker
Open-source tablet perimeter (Eye catcher): *Jones et al., 2021*	1. Tablet screen presented Goldmann III stimuli of variable intensity, at 24-2 perimetric grid/22 paracentral locations (ZEST algorithm) 2. Detection thresholds were determined on the basis of eye movements (seen/unseen) using a remote eye-tracker

*ZEST – Zippy Estimation of Sequential Testing

Even if the participant initiates a random eye movement during the instances where he/she has less surety that a stimulus was seen, the well-defined EMP decision algorithm is capable to differentiate the 'reliably seen' response

from arbitrary search behaviour. The application of this advanced technique and its evolution provides the options to acquire wider knowledge and a deeper understanding of the human visual system (Wade et al., 2010; Harezlak et al., 2018). Table 8.1 consolidates four EMP systems proposed in the literature with their key specifications including the technical components, measurement strategies, and outcome measures. Subsequently, their study methodologies are compared and contrasted with the approach proposed in this thesis.

8.2.2 Features of the proposed EMP prototype and protocol

In my experiments (Chapters 2 to 6), I used a remote eye tracking system (Tobii T120, Tobii, Sweden) that relied upon the principle of Pupil Centre Corneal Reflection (PCCR). The eye tracking system was comprised of near Infrared (IR) projectors and sensors that use IR light reflection to capture high frame rate images of eyes integrated with image processing algorithms to determine specific details of the gaze data.
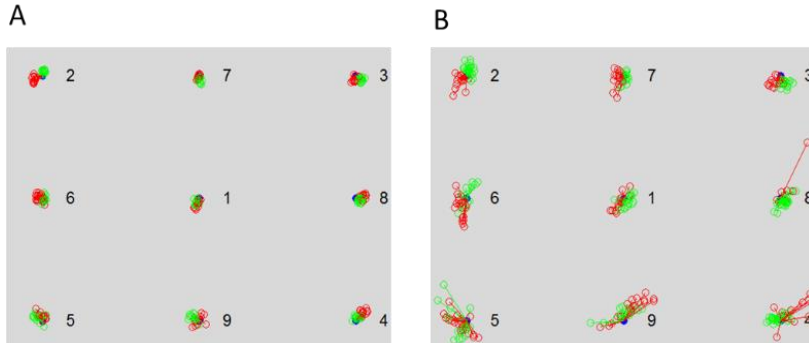

Figure 8.2: Calibration plot illustrating the simple and concise representation of two performed calibrations showing an acceptable calibration (Panel A) and a significant offset between the mapped sample points (Panel B). Green and red lines denote the error vectors for the right and the left eye respectively.

The measurement setup was easy to establish and enabled freedom of head movement (inside the headbox within which the tracking was possible). The spatial accuracy, the average offset between the point of gaze and the point reported by the tracker, and the precision, the sample-to-sample difference

in what the eye-tracker reports, when compared to the true gaze point of the eye tracking device, were optimal to serve the research purpose (Niehorster et al., 2018). Each of the measurement series began with a nine-point calibration process using a smooth pursuit task, whereby the geometric features of the participants' eyes were estimated and taken as a basis to accurately analyse the gaze points for each image sample. The quality of the calibration was checked (Figure 8.2) by inspecting a schematic representation of calibration success that contained error vectors (green and red lines of varying extent) in which the length of the vectors denoted the offset between each sampled gaze point and the centre of the calibration dot (colour coded as blue). Calibration was deemed to be successful and accepted if the offset between each sampled gaze point and the centre of the calibration dot was well within the permissible window (Figure 8.2: Panel A). Large offsets were noticed when the participants were either distracted during the calibration or the eye tracker was not being set up in the approved way and the calibration was rerun (Figure 8.2: Panel B). This step helped in the attainment of good quality gaze data throughout the actual experiments.

There were instances of data loss or poor data quality even if the participant's eyes remain within the trackable area. Data loss was defined as the time period during which the eye tracker was unable to report a gaze position whereas poor data quality was the property of the sequence of raw data samples produced by the tracker. Though the majority (≥ 92%) of the enrolled study participants successfully performed EMP, data loss was observed in participants with mitotic pupils (less than 2 millimeters) and ptosis (droopy eyelids). Miotic pupils were observed in glaucoma patients who were on parasympathomimetic drugs. Apart from these, eye tracking possibility was expected to be limited in those sets of patients with a corneal scar, dense cataract > LOCS III (Lens Opacification Classification System), ocular motility restrictions, and large-angle strabismus (> 6 prism diopter), hence restricted in the selection criteria. Optimal data quality was ensured by an appropriately arranged experimental setup, proper positioning of the participants with necessary instructions, and a suitable physical recording environment including the lighting conditions (Nyström et al., 2013; Niehorster et al., 2018). In spite

8

of the precautions, there were situations of data loss or poor data quality in glaucoma patients, which can be attributed to the adverse effects of the long-standing use of anti-glaucoma medications causing ocular surface alterations including dry eye (Actis et al., 2014).
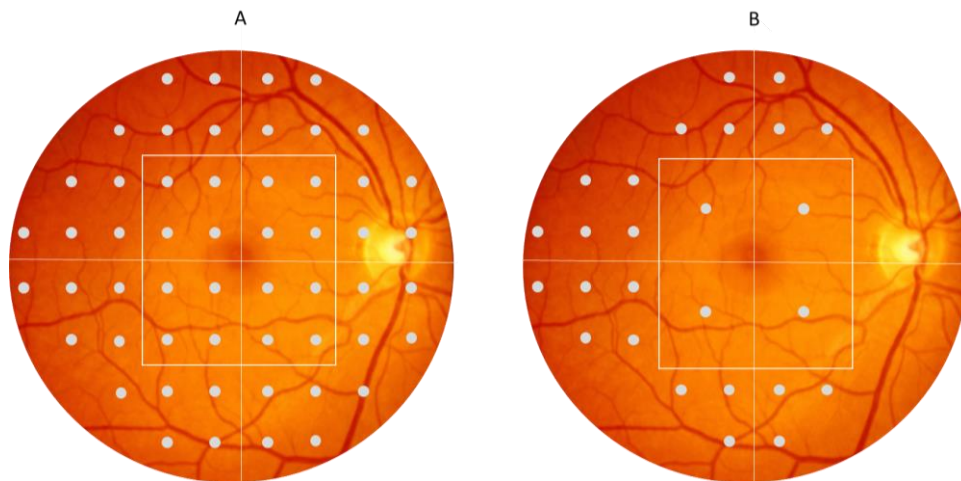

Figure 8.3: Illustration of stimulus grids used, full-field (Panel A) and the Screening (Panel B) mode, during the EMP measurements with corresponding locations on the retinal surface.

Like many other modern psychophysical studies of visual perception, this proposed method also relied on computer-generated stimuli presented on a flat Thin-Film-Transistor (TFT) monitor. While this method permitted the precise and well-controlled display of stimuli, it suffered from a restriction in terms of the maximum attainable spatial coverage (Yu et al., 2010). In order to evaluate foveal, parafoveal, and near peripheral VF (30° on either side of the line of fixation) using a flat projection screen instead of a hemispherical bowl as in Humphrey Field Analyser (HFA) the Fixation Target (FT) was not only kept at the centre of the screen (primary gaze) but also moved to four different eccentric positions (± 20°) with inclined gaze angles. This facilitated the coverage of maximum visual angles of 27° horizontally (a total of 54°) and 21° vertically (a total of 42°). This thesis hypothesised that the SRT would be similar when the horizontal, vertical, or oblique SEMs are initiated with eyes aligned in a primary compared to cardinal positions of gaze (Levo and dextro

elevation or depression). But the effect of the viewing angle on the oculomotor behaviour and SRT should be further investigated.

Three proposed prototypes detailed in the previous literature (Table 8.1) also used flat display screens (LCDs and tablet screens) for stimulus presentation that was analogous to the one described in this thesis (Murray et al., 2009; Leitner et al., 2021; Jones et al., 2021). In the meantime, the pediatric perimeter used a hemispherical dome built with a dimension to comfortably place their infant participants (aged between 2.3 to 12 months) in a supine position. This projection surface enabled the assessment of 90° VF in all the quadrants except for the inferior (Satgunam et al., 2017). This is certainly in view of the spherical geometry of the human VF coordinates. So during the course of future refinement, the currently proposed and validated EMP protocol can even be integrated with a hemispheric projection screen to create a large spatial area coverage. This might outspread the possibilities to evaluate VF responsiveness even at the farther periphery. This prototype was acquainted with two customised protocols (Figure 8.3) that relied on a 54-point grid (Panel A), similar to the standard grid used in HFA, and a 26-point grid (Panel B). The latter one was a screening grid, a subset of the full-field grid that comprised specifically chosen locations exhibiting the highest susceptibility to glaucomatous damage (Supplementary Table 3.1). The protocol used a typical Goldmann size III visual stimulus (subtending 0.43° of visual angle) for the adult cohort (Chapters 2 to 4, 6) and a circular smiley symbol for the pediatric cohort (Chapter 5).

Each of the test locations was evaluated once at four levels of SI i.e. 192, 214, 249, and 276 cd/m^2 in the full-field mode, and at two levels of SI i.e. 214 and 276 cd/m^2 in the screening mode. This selection of two stimuli was on the basis of a Receiver Operating Curve (ROC) analysis with the maximum Area Under the Curve (AUC) value for the 214 cd/m^2 to discriminate glaucoma patients from the age-matched healthy controls (Chapter 3). In the literature, the majority of the test stimuli were suprathreshold or fixed-intensity test stimuli, as in the EFA study that had a luminance level of 10 cd/m^2 (Leitner et al., 2021) whereas the pediatric perimeter used LED lights set to match 550 nm wavelength (Satgunam et al., 2017). Although the previous studies used

8

comparable stimulus sizes, their intensity/luminance is not directly comparable with those used in this thesis. The intensities of the test background and stimuli were rather close to the ones used in the screen-based and Virtual Reality (VR) based eye tracker settings proposed by Soans et al. (Soans et al., 2021). Though the chosen intensities aided in accurately discriminating cases from their age-matched controls, a wider range of intensity levels for the purpose of thresholding might be recommended during the course of future refinements.
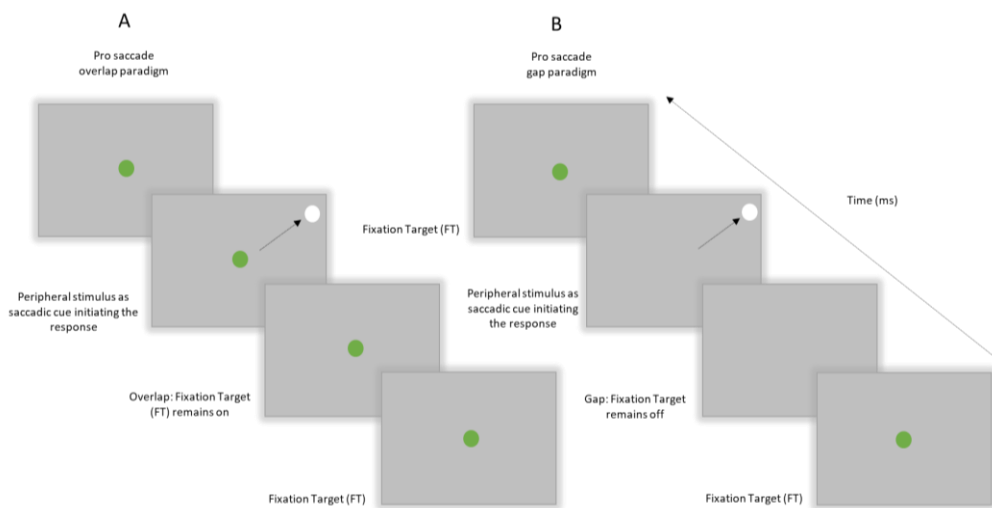
Figure 8.4: Illustration of the experimental paradigm, overlap (Panel A), and gap (Panel B) where the Fixation Target (FT) is kept on while the peripheral visual stimuli are projected to initiate saccades during the overlap paradigm whereas the FT is taken off in the gap paradigm.

The Reaction Time (RT) to initiate an SEM is reported to be influenced by the type of fixation task due to the underlying neuronal mechanisms conveying signals to gaze shifting and holding mechanisms (Figure 8.4). When the FT is switched off before the stimulus presentation (gap paradigm), the saccade behaviour is expected to be altered when compared to an overlap paradigm. In the gap task, a period without visual stimulation is presented between the offset of the FT and the onset of a saccade stimulus, resulting in significantly faster mean RT values recorded along with an increased rate of express saccades (RT as low as 80 to 120 ms) and/or anticipatory saccades. Moreover,

saccade performance in the gap task demands cognitive control to sustain fixation if the gap interval is longer (> 200 ms) where actually there is no FT present.

With regard to saccade performance in the overlap task, an effortful choice seems to be required for saccade initiation to overcome the ocular fixation reflex induced by the FT when a saccade target is projected in the peripheral VF. The EMP paradigm defined in this thesis relied upon an overlap paradigm for being analogous to the HFA method, and to reduce the occurrence of search behaviour and limit the generation of express saccades (Takagi et al., 1995; Bucci et al., 2005; Özyurt & Greenlee, 2011). From the literature that evaluated the effect of gap-overlap stimuli on the distribution of SRTs, I hypothesise the SRT values recorded using overlap stimuli to have a different offset and range. Hence a direct comparison across diverse types of fixation tasks might not be reliable.

8.2.3 EMP analysis algorithm

The eye tracking sensors used in my experiments collected sufficient gaze data samples to notify the stability, location, and duration of eye fixation within the Area of Interest (AOI) of the FT. The customised post-test analysis window (MATLAB, MathWorks. Natick, USA) could successfully detect Fixation Losses (FL) and False Positive (FP) responses. Although the possibility of FP feedbacks is very minimal due to the reliance on natural reflexive eye movements, the algorithm still incorporated a quality check to determine the presence of FP responses. These kind of responses were determined and eliminated by inspecting each SEM trial relying on the well-defined classification criteria (detailed in chapters 2 to 6). False Negative (FN) rates are also one of the valuable indicators as they flag the periods of participants' inattention. FN response occurs when the participant fails to give a positive response to a stimulus presented at an intensity level likely to be seen. Despite stating the patient consistency, FN rates can also give valuable information about the VF status of glaucoma patients. This is due to the increased rate of random threshold variability and visual fatigue observed in glaucoma patients (Bengtsson & Heijl, 2000; Chandrinos et al., 2020). Incorporation of

catch trails to determine FN rates is advised during the future refinement of the test .

8.3 Disrupted saccades in visual system dysfunctions: pathophysiological background

Visual orienting behavior in humans results from a composite interaction between the cortical neural networks specialised for stimulus choice, motor preparation, and generation of SEMs. SRT, a quantifiable parameter of SEM, is the totality of the processing time that comprises localising the stimulus, preparing, and initialising a directional SEM towards the detected stimulus (Pierrot-Deseilligny et al., 2003; Gaymard et al., 2012). Since SRT is one of the indicators for human perceptual performance this thesis utilised SRT as a reliable parameter to create VF plots during EMP.
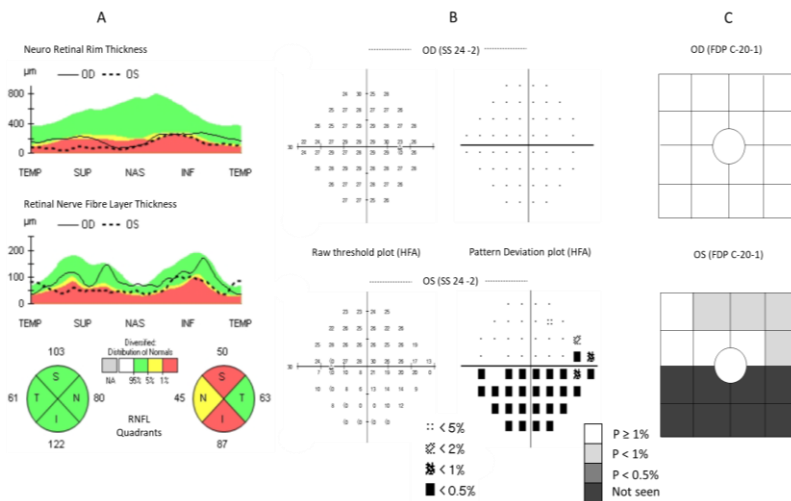

Figure 8.5: Optical Coherence Tomography (OCT) reports of a patient displaying healthy Neuro Retinal Rim (NRR) and normal Retinal Nerve Fibre Layer (RNFL) thickness but RNFL thinning in the superior and inferior quadrants (Panel A). HFA (SS 24 -2 protocol) and FDP (C-20-1 protocol) plots (Panels B and C respectively) showed normal VF in the right eye (OD) and an inferior arcuate defect and an early superior arcuate defect in the left eye (OS).

Glaucoma (Chapters 2 to 4) and neuro-ophthalmic patients (Chapters 5,6) who underwent EMP measurement as a part of this thesis exhibited significantly delayed SRT (temporal lag) as compared to their age-matched normal-sighted controls. This was in accordance with the previously published literature that reported disruptive eye movements in glaucoma (Kim et al., 1995; Mazumdar et al., 2014; Najjar et al., 2017; Thatham et al., 2020; Soans et al., 2021) and neuro-ophthalmic diseases (Reulen et al., 1984; Brigell et al., 1988). Here is a clinical case-based description of a patient (40 years old male) diagnosed with unilateral Primary Open Angle Glaucoma (POAG) with a definite glaucomatous structural damage in the left eye with a corresponding functional defect detected using HFA and FDP (Figure 8.5). The custom-generated EMP plots correlated well with the conventional clinical findings (Figures 8.5 and 8.6). Similar to the previously reported EMP systems, the current EMP system also generated plots on the basis of eye movement responses (seen, unseen, and invalid). However, the surplus strength of this thesis is the establishment of a normative database and VF responsiveness plots generated on the basis of SRTs adjusted for the factors relating to the patient and stimulus characteristics.

The neuroanatomic substructures for SEM control are better described through the studies involving transcranial magnetic stimulation and functional imaging (Pierrot-Deseilligny et al. 2002; Pierrot-Deseilligny et al., 2003). The studies emphasised the contribution of a complex interconnected network of cortical and subcortical structures in which the Frontal Eye Field (FEF) and the Parietal Eye Field (PEF) are critical control centres for planned as well as reflexive SEMs. The Supplementary Eye Field (SEF) is considered a monitoring centre to evaluate the framework of SEM and regulate saccade generation during a task performance. The presence of this intricate network suggests that any structural alterations due to degeneration or injury have a high likelihood of affecting the SEM control. The delays in SEM initiation among patients with glaucomatous neurodegeneration or neuro-ophthalmic diseases could be attributed to either the loss of axonal fibres of the

8

Opti Nerve (ON) or an insult to the ON that provide direct retinal feedback to Superior Colliculus (SC) and/or that drive the information through the visual cortex (Yucel et al., 2003; Kanjee et al., 2012).
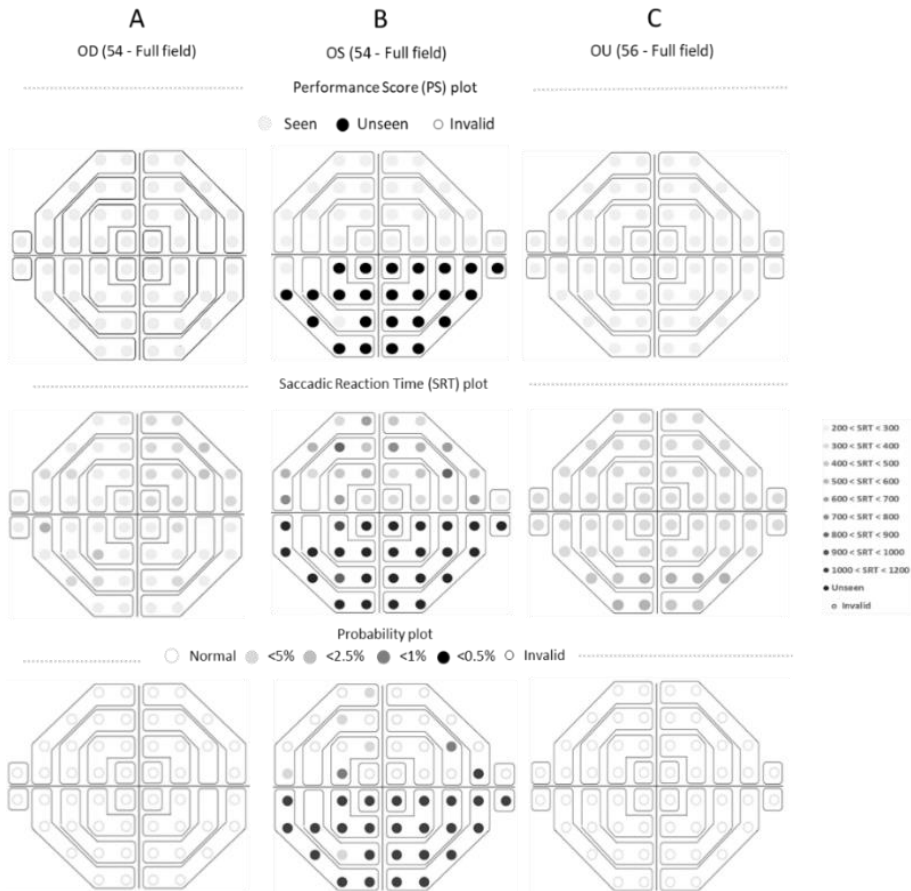

Figure 8.6: Custom-generated EMP plots (Performance Score, SRT plot, and Probability plot) exhibiting a normal VF in the right eye (Panel A) and inferior arcuate defect with an early VF depression in the superior hemifield in the left eye (Panel B).

This case example shows how this thesis effectively translated the recorded delays in SEM initiation as a clinical index to plot VF responsiveness plots that were well compared to VF plots generated by the clinical standard, HFA. Even the screening protocol of EMP accurately identify glaucoma and was well comparable with the FDP outputs (Chapter 3).

It would be advisable to conduct an in-depth structural-functional correlation (OCT and EMP) assessment in a group of patients with glaucoma. Recent studies have reported the presence of delayed SRT even before the functional changes are detectable in SAP (Najjar et al., 2017; Thepass et al., 2021). Since it is essential to detect/screen the early forms of glaucoma to initiate therapy it seems worthwhile to explore the possibility of SRT as an early glaucoma detection index. Despite being a screening/diagnostic index SRT might also be useful as a predictor for disease progression in glaucoma or prognosis in neuro-ophthalmic diseases like Optic Neuritis (Chapter 6).

8.4 Natural variability of the reaction time during a prosaccade task performance

SRT of a saccade initiated towards visual stimuli reflects the responsiveness of the oculomotor-orienting system and it is influenced by various endogenous factors including those related to the participants as well as the test stimulus. Previous literature has explored the influence of such factors on SRT in isolation and in combination (Munoz et al., 1998; Darrien et al., 2001; Irving et al., 2011; Pel et al., 2013; Woods et al., 2015; Mazumdar et al., 2019; Yamagishi et al., 2020) among healthy adults and in children. Mazumdar et al. investigated the SRT characteristics among healthy controls and the influence of participants' age, gender, stimulus intensity, and eccentricity on the response times (Mazumdar et al., 2019). The study suggested the need to analyse such an interaction in order to refine the use of SRT as an index for VF responsiveness especially while building a normative database for the proposed EMP method. Hence this thesis encompassed the analysis of participants' characteristics such as age, and ethnicity along with the stimulus characteristics such as intensity, and eccentricity.

Apart from these factors, it might be worthwhile to investigate the intra and inter trial variabilities in saccade initiation, since the SEMs are subjected to dissimilarities when made repeatedly to the same experimental stimulus (Smeets et al., 2003). Here is a first-line impression of the repeatability of EMP (Figure 8.7) from the data obtained from five series of measurements

(one baseline and four repetitions) performed on a healthy control (26 years/female). The EMP measurement was performed using the 54-point grid (Figure 8.3: Panel A) wherein each test location was evaluated using four levels of SI i.e. 192, 214, 249, and 276 cd/m2. Five trials were conducted on consecutive days with an inter-test interval of ~24 hours. In the direction of obtaining a global view of the results, the percentage of reliably 'seen' responses (Figure 8.7: Top panel) and corresponding mean SRT values (Figure 8.7: Bottom panel) were calculated for each of the EMP trials and were found to be closely comparable.
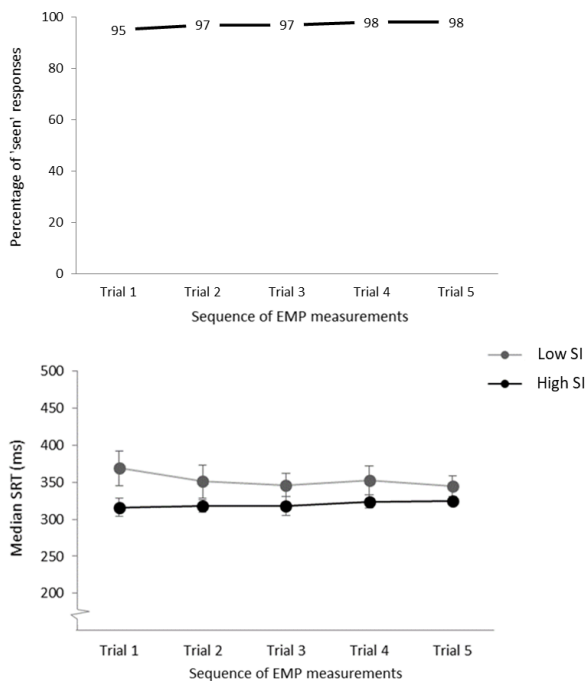

Figure 8.7: Line graphs showing the numerically comparable 'seen' responses (%) ranging from 95 to 98% (Left panel) and corresponding median SRT values in ms (Right panel) obtained for the lower (192 cd/m^2) and higher (276 cd/m^2) intensity/contrast test stimuli across the measurement series. The error bars represent the corresponding Inter Quartile Ranges (IQR).

There are several factors that contribute to test-retest variability in perimetry, including the amount of participants' test familiarity and the time of day.

However, a prominent source of variability is short-term fluctuations in relation to the psychometric function. The natural response to a presented visual stimulus triggers an increase in the rate at which Retinal Ganglion Cells (RGCs) produce neural spikes, but at inconstant intensities causing variability in the psychometric function. It is also suggested that this raised variability might vary as a function of distance from the central fixation target whose magnitude is expected to be lower in the central areas of the VF compared to the peripheral regions in healthy or eyes with near-normal retinal sensitivity (Heijl et al., 1989). Whenever the VF regions are altered due to underlying ocular conditions, not only does the sensitivity decrease but also the psychometric function becomes shallower. This contributes to an increase in intra-test variability (Gardiner et al., 2018).
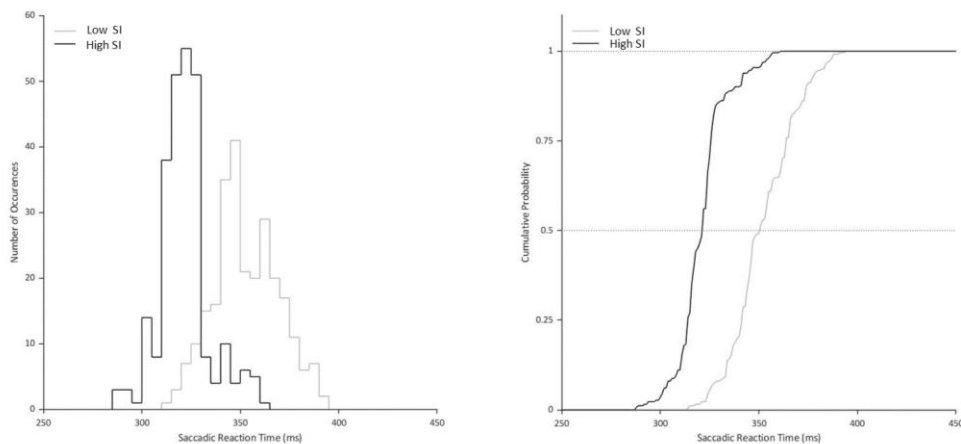

Figure 8.8: Representation of the SRT data distribution (n = 1044 observations) using a histogram/frequency distribution (Left Panel) and the CDF (Right Panel) for the lower (192 cd/m^2) and higher (276 cd/m^2) intensity/contrast test stimuli.

Here in this thesis classification decisions are made by considering the overall mean SRT values or zone-wise SRTs. Even though the global SRT values

showed reasonable discriminatory ability, efforts should be taken in the future to best characterise the SRT data by reducing the influence of variability

and outliers in the distributions. Henceforward, instead of the individual values of SRTs, examining the shape of SRT distributions obtained from repeated observations should be relied upon to summarise the data. The changes in the spread and shape of this distribution can be examined across measurement trials for greater clinical information (Cooper et al., 2012). These distributions can be represented using either Probability Density Functions (PDF) or Cumulative Density Functions (CDF). Considering the natural variability of SRT might improve the existing diagnostic/screening ability of the proposed EMP protocols by zooming into localised decline in VF responsiveness.

Here is a preliminary effort to generate empirical models (Figure 8.8) to visualise the shape of SRT distributions that helped in getting a pragmatic view of the data distributions across the measurement trails. Frequency distribution was generated by dividing the SRT scale into intervals and calculating the number of observations/occurrences in each interval. The distribution of lower (196 cd/m^2) and higher intensity test stimuli (276 cd/m^2) was distinct from each other wherein the lower intensity data had a comparatively wider spread and shorter clusters of bars (Figure 8.8: Left panel). The empirical CDF plots were generated by plotting SRT data values (x-axis) against the percentile scale (y-axis) thereby displaying the cumulative distribution observed in the SRT data sample as a stepped function. When compared between the lower and higher intensity stimuli, the CDF curve for the latter is shifted towards the left indicating a faster SRT distribution. The overall slope of the CDF function was found to be steeper for the higher intensity data, therefore lower variability (Figure 8.8: Right panel).

In par with the assessment of contrast sensitivity threshold variability assessment, the spatiotemporal variabilities in SEM initiation and trajectories as a function of orientation, amplitude, and SI should be measured (Heijl et al., 1989). This might offer a critical piece of information concerning the expected variability when further refining the EMP algorithm by keeping an optimal balance between stimulus size, stimulus intensity, stimulus location, and the number of presentations/intra-test repetitions.

8.5 Existing methods of binocular visual field estimation and possibilities of EMP

Routine ocular diagnostics rely on M/O perimetry methods for the diagnosis and monitoring of disease. But it is of great clinical implication to appreciate a patient's BVF, the superimposition of the two M/O fields (Figure 8.9: Panel A), to recognise the effect of VFDs on a patient's Vision-Related Quality of Life (VRQoL). Among the several testing programs offered by the automated perimeters, the Esterman Visual Field test (EVFT) is a binocular testing method that consists of 120 white test points shown at a suprathreshold light intensity of 10 dB. HEVF examines ~ 130° of the field and classifies the patient as pass or fail by calculating 'seen' and 'unseen' points and summarising the performance into an Esterman efficiency score (Crabb et al., 2004). This test indeed offers a gross estimation of the functional VF under normal/natural-istic viewing conditions but it is impossible to understand the actual respon-siveness of the VF as it offers a binary output (seen/unseen).
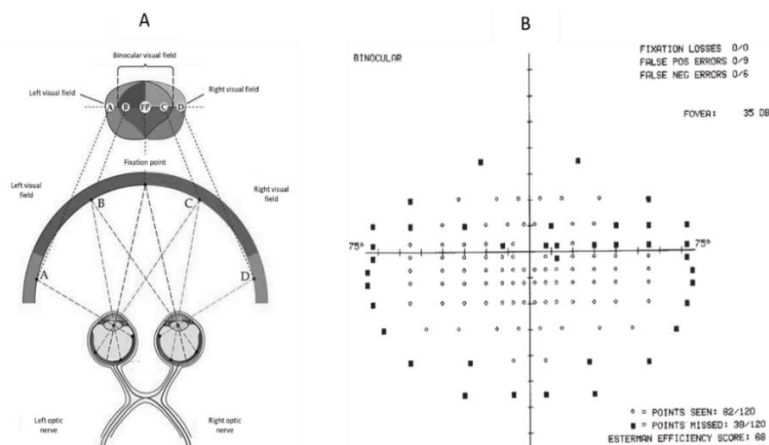

Figure 8.9: An illustration of the superimposition of M/O fields to form the B/O field of vision (Panel A, Image reproduced from Aboali et al., 2021) and a sample report generated using the Esterman Visual Field Test (EVFT) with reliability indices (False positive and Negative errors) and Esterman efficiency score, a calculated percentage of total seen responses/total tested points (Panel B, Image reproduced from Crabb & Viswanathan, 2005).

However, EVFT is not often performed in regular clinical settings and subsequently, the Integrated VF (IVF) is often used to estimate a patient's binocular field of vision without extra perimetric testing. As compared to EVFT, IVF is reported to provide a better prediction of a patient's perceived inability to perform daily visual tasks. Still, this analytical method is only an estimate of the BVF and not an actual measure of the field (Crabb et al., 2003; Crabb et al., 2005). Here the proposed EMP method delivers possibilities for B/O EMP estimation, besides the MVF estimation, by providing an in-depth analysis of the functional vision by providing B/O reaction times.

Figure 8.10 is a clinical case-based example, the glaucoma patient from figure 8.5, who presented with asymmetric VFDs (non-overlapping), where B/O SRTs seemed to be comparable with the structurally and perimetrically normal eye (right eye). This could be perhaps explained by the fact that B/O viewing doubles the likelihood of visual stimuli detection. Previous literature has documented the statistical models to predict B/O sensitivities (Crabb et al., 1998; Crabb et al., 2004; Nelson-Quigg et al., 2000). Henceforward a scientific probe with a specific focus on B/O EMP might help to better understand the nature and extent of spatial and temporal summation that occurs in the visual areas of the brain. Apart from the temporal lag (SRT delay), glaucoma patients also revealed spatial uncertainty when they had to make saccades toward the central or near peripheral stimuli.

In the exploratory report described in Chapter 6, the requirement for a re vised experimental setup by including a dual-screen (haploscope) system is stated. Such a revision of the system was proposed to allow an independent, simultaneous, or alternating control of visual stimulation thereby providing a convenient testing environment for BVF and pupillometry. Concerning the perimetry protocol, the dual-screen prototype with the dichoptic/haploscopic viewing would aid in the projection of 3D visual images thus enabling the assessment of eye movement behaviour not just in a 2D surface but also in a 3D mode. In real-life situations, the eye movements initiated while looking at diverse objects in 3D visual space typically involve components of both

vergence and saccades. Several studies have suggested while a decision is made to initiate eye movements towards a visual target, two distinct oculomotor subsystems (saccades and vergence) are triggered. Earlier studies stated that the two oculomotor subsystems, that of saccades and of vergence, exhibit markedly contrasting dynamic characteristics, such as speed and duration. The evaluation of the dynamic characteristics of these combined movements might bring important insights into the parallel sensory processing of direction and depth information (Yang et al., 2002).
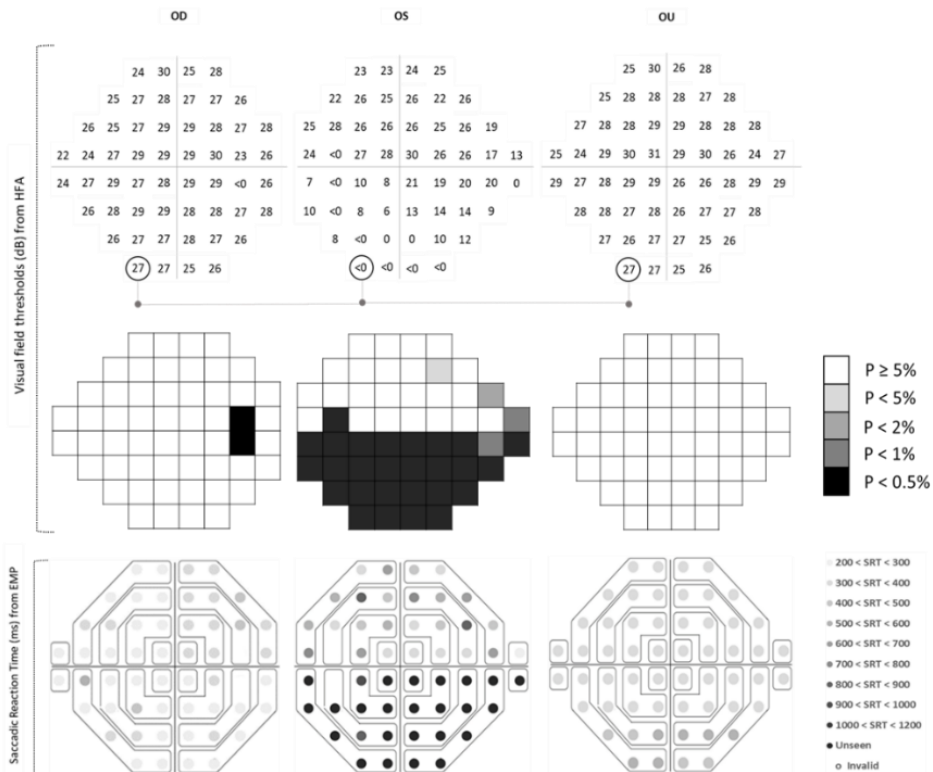

Figure 8.10: A comparative illustration of the M/O and B/O raw threshold plots generated using HFA and EMP. Top panel: Illustrates the M/O HFA reports along with the integrated field report generated by relying on the binocular summation method (Nelson-Quigg et al). Bottom panel: M/O and B/O reaction time values recorded using the EMP protocol. Encircled locations are a sample illustration of the corresponding VF locations and the greyscale denotes the probability levels.

8.6 Participants' preferences and perceptions of the proposed method of perimetry

Perimetry is a psychophysical procedure and relies on reliable subjective responses to generate valuable clinical information. Hence it seemed mandated to evaluate patient preference and perception of the newly proposed method for VF estimation. This thesis used a previously validated questionnaire (Meethal et al., 2019), refined for the current study (Appendix 4.1), to assess participants' preferences with regard to the experimental setting, test pattern, target characteristics, and physiological and psychological aspects affecting the perimetry, therefore such specific details can be considered while further refining the testing method. A previous study that compared the patient preference for HFA and FDP reported that pressing the response button on detecting a peripheral stimulus and the inability to maintain steady central fixation for a prolonged duration were the most commonly reported factors that increased the level of difficulty of the conventional perimetry tasks (Meethal et al., 2019). The current sample population (Chapter 4) also responded on par with these observations and this difficulty might be the reason behind a higher preference for EMP as it permits natural reflexive eye movements. In addition, the fear of failing/repeating the test was found to be the most common factor that is probably affecting the participants' concertation while performing the perimetry task. Similarly, yet another study evaluated the patient preference for HFA and two EMP setups, one a screen-based and the other a VR based one. The participant's preference pattern was evaluated using a User Experience Questionnaire (UEQ) that incorporated six dimensions such as competence, perspicuity, Immersion, Aesthetics, and Attractiveness. A high preference was found for the EMP method specifically the VR-based prototype due to freedom of head movements, aesthetics, and attractiveness (Soans et al., 2021). Though their study group included healthy controls, glaucoma and neuro-ophthalmic patients, the mean age (years) of their subgroups was descriptively lesser when compared to the study population studied in this thesis. Hence the results are not directly

comparable but the preference pattern was similar where both the study groups preferred SEM-based perimetry rather than the conventional method.

8.7 Eye tracking as a tool for pupillometry

8.7.1 State-of-the-art pupillometer systems and strategies

The conventional approach to pupillary assessment, Swinging Flashlight Test (SFT), depends on a qualitative judgment regarding the speed and magnitude of pupil constriction and its comparison with the contralateral pupil. RAPD or Marcus Gunn pupil is detected whereupon one pupil constricts comparatively less when a light source is swung between the pupils (Pillai et al., 2019). SFT is a simple, quick, non-invasive, inexpensive method that is indispensable in routine ophthalmic evaluation to rule out ON damage (Levatin et al., 1959; Pillai et al., 2019). But, this procedure is exposed to various levels of inconsistency put forward by the ambiance of the testing room, amount and angulation (off-axis) of the projected light, the clinical expertise of the examiner, inter-examiner inconsistency, and lack of any particular criteria for quantification and documentation. The evaluation and conclusions often become challenging in the presence of anisocoria (unequal pupil sizes), minimally reacting pupil, dark iris, etc. Thus, pupilometer systems were constructed in which the first was based on photography techniques that were less in precision with long time consumption for data processing. Later in time, they were replaced using photoelectric measurements of the light reflected from the iris followed by television-based systems, and then Charged Couple Device-based (CCD) ones (Szczepanowska-Nowak et al., 2004). Recent advancements have introduced ETT based automatic high-resolution infrared pupillometry systems to objectively and precisely quantify the pupil parameters and they were recommended for various clinical or research applications (Kalaboukhova et al., 2006). Table 8.2 consolidates a few pupillometer systems proposed in the literature with their key specifications including the technical components, measurement strategies, and outcome measures. Subsequently, their study methodologies are compared and contrasted with the approach recommended in this thesis.
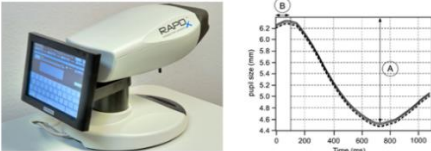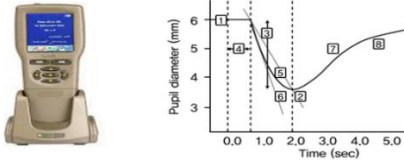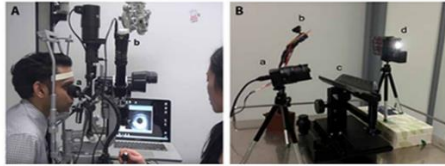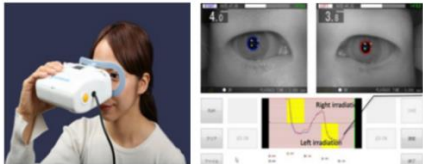
8

8.7.2. Features of the haploscope-based prototype and pupillometry protocol

The haploscope based binocular prototype, mentioned in chapter 6 and described in the following chapter, was found to be suitable for a well-controlled stimulation of the pupils with a paradigm that replicated the conventional SFT procedure. This was a haploscope-based binocular system (Figure 7.1) where a mirror-based dichoptic stimulation was combined with a portable eye tracking device (Tobii Pro X3-120). Dichroic mirrors were selectively transparent to the infrared wavelength range in which the eye trackers record their signals (Ramey et al., 2008; Naber et al., 2011; Brascamp & Naber, 2017). These mirrors were placed at a 45° angle relative to the participant's midline thereby diverting the two eyes' visual line of sight in opposite directions to two different monitor displays without obstructing the camera's view. This was indeed a straightforward system that permitted unilateral or bilateral stimulation and simultaneous recording of the pupillary and oculomotor responses during pupillometry and perimetry respectively. The dichoptic viewing systems designed exclusively for the purpose of pupillometry are marginally described in the previous literature, wherein similar or comparable optical systems were found in two studies. A former scientific study that aimed to assess pupil size variability (Nowak et al., 2014) and another one that evaluated pupillary reflex as an index for perceptual rivalry (Naber et al., 2011) have used systems with analogous optical aspects.

Aside from the prototype design, assemblage, and geometry, the system proposed in the thesis differs from the previously suggested ones in terms of the test protocol (Figure 7.2: Top panel) and the analysis algorithm (Figure 7.3). With regard to the light stimulation protocol, previous pupillometer settings have relied upon diverse light stimulus paradigms. RAPDx® pupillometer records B/O pupil response evoked using a white stimulus illuminance of 30.9 lux against a background illuminance of 0.5 lux where the field of view was 30° (Satou et al., 2015; Satou et al., 2016). On the other hand, Yoo et al. used a pupillometry technique which was performed after 3 minutes of dark adaption and the stimuli consisted of light pulses at a fixed intensity of 180 microwatts/cm^2 projected for a duration of 185 ms (Yoo et al., 2017).

Chang et al. used a smartphone with an LED strobe light (0.2 s light ON, 5 s light OFF cycles) as the stimulus and an IR camera (video pupillography) to record pupil kinetics (Chang et al., 2017). The Hitomiru® pupillometer shined visible light onto one side of the pupil to induce pupillary miosis and then used an IR light to gauge and monitor the PD by using infrared short-range sensors (Kotani et al., 2021).

Table 8.2: The consolidation of the recently proposed EMP systems in the literature with their key specifications.

This thesis put forward a B/O pupillometer system with a stimulation protocol that is a computerised replica of the SFT with three distinct stimulation

phases namely, (a) Simultaneous stimulation phase, (b) Unilateral stimulation phase, and (c) Alternating stimulation phase (Figure 7.2: Top panel). The PLR was induced by one of two stimuli that transitioned from a black to white elliptical slide. Due to the customisable nature of the protocol, the system has possibility to incorporate chromatic pupillometry and evaluate the Post Illumination Pupillary Response (PIPR). In addition, the haploscopic view offers a possibility for Pupillary Near Reflex (PNR) thereby aiding in the assessment of light-near dissociation signs (Ellis et al., 1981; Rukmini et al., 2019; Lei et al. 2014). Pupil data underwent outlier removal using filtration techniques and from the raw traces, parameters were computed using a double exponential fit function. Apart from the pupillogram with the traces generated for each of the stimulation panels, the proposed method is equipped with a PRS co-efficient (Chapter 7) calculated from the diameter and time-based pupil parameters. The co-efficient is a summary index for inter-pupil symmetry aiding the clinicians to get a quick impression of the afferent pupillary defect.

8.8 Glimpse towards clinical implementation: Visual diagnostic/screening practice

This thesis designed, developed, and validated ETT based prototype(s) merging both perimetry and pupillometry protocols for clinical predictions. The protocols extracted ocular biomarkers i.e. SEM and PLR-based parameters that successfully estimated the functional integrity of the visual pathways. These are robust and reliable objective indices that showed promising capability in detecting the disease affecting the ON functionality. Integration of these measures as a clinical index would pave the way to provide a surrogate means to better characterise the oculomotor and pupil behaviour. This would be a feasible method in routine clinical practice and later translated it into population-based screening strategies. Here is a case-based example of a 50-year-old female (Figure 8.11) who visited the neuro-ophthalmology clinic with a complaint of progressive unilateral vision loss in the right eye. Routine clinical evaluation revealed a decline in visual acuity, presence of RAPD in the right eye, delayed latency, and reduced amplitude on Visual Evoked Potential (VEP). Magnetic Resonance Imaging (MRI) report revealed irregular lobulated

plaque like enhancement in the inferior tentorium, thickened right ON sheath complex suggesting the possibility of a granulomatous etiology. In addition to the regular battery of investigations, the patient underwent EMP and pupillometry using the haploscope prototype.
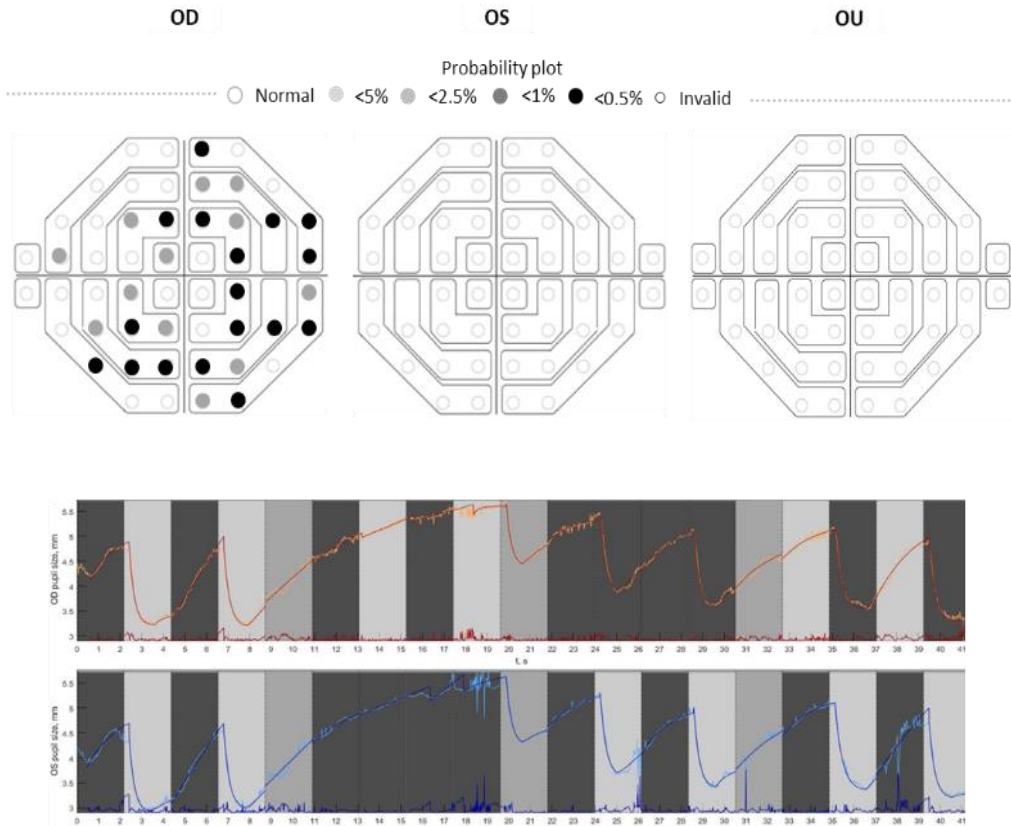
Figure 8.11: Custom-generated EMP plots (Probability plot) exhibiting temporal and inferonasal VFDs in the right eye with a normal VF in the left eye and binocular condition (Top panel). Pupillogram that shows the raw pupillary traces from the right (in orange) and left eye (in blue). The superimposed red and blue traces are the best fit line created on the basis of the double exponential fitting procedure displayed along with the residual errors. Unilateral stimulation phase OD showed no constriction responses from the pupil on light stimulation and the same is persistent in the final stimulation phase, thus revealing a right RAPD.

Here I am furnishing the integrated outputs showing a definite decline in VF responsiveness (Figure 8.11: Top panel) and a corresponding pupillary

defect (Figure 8.11: Bottom panel). These unified measures support to draw valuable insights into the functional status of the visual system. The conventional methods indeed show promising diagnostic ability but the integration of multiple functional indices (sensory and motor aspects of the visual systems) might aid in extending the boundaries of applicability. Together with the integrated approach, this thesis recommends a structural-functional coupling based clinical decision making for better diagnostic ability and progression/prognosis estimation.

The current prototype is a laboratory based experimental setup and a miniature and portable version of this seemed ideal for the clinical implementation. Hence, the research insights obtained from this thesis were translated and incorporated into a Head-Mounted haploscopic Device (HMD) in collaboration with a technological company based in Norway (Bulbitech AS, Trondheim, Norway). The HMD, named BulbiCAM (Figure 8.12) is a miniature replica of the haploscope prototype described in this thesis integrated with the proposed EMP and pupillometry protocols. The commercialised product version of the haploscope prototype is currently under technical development, refinement, and validation process. From the previous literature, we hypothesise that the patient preference toward this VR-based product will be equal to higher when compared to the table-mounted experimental prototype (Soan et al., 2021).

Fundamentally all areas of the oculomotor and pupillary networks are reported to be implicated in visual perception, decision making, cognition, attention, etc., and have been proposed to reflect both conscious and preconscious brain activity. Although this research has created a resilient base for understanding the deviations in eye movements and PLR dynamics in glaucoma and neuro-ophthalmic diseases, there remain many unexplored areas that merit further investigation. For instance, apart from the specific ocular conditions investigated in this thesis, the disruption of SEM and PLR responses could be linked to the neurodegeneration observed in diseases such as Parkinson's and Alzheimer's (Mosimann et al., 2005; MacAskilla et al., 2016; DiNuzzo et al., 2019).

Therefore, regardless of whether a neurodegenerative process or neuronal damage is relatively focal (e.g. glaucoma) or widespread (e.g. Parkinson's), effects are therefore likely to be evident as altered oculomotor performance and PLR dynamics.
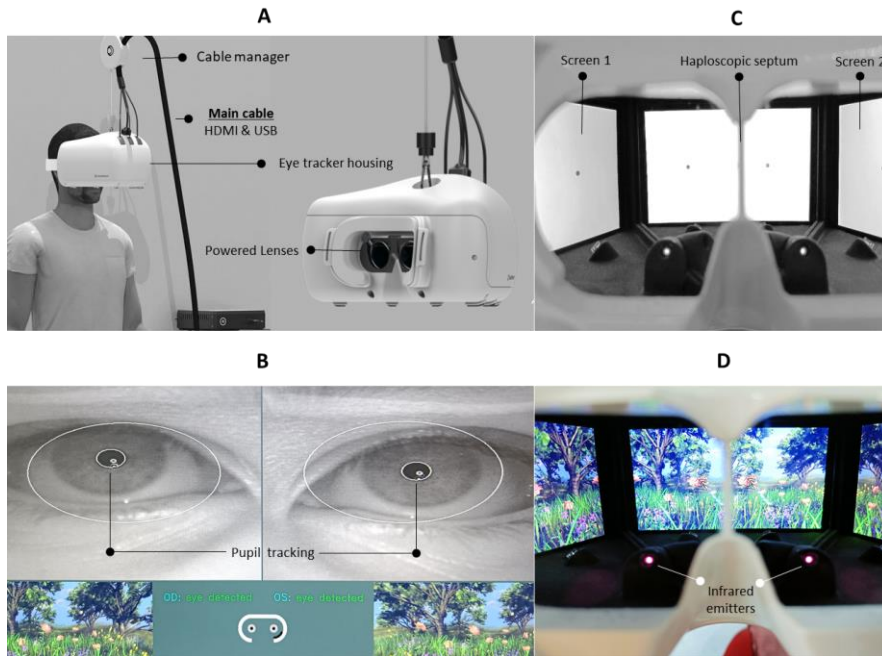
Figure 8.12: Panel A - the Head-Mounted haploscopic Device, the BulbiCAM labeled with its power/data cables, eye tracker housing, and power lenses. Panel B - The examiner's screen displays the pupil tracking status along with the BulbiCAM display. Panel C and D – A closer view of the dual Liquid Crystal Display (LCD) screens and the two infrared (IR) sensors.

In summary, patients with a wide spectrum of neuro/neuro-degenerative conditions experience significant changes to the basic neurochemistry that in turn cause alterations to eye movement circuitry and pupillary dynamics. Hence, the integrated approach proposed in this thesis might be an index for a wider range of diseases that need to be further explored in the future. It might be worthwhile including similar psychophysical approaches to investigate other functional aspects of vision such as colour, contrast and adaptation thereby including a wide spectrum of potential markers for the visual system integrity.

8.9 Extended future directions for ETT in ophthalmology/optometry

8.9.1: Gaze re-training:

Central, paracentral, and peripheral VFDs due to any underlying etiology pose difficulties in functional vision in turn leading to a decline in VRQoL. The presence of such VFDs leads to differential visual search methods. Various studies have evaluated patients with VFDs for understanding their SEM behaviour and found impaired visual scanning patterns and substantial deviations in the SEM responses (increased search times, number of fixations, and errors) when compared to the age-matched controls (Coeckelbergh et al., 2002). Specific SEM patterns such as the number of saccades and fixations, corrective saccades, hypo/hypermetric saccades, regressive saccades, etc. recorded while passively viewing real-life images or specific visual tasks can be further explored (Crabb et al., 2010; Smith et al., 2012; Asfaw et al., 2018).

Figure 8.13: Gaze plot that shows the 'time sequence of looking' by including the location, order, and duration of gaze (Panel A). Heat map that shows the 'distribution of looking' by including the illustration of the visual attention (Panel B).
(Note: Gaze and heat maps from a female healthy volunteer aged 24-years-old).

Previous studies have revealed that it is possible to detect the presence of VFDs based on free viewing eye movements (Smith et al., 2012; Asfaw et al., 2020; Gestefeld et al., 2021). However, at times certain patients with VFDs are not even conscious of the presence of VFD due to their brains filling-in the

missing visual information (Carvalho et al., 2019). A very recent study has even attempted to reconstruct the VFD location by mapping the basic properties of fixations and SEMs across their VF (Gestefeld et al., 2021). Moreover, individual glaucoma patients not only have different VFD, they also appear to differ in their ability to cope with it. Consequently, it might be beneficial to have a well-established VF grid for standardised perimetry (as described in this thesis) followed by a real-life scenario (static or dynamic images) based analysis methods. These not only stand as indices for real functional vision in patients diagnosed with VFDs but also helps in designing effective interventions/gaze re-training programs with the goal of rectifying the impaired eye movement behaviour (Smith et al., 2012; Gunn et al., 2019). Here I am presenting a preliminary proof of concept report to evaluate the search behaviour pattern of a healthy control while viewing a traffic scene recorded using the proposed prototype (Figure 8.13). Further investigations on the basis of these scientific particulars might help spread the prototype's possibilities from a diagnostic/screening approach to a visual training platform.

8.9.2: Gaze analysis in ophthalmic/optometry education

Advancements in the ETT not only find possibilities in the diagnosis and monitoring of diseases but also in the field of medical education. Previous studies have adopted eye movements to assess clinical skill acquisition specifically in the interpretation of diagnostic reports (Yang G-Z Dempere-Marco et al., 2002; Leong et al., 2007; O'Neill et al., 2011). Pertaining to ophthalmology, a previous study has compared the visual gaze behaviour of glaucoma subspecialists with a set of ophthalmology trainees during Optic Nerve Head (ONH) and RNFL examination (O'Neill et al., 2011). Here is an initial proof of concept report to evaluate gaze patterns while viewing and interpreting a single-field report generated by HFA recorded using the proposed prototype (Figure 8.14).

Since the possibilities of ETT in ophthalmic/optometry education and teaching methods are minimally explored, it would be worthwhile to study gaze

8

pattern behaviors of clinicians with varying levels of expertise. The insights from such research can be utilised while creating student training strategies.
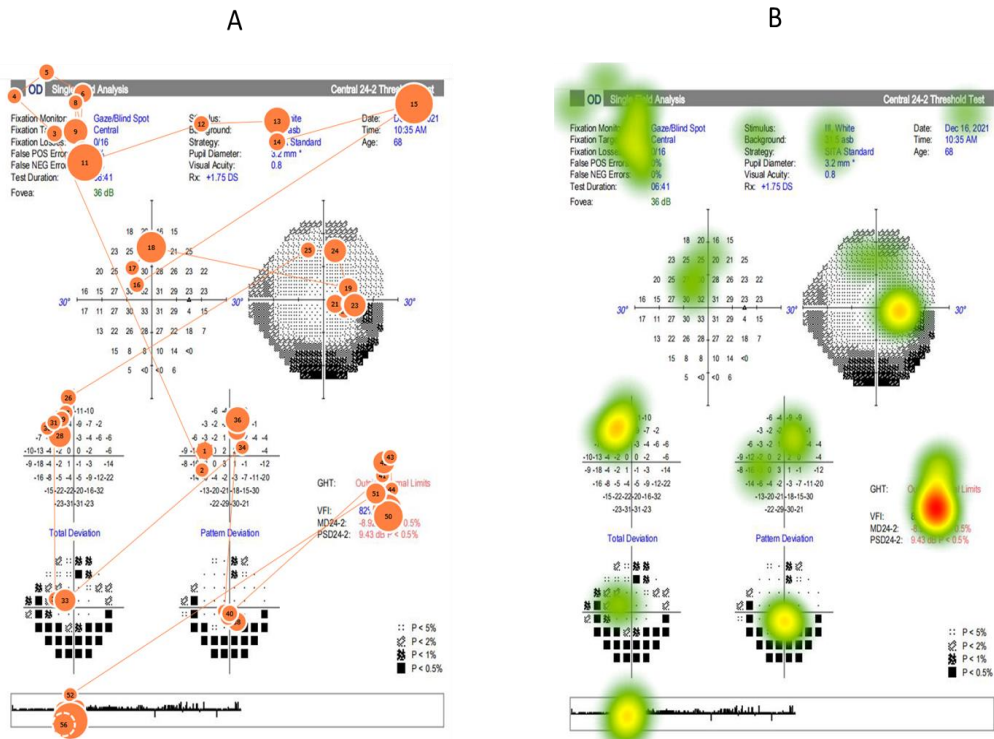
Figure 8.14: Gaze plot that shows the 'time sequence of looking' (Panel A) whereas the heat map (Panel B) that shows the 'distribution of looking' by including the illustration of the visual attention.
(Note: Gaze and heat maps from a female healthy volunteer aged 18-years-old optometry student).

8.10 Conclusive remarks

The culmination of my research findings demonstrated that eye tracking based perimetry and pupillometry approaches can derive reliable functional biomarkers to obtain comprehensive clinical information regarding the visual system integrity. While the groundwork has been set, with further

refinements as suggested, the method could supplement the existing neuro-physiological measures and aid in enhanced clinical diagnoses and prognosis estimations.

8

APPENDICES

- General Summary

- References

- Portfolio

- List of Publications

- List of Awards and Accolades

- Acknowledgments

- Curriculum Vitae

GENERAL SUMMARY

Visual function declines resulting from the structural defects concomitant with glaucoma or any neurologic origin lead to a decline in Quality of Life (QoL). Visual function impairment impacts the Activities of Daily Living (ADL), confines social interactives, and limits real-life independence. This eventually brings about a variety of public health, social and economic burdens, particularly in underdeveloped/developing countries. Hence it is important to detect abnormalities in the visual pathways so as to provide appropriate intervention or rehabilitative care. Conventionally the integrity of the Optic Nerve (ON) and the other components of the visual pathway is appreciated by relying on the intactness of the Visual Field (VF) and normality of the Pupillary Light Reflex (PLR). These are evaluated using Standard Automated Perimetry (SAP) and Swinging Flashlight Test (SFT) respectively. However, the existing methods put forward certain challenges and the introduction of Eye Tracking Technology (ETT) into ophthalmic care assure to overcome certain of those drawbacks.

At our lab (Vestibular and Oculomotor Research Group, Erasmus MC, Rotterdam, The Netherlands), an ETT-based prototype was designed to evaluate visual orienting responses in children and was found to be feasible in detecting deficits pertaining to visual information processing. For the present thesis, the EMP protocol, integrated into the standard prototype, was further explored and evaluated for its feasibility and reliability among adults with glaucoma and children and adult with neuro-ophthalmic diseases. In this thesis, the EMP test protocol (Full-field and screening modes) were found to be clinically promising in identifying the decline in VF responsiveness on the basis of reflexive eye movement behaviour and Saccadic Reaction Time (SRT). The prototype was further reformed to develop a dual-screen based haploscope system to fit in the options for binocular EMP along with the binocular pupillometry technique. EMP and pupillometry based parameters were extracted as the potential functional biomarkers of visual system integrity to flag out visual system defects associated with glaucoma and neuro-ophthalmic conditions. In addition to diagnosis, the preliminary reports finished in

this thesis show the ability to predict the progress/prognosis of the listed diseases.

Chapter 2:

Evaluated the influence and interaction between the participant (age, ethnicity) and the stimulus related (eccentricity, intensity) factors on SRT and the interaction between these factors using a Generalised Linear Mixed Model (GLMM) analysis. This study group included healthy controls and primary glaucoma patients from 20 to 85 years of age belonging to two different ethnic groups i.e. Indian and Dutch. All the participants underwent EMP using a full-field grid consisting of 54 VF locations tested at four Stimulus Intensity (SI) levels (192, 214, 249, and 276 cd/m^2) against a background of 152 cd/m^2. For the purpose of analysis, the participants were divided into five age bins and VF was segregated into five distinct zones based on the stimulus eccentricities. The model revealed an overall statistically significant interaction between the four tested factors wherein the maximum difference in SRT was found in the age groups greater than 40 years for the farthest peripheral zone at 214 cd/m^2 SI level (The Indian cohort exhibited faster SRT than their Dutch counterparts). SRT cut-off values for discriminating between healthy control and glaucoma were found to be statistically comparable for the two ethnic cohorts. Although screening for the decline in VF responsiveness can be done on the basis of global mean SRT, this chapter recommends the reliance on an ethnicity-specific normative database adjusted for the evaluated factors to accurately predict/quantify the location-wise SRT delay and corresponding pattern and depth of VFD.

Chapter 3:

Focused on the development and first-line evaluation of a rapid and novel protocol on the basis of EMP to screen VFDs associated with glaucoma. The study group included healthy controls and primary glaucoma patients aged above 20 years recruited from the Indian subcontinent. The full-field grid

(fixed protocol) consisting of 54 VF locations tested at four levels of SI (192, 214, 249, and 276 cd/m^2) was further refined into a screening grid (interactive protocol) consisting of 26 VF locations at two SI levels (214 and 276 cd/m^2) on the basis of Receiver Operating Characteristic (ROC) analysis. An internal validation analysis revealed a 90.4% screening accuracy to classify healthy controls and patients on the basis of mean global SRT values.

Chapter 4:

Compared the clinical reliability of the SRT-based screening protocol with the Standard Automated Perimetry (SAP) and Frequency Doubling Perimetry (FDP). This validation stage considered another set of healthy controls and primary glaucoma patients (not inclusive of the sample used for the development phase) aged above 20 years recruited from the Indian subcontinent. The Area Under the Curves (AUC) generated on the basis of Robin's scores obtained from the C-20-1 screening protocol of FDP and the mean SRT values obtained from the 26-point screening protocol of EMP were statistically comparable. This chapter also evaluated the participants' pattern of preference and perception towards the conventional perimetry techniques and the proposed EMP screening approach. A majority of elderly healthy controls and patients with moderate and severe glaucomatous defects preferred EMP over the existing clinical methods.

Chapter 5:

Refined the EMP protocol developed for the adult cohort into Eye Movement Pediatric Perimetry (EMPP) and examined its feasibility and clinical applicability among children with VFDs associated with Intracranial lesions (IL). The study group included healthy controls and patients diagnosed with IL recruited from the Netherlands. The customised method (Monocular and binocular EMPP) could be successfully performed by 94% of the controls and 89% of the cases, which included even children under four years of age. EMPP appeared to be a reliable method to estimate and characterise the central 30° VF in greater detail in children with IL, thereby supplementing the conventional methods.

Chapter 6:

Described a clinical case example wherein the reliability of SRT as an index to detect the presence and extent of VFDs associated with the neuro-ophthalmic condition was explored. This primary report discussed the clinical course of a 26-year-old female diagnosed with optic neuritis who underwent EMP (full-field grid) in addition to the routine battery of ophthalmic evaluations during the baseline and the follow-up visit post treatment. The EMP based VF plots revealed functional deficits that correlated well with the

conventional structural and functional diagnostic outcomes during the active as well as the recovery stage of the disease. In addition to the monocular EMP plots, this chapter presented the binocular EMP evaluation and generated corresponding VF plots. These outcomes at an individual subject level are an introductory basis to further explore the possibility of SRT as not just a diagnostic index but also as a prognostic index in neuro-ophthalmic diseases. This chapter also recommended modification of the EMP system for an inclusive pupillometry for a better comprehensive evaluation of the visual system integrity.

Chapter 7:

Elaborated on the development and feasibility of a haploscope-based pupilometer for the parametrisation of the PLR dynamics. The study group included healthy controls and patients diagnosed with Relative Afferent Pupillary Defect (RAPD). Healthy controls, aged between 20 to 29 years, with light or dark-coloured irides were recruited at the collaborative institutes in Rotterdam, The Netherlands, and Chennai, India to evaluate the influence of iris colour on PLR dynamics. All the participants underwent a prelim nary ophthalmic evaluation including pupillary examination using SFT, followed by pupillometry using the customised binocular haploscope based system (two identical setups in both the laboratories). Pupil responses were captured using an eye tracking camera and analysed using a double exponential fitting procedure to yield diameter and time-based pupil parameters. Except for the

initial Pupil Diameter (PD) during dilation and minimum PD during con-striction rest of the pupil parameters were statistically comparable between the light and dark iris groups. This chapter introduced an inter-pupillary comparison co-efficient called Pupil Response Symmetry (PRS) that could identify patients with clinically reported RAPD.

Chapter 8:

Apart from highlighting the specific findings of this thesis, the general discussion chapter described the State-of-the-art EMP and pupillometry systems and strategies. The features of the proposed method were compared and contrasted with the existing approaches in terms of the technicalities, test protocols/paradigms, generated outputs, and extracted parameters. The in-depth discussion about the structural-functional correlation of SRT delay, natural variabilities of the reaction time, and clinical applicability of binocular (B/O) EMP were demonstrated and discussed through case-based examples drawn from the samples of study participants. The translation of an experimental lab-based prototype into a clinically implementable version is also described in this chapter as a glimpse toward the future. This chapter was concluded by mentioning the potential extended future directions for ETT in gaze re-training (visual rehabilitation) in patients with functional deficits and also as a potential teaching tool in ophthalmology/optometry education.

Overall, the thesis presents eye tracking based approach to quantify oculomotor and pupillary dynamics integrated with the proposed analysis strategies to extract reliable parameters. The derived parameters are found to be dependable biomarkers to assess the functional integrity of the visual system. These findings make a base for an improved understanding of the clinical utility of such parameters and further refinements to the system and protocol are recommended for clinical implementation. Given the use of reflexive eye movements and comprehensive PLR dynamics, this proposed approach could be a potential supplementary method to the existing diagnostic modalities thereby providing useful and additional clinical information.

REFERENCES

- Aboali M, Abd Manap N, Hamzah RA, et al., A New Post-Processing Method for Stereo Matching Algorithm. International journal of Engineering Research and Technology. 2021: 1-13
- Actis AG, Rolle T. Ocular surface alterations and topical anti-glaucomatous therapy: a review. The Open Ophthalmology Journal. 2014; 8:67.
- Adams CW, Bullimore MA, Wall M. et al., Normal aging effects for frequency doubling technology perimetry. Optometry and vision science. 1999 Aug 1; 76(8):582-7.
- Agarwal HC, Gulati V, Sihota R. Visual field assessment in glaucoma: comparative evaluation of manual kinetic Goldmann perimetry and automated static perimetry. Indian journal of ophthalmology. 2000 Dec 1; 48(4):301.
- Alotaibi A, Underwood G, Smith AD. Cultural differences in attention: Eye movement evidence from a comparative visual search task. Consciousness and cognition. 2017 Oct 1; 55:254-65.
- Anderson RD, Patella VM (1999) Automated static perimetry, 2nd edn. Mosby, St. Louis
- Armaly MF. The size and location of the normal blind spot. Archives of Ophthalmology. 1969 Feb 1;81(2):192-201.
- Asaoka R, Crabb DP, Yamashita T et al., Patients have two eyes! binocular versus better eye visual field indices. Investigative ophthalmology & visual science. 2011 Aug 1;52(9):7007-11.
- Asfaw DS, Jones PR, Edwards LA et al., Using eye movements to detect visual field loss: a pragmatic assessment using simulated scotoma. Scientific reports. 2020 Jun 17;10(1):1-3.
- Atkinson J, Braddick O. Visual attention in the first years: typical development and developmental disorders. Developmental Medicine & Child Neurology. 2012 Jul;54(7):589-95.
- Behnke S. Hierarchical neural networks for image interpretation. Springer; 2003 Nov 18.
- Bee YS, Lin MC, Wang CC et al., Optic neuritis: clinical analysis of 27 cases. The Kaohsiung journal of medical sciences. 2003 Mar 1;19(3):105-11.
- Bengtsson B, Heijl A. False-negative responses in glaucoma perimetry: indicators of patient performance or test reliability? Investigative ophthalmology & visual science. 2000 Jul 1;41(8):2201-4.
- Bengtsson B, Heijl A. A visual field index for calculation of glaucoma rate of progression. American journal of ophthalmology. 2008 Feb 1;145(2):343-53.
- Bergamin O, Schoetzau A, Sugimoto K et al., The influence of iris colour on the pupillary light reflex. Graefe's archive for clinical and experimental ophthalmology. 1998 Jul 1;236(8):567-70

- Bergamin O, Kardon RH. Latency of the pupil light reflex: sample rate, stimulus intensity, and variation in normal subjects. Investigative Ophthalmology & Visual Science. 2003 Apr 1;44(4):1546-54.
- Biousse V, Newman NJ. Ischemic optic neuropathies. New England Journal of Medicine. 2015 Jun 18;372(25):2428-36.
- Bos JE. Clinical quantitative pupillometry: The latency of pupillary constriction as measured with the IRIS system (preliminary results). Neuro-ophthalmology. 1988 Jan 1; 8 (6):299-305
- Bradley JC, Bentley KC, Mughal AI et al., The effect of gender and iris colour on the dark-adapted pupil diameter. Journal of ocular pharmacology and therapeutics. 2010 Aug 1;26(4):335-40
- Brascamp JW, Naber M. Eye tracking under dichoptic viewing conditions: a practical solution. Behavior research methods. 2017 Aug; 49(4):1303-9.
- Bremner FD. Pupil assessment in optic nerve disorders. Eye. 2004 Nov;18(11):1175-81.
- Bremner FD. Pupillometric evaluation of the dynamics of the pupillary response to a brief light stimulus in healthy subjects. Investigative ophthalmology & visual science. 2012 Oct 1;53(11):7343-7.
- Brigell MG, Goodwin JA, Lorance R. Saccadic latency as a measure of afferent visual conduction. Investigative ophthalmology & visual science. 1988 Aug 1;29(8):1331-8.
- Broadway DC. Visual field testing for glaucoma–a practical guide. Community eye health. 2012;25(79-80):66.
- Bucci MP, Pouvreau N, Yang Q. et al., Influence of gap and overlap paradigms on saccade latencies and vergence eye movements in seven-year-old children. Experimental brain research. 2005 Jul;164(1):48-57.
- Buijs RM, Escobar C, Swaab DF. The circadian system and the balance of the autonomic nervous system. Handbook of clinical neurology. 2013 Jan 1;117:173-91.
- Carvalho J, Renken RJ, Cornelissen FW. Predictive masking is associated with a system-wide reconfiguration of neural populations in the human visual cortex. bioRxiv. 2019 Jan 1:758094.
- Casson RJ, James B. Effect of cataract on frequency doubling perimetry in the screening mode. Journal of Glaucoma. 2006 Feb 1;15(1):23-5.
- Chang LY, Turuwhenua J, Qu TY et al., Infrared video pupillography coupled with smart phone led for measurement of pupillary light reflex. Frontiers in Integrative Neuroscience. 2017 Mar 7;11:6.
- Chen JW, Vakil-Gilani K, Williamson KL et al., Infrared pupillometry, the Neurological Pupil index and unilateral pupillary dilation after traumatic brain injury: implications for treatment paradigms. Springerplus. 2014 Dec;3(1):1-0.

- Chen C. The Evaluation of Driving Performance in Glaucoma Patients Using Binocular or Monocular Visual Field Parameters. Investigative Ophthalmology & Vision Science 2013 Jun 1 (Vol. 54, No. 15).
- Chew SS, Kerr NM, Wong AB et al., Anxiety in visual field testing. British Journal of Ophthalmology. 2016 Aug 1;100(8):1128-33.
- Chylack LT, Leske MC, McCarthy D, et al., Lens opacities classification system II (LOCS II). Archives of ophthalmology. 1989 Jul 1;107(7):991-7.
- Clark R, Blundell J, Dunn MJ et al., The potential and value of objective eye tracking in the ophthalmology clinic. Eye. 2019 Aug;33(8):1200-2.
- Coeckelbergh TR, Cornelissen FW, Brouwer WH et al., Kooijman AC. The effect of visual field defects on eye movements and practical fitness to drive. Vision research. 2002 Mar 1;42(5):669-77.
- Cohen LM, Rosenberg MA, Tanna AP et al., A novel computerised portable pupillometer detects and quantifies relative afferent pupillary defects. Current eye research. 2015 Nov 2;40(11):1120-7.
- Contestabile MT, Perdicchi A, Amodeo S et al., Effect of refractive correction on the accuracy of frequency-doubling technology Matrix. Journal of Glaucoma. 2013 Jun 1;22(5):413-5.
- Cooper HE, Camic PM, Long DL et al., APA handbook of research methods in psychology, Vol 1: Foundations, planning, measures, and psychometrics. American Psychological Association; 2012.
- Crabb DP, Viswanathan AC, McNaught AI et al., Simulating binocular visual field status in glaucoma. British Journal of Ophthalmology. 1998 Nov 1;82(11):1236-41.
- Crabb DP, Fitzke FW, Hitchings RA et al., A practical approach to measuring the visual field component of fitness to drive. British Journal of Ophthalmology. 2004 Sep 1;88(9):1191-6.
- Crabb DP, Viswanathan AC. Integrated visual fields: a new approach to measuring the binocular field of view and visual disability. Graefe's Archive for Clinical and Experimental Ophthalmology. 2005 Mar;243(3):210-6.
- Crabb DP, Smith ND, Rauscher FG et al., Exploring eye movements in patients with glaucoma when viewing a driving scene. PloS one. 2010 Mar 16;5(3):e9710.
- C Kawasaki D, Boumaza D, Grisotto C et al., Reliability of standard pupillometry practice in neurocritical care: an observational, double-blinded study. Critical Care. 2016 Dec;20(1):99.
- Dain SJ, Cassimaty VT, Psarakis DT. Differences in FM100-Hue test performance related to iris colour may be due to pupil size as well as presumed amounts of macular pigmentation. Clinical and experimental optometry. 2004 Jul;87(4-5):322-5.
- Darrien JH, Herd K, Starling LJ et al., An analysis of the dependence of saccadic latency on target position and target characteristics in human subjects. BMC neuroscience. 2001 Dec;2(1):1-8.

- Daw NW, Daw NW. Visual development. New York: Springer; 2006 Jul 4.
- Delinte A, Gomez CM, Decostre MF et al., Amplitude transition function of human express saccades. Neuroscience research. 2002 Jan 1;42(1):21-34.
- De Nava AS, Somani AN, Salini B. Physiology, Vision. InStatPearls [Internet] 2021 May 9. StatPearls Publishing.
- DiNuzzo M, Mascali D, Moraschi M et al., Brain networks underlying eye's pupil dynamics. Frontiers in neuroscience. 2019 Sep 18;13:965.
- Ellis CJ. The pupillary light reflex in normal subjects. British Journal of Ophthalmology. 1981 Nov 1;65(11):754-9.
- Foster PJ, Buhrmann R, Quigley HA et al., The definition and classification of glaucoma in prevalence surveys. British journal of ophthalmology. 2002 Feb 1;86(2):238-42.
- Gardiner SK. Differences in the relation between perimetric sensitivity and variability between locations across the visual field. Investigative ophthalmology & visual science. 2018 Jul 2;59(8):3667-74.
- Garg S, Lehtonen A, Huson SM et al., Autism and other psychiatric comorbidity in neurofibromatosis type 1: Evidence from a population-based study. Developmental Medicine & Child Neurology. 2013 Feb;55(2):139-45.
- Gaymard B. Cortical and sub-cortical control of saccades and clinical application. Revue neurologique. 2012 Oct 1;168(10):734-40.
- Gella L, Nittala MG, Raman R. Retinal sensitivity in healthy Indians using microperimeter. Indian Journal of Ophthalmology. 2014 Mar;62(3):284.
- George R, Ramesh SV, Vijaya L. Glaucoma in India: estimated burden of disease. Journal of glaucoma. 2010 Aug 1;19(6):391-7.
- Gestefeld B, Marsman JB, Cornelissen FW. How Free-Viewing Eye Movements Can Be Used to Detect the Presence of Visual Field Defects in Glaucoma Patients. Frontiers in medicine. 2021;8.
- Glen FC, Baker H, Crabb DP. A qualitative investigation into patients' views on visual field testing for glaucoma monitoring. BMJ open. 2014 Jan 1;4(1):e003996.
- Grillini A, Renken RJ, Vrijling AC et al., Eye movement evaluation in multiple sclerosis and Parkinson's disease using a standardised oculomotor and neuro-ophthalmic disorder assessment (SONDA). Frontiers in neurology. 2020 Sep 8;11:971.
- Grillini A, Ombelet D, Soans RS et al., Towards using the spatio-temporal properties of eye movements to classify visual field defects. In proceedings of the 2018 ACM Symposium on Eye Tracking Research & Applications 2018 Jun 14 (pp. 1-5).
- Goodale MA. Action without perception in human vision. Cognitive neuropsychology. 2008 Dec 1;25(7-8):891-919.
- Gunn SM, Lajoie K, Zebehazy KT et al., Mobility-related gaze training in individuals with glaucoma: a proof-of-concept study. Translational Vision Science & Technology. 2019 Sep 3;8(5):23-.

- Hajian-Tilaki K. Receiver operating characteristic (ROC) curve analysis for medical diagnostic test evaluation. Caspian journal of internal medicine. 2013;4(2):627.
- Hall CA, Chilcott RP. Eyeing up the future of the pupillary light reflex in neurodiagnostics. Diagnostics. 2018 Mar 13;8(1):19.
- Hamdy M, Sherif H, Ibrahim I. Value of saccadic latency as a diagnostic tool for multiple sclerosis: a review and meta-analysis study. Hearing, Balance and Communication. 2021 Mar 15;19(2):73-9.
- Harwerth RS, Carter-Dawson L, Shen et al., Ganglion cell losses underlying visual field defects from experimental glaucoma. Investigative ophthalmology & visual science. 1999 Sep 1;40(10):2242-50.
- Harezlak K, Kasprowski P. Application of eye tracking in medicine: A survey, research issues and challenges. Computerised Medical Imaging and Graphics. 2018 Apr 1;65:176-90.
- Hayreh SS. Anatomy and physiology of the optic nerve head. Transactions-American Academy of Ophthalmology and Otolaryngology. 1974;78(2):OP240-54.
- Heijl A, Lindgren A, Lindgren G. Test-retest variability in glaucomatous visual fields. American journal of ophthalmology. 1989 Aug 1;108(2):130-5.
- Heijl A, Patella VM. Essential perimetry: the field analyzer primer. Carl Zeiss Meditec; 2002.
- Hess AS, Shardell M, Johnson JK et al., Methods and recommendations for evaluating and reporting a new diagnostic test. European journal of clinical microbiology & infectious diseases. 2012 Sep;31(9):2111-6.
- Hitchings RA, Spaeth GL. The optic disc in glaucoma. I: Classification. British journal of ophthalmology. 1976 Nov 1;60(11):778-85.
- Irving EL, González EG, Lillakas L et al., Effect of stimulus type on the eye movements of children. Investigative ophthalmology & visual science. 2011 Feb 1;52(2):658-64.
- Jernigan ME. Structural analysis of eye movement response to visual field stimuli. Computers in Biology and Medicine. 1980 Jan 1;10(1):11-22.
- Johnson CA, Samuels SJ. Screening for glaucomatous visual field loss with frequency-doubling perimetry. Investigative Ophthalmology & Visual Science. 1997 Feb 1;38(2):413-25.
- Jones PR, Kalwarowsky S, Atkinson J et al., Automated measurement of resolution acuity in infants using remote eye-tracking. Investigative ophthalmology & visual science. 2014 Dec 1;55(12):8102-10.
- Jones PR, Campbell P, Callaghan T et al., Glaucoma home monitoring using a tablet-based visual field test (Eyecatcher): an assessment of accuracy and adherence over 6 months. American journal of ophthalmology. 2021 Mar 1;223:42-52.

- Kalaboukhova L, Fridhammar V, Lindblom B. An objective method for measuring relative afferent pupillary defect in glaucomatous optic neuropathy—stimulus optimisation. Neuro-ophthalmology. 2006 Jan 1;30(1):7-15.
- Kawasaki A. Physiology, assessment, and disorders of the pupil. Current opinion in ophthalmology. 1999 Dec 1;10(6):394-400.
- Kedar S, Ghate D, Corbett JJ. Visual fields in neuro-ophthalmology. Indian journal of ophthalmology. 2011 Mar;59(2):103.
- Kelly DJ, Jack RE, Miellet S et al., Social experience does not abolish cultural diversity in eye movements. Frontiers in psychology. 2011 May 18;2:95.
- Kim DE, Eizenman M, Trope GE, Kranemann C. Eye movement perimetry. In Proceedings of 17th International Conference of the Engineering in Medicine and Biology Society 1995 Sep 20 (Vol. 2, pp. 1629-1630).
- Kleiner M, Brainard D, Pelli D et al., What's new in Psychtoolbox-3. Perception. 2007 Aug 27; 36(14):1
- Knox PC, Wolohan FD. Cultural diversity and saccade similarities: Culture does not explain saccade latency differences between Chinese and Caucasian participants. PloS one. 2014 Apr 7;9(4):e94424.
- Kotani J, Nakao H, Yamada I et al., A Novel Method for Measuring the Pupil Diameter and Pupillary Light Reflex of Healthy Volunteers and Patients With Intracranial Lesions Using a Newly Developed Pupilometer. Frontiers in Medicine. 2021:1362.
- Kotecha M, Gotecha S, Chugh A et al., Neuroophthalmic Manifestations of Intracranial Tumours in Children. Case Reports in Ophthalmological Medicine. 2021 May 15;2021.
- Kowler E. Eye movements: The past 25 years. Vision research. 2011 Jul 1;51(13):1457-83.
- Kozak I, Rahn U. Navigation technology/eye-tracking in ophthalmology: principles, applications and benefits—a narrative review.
- Kravitz DJ, Saleem KS, Baker CI et al., A new neural framework for visuospatial processing. Nature Reviews Neuroscience. 2011 Apr;12(4):217-30.
- Kupersmith MJ, Gal RL, Beck RW et al., Optic Neuritis Study Group. Visual function at baseline and 1 month in acute optic neuritis: predictors of visual outcome. Neurology. 2007 Aug 7;69(6):508-14.
- Kurz S, Krummenauer F, Pfeiffer N et al., Monocular versus binocular pupillometry. Journal of Cataract & Refractive Surgery. 2004 Dec 1;30(12):2551-6.
- Lee JY, Cho HK, Kee C. Assessment of the Vision-Specific Quality of Life Using Binocular Esterman Visual Field in Glaucoma Patients. Journal of the Korean Ophthalmological Society. 2013 Oct 15;54(10):1567-72.
- Leiba H, Glaser JS, Schatz NJ et al., Postpartum optic neuritis: etiologic and pathophysiologic considerations. Journal of Neuro Ophthalmology. 2000 Jun 1;20(2):85-8.

- Leigh RJ, Zee DS. The neurology of eye movements. Contemporary Neurology; 2015
- Lei S, Goltz HC, Chandrakumar M et al., Full-field chromatic pupillometry for the assessment of the postillumination pupil response driven by melanopsin-containing retinal ganglion cells. Investigative Ophthalmology & Visual Science. 2014 Jul 1;55(7):4496-503.
- Leitner MC, Hutzler F, Schuster S et al., Eye-tracking-based visual field analysis (EFA): a reliable and precise perimetric methodology for the assessment of visual field defects. BMJ open ophthalmology. 2021 Mar 1;6(1):e000429.
- Leong JJ, Nicolaou M, Emery RJ et al., Visual search behaviour in skeletal radiographs: a cross-speciality study. Clinical radiology. 2007 Nov 1;62(11):1069-77.
- Levatin P. Pupillary escape in disease of the retina or optic nerve. AMA Archives of Ophthalmology. 1959 Nov 1;62(5):768-79
- Litvan I, Saposnik G, Maurino J et al., Pupillary diameter assessment: need for a graded scale. Neurology. 2000 Jan 25;54(2):530-.
- Litzinger TC, Del Rio-Tsonis K. Eye anatomy. Encyclopedia of life science. 2002.
- Luna B, Velanova K, Geier CF. Development of eye-movement control. Brain and cognition. 2008 Dec 1;68(3):293-308.
- MacAskill MR, Anderson TJ. Eye movements in neurodegenerative diseases. Current opinion in neurology. 2016 Feb 1;29(1):61-8.
- Mardanbegi D, Wilcockson TD, Killick R et al., A comparison of post-saccadic oscillations in European-Born and China-Born British University Undergraduates. Plos one. 2020 Feb 25;15(2):e0229177.
- Martin JT, Pinto J, Bulte D et al., PyPlr: A versatile, integrated system of hardware and software for researching the human pupillary light reflex. Behavior Research Methods. 2021 Dec 16:1-20.
- Martinez-Conde S, Macknik SL, Hubel DH. The role of fixational eye movements in visual perception. Nature reviews neuroscience. 2004 Mar;5(3):229-40.
- Mathôt S. Pupillometry: Psychology, physiology, and function. Journal of Cognition. 2018;1(1).
- Mazumdar D, Pel JM, Panday M et al., Comparison of saccadic reaction time between normal and glaucoma using an eye movement perimeter. Indian journal of ophthalmology. 2014 Jan;62(1):55.
- Mazumdar D, Meethal NS, Panday M et al., Effect of age, sex, stimulus intensity, and eccentricity on saccadic reaction time in eye movement perimetry. Translational Vision Science & Technology. 2019 Jul 1;8(4):13-.
- Mazumdar D, Pel JJ, Kadavath Meethal NS et al., Visual field plots: A comparison study between standard automated perimetry and eye movement perimetry. Journal of Glaucoma. 2020 May 21;29(5):351-61.

- McDougal, D. H. & Gamlin, P. D. Autonomic control of the eye. Compr. Physiol. 2015; 5(1), 439.
- McKone E, Davies AA, Fernando D et al., Asia has the global advantage: Race and visual attention. Vision research. 2010 Jul 21;50(16):1540-9.
- McTrusty AD, Cameron LA, Perperidis A et al., Comparison of threshold saccadic vector optokinetic perimetry (SVOP) and standard automated perimetry (SAP) in glaucoma. Part II: patterns of visual field loss and acceptability. Translational vision science & technology. 2017 Sep 1;6(5):4-.
- Meeker M, Du R, Bacchetti P et al., Pupil examination: validity and clinical utility of an automated pupillometer. Journal of Neuroscience Nursing. 2005 Feb 1;37(1):34.
- Meethal NS, Pel JJ, Mazumdar D et al., Eye movement perimetry and frequency doubling perimetry: clinical performance and patient preference during glaucoma screening. Graefe's Archive for Clinical and Experimental Ophthalmology. 2019 Jun;257(6):1277-87.
- Meethal NS, Lokapavani V, Asokan R et al., SITA standard testing with Humphrey visual field analyzer versus full threshold testing with frequency doubling perimetry: a comparison of patient preference and perception. Asian Journal of Ophthalmology. 2019;17(1):45-55.
- Meethal NS, Robben J, Mazumdar D et al., Detection of visual field defects using Eye Movement Pediatric Perimetry in children with intracranial lesions: feasibility and applicability. Heliyon. 2022 Nov 17:e11746.
- Miguel CS, Chaim-Avancini TM, Silva MA et al., Neurofibromatosis type 1 and attention deficit hyperactivity disorder: a case study and literature review. Neuropsychiatric disease and treatment. 2015;11:815.
- Mosimann UP, Müri RM, Burn DJ et al., Saccadic eye movement changes in Parkinson's disease dementia and dementia with Lewy bodies. Brain. 2005 Jun 1;128(6):1267-76.
- Monkhouse S. Cranial nerves: functional anatomy. Cambridge University Press; 2005 Oct 13.
- Montaleone P. The optic nerve: A clinical perspective. Univ West Ont Med J. 2010;79:37-9.
- Munoz DP, Broughton JR, Goldring JE et al., Age-related performance of human subjects on saccadic eye movement tasks. Experimental brain research. 1998 Aug;121(4):391-400.
- Murray IC, Fleck BW, Brash HM et al., Feasibility of saccadic vector optokinetic perimetry: a method of automated static perimetry for children using eye tracking. Ophthalmology. 2009 Oct 1;116(10):2017-26.
- Murray I, Perperidis A, Brash H et al., Saccadic Vector Optokinetic Perimetry (SVOP): a novel technique for automated static perimetry in children using eye tracking. In 2013 35th Annual International Conference of the IEEE Engineering in Medicine and Biology Society (EMBC) 2013 Jul 3 (pp. 3186-3189). IEEE.

- Murray IC, Schmoll C, Perperidis A, Brash HM, McTrusty AD, Cameron LA, Wilkinson AG, Mulvihill AO, Fleck BW, Minns RA. Detection and characterisation of visual field defects using Saccadic Vector Optokinetic Perimetry in children with brain tumours. Eye. 2018 Oct;32(10):1563-73.
- Naber M, Frässle S, Einhäuser W. Perceptual rivalry: reflexes reveal the gradual nature of visual awareness. PLoS One. 2011 Jun 3;6(6):e20910.
- Najjar RP, Sharma S, Drouet M et al., Disrupted eye movements in preperimetric primary open-angle glaucoma. Investigative ophthalmology & visual science. 2017 Apr 1;58(4):2430-7.
- Nakano T, Higashida N, Kitazawa S. Facilitation of face recognition through the retino-tectal pathway. Neuropsychologia. 2013 Aug 1;51(10):2043-9.
- Nelson-Quigg JM, Cello K, Johnson CA. Predicting binocular visual field sensitivity from monocular visual field results. Investigative ophthalmology & visual science. 2000 Jul 1;41(8):2212-21.
- Niehorster DC, Cornelissen TH, Holmqvist K et al., What to expect from your remote eye-tracker when participants are unrestrained. Behavior research methods. 2018 Feb;50(1):213-27.
- Nieuwenhuys R, Voogd J, Van Huijzen C. The human central nervous system: a synopsis and atlas. Springer Science & Business Media; 2007 Dec 31.
- Nowak W, Żarowska A, Szul-Pietrzak E et al., System and measurement method for binocular pupillometry to study pupil size variability. Biomedical engineering online. 2014 Dec;13(1):1-6.
- Nyström M, Andersson R, Holmqvist K et al., The influence of calibration method and eye physiology on eyetracking data quality. Behavior research methods. 2013 Mar;45(1):272-88.

- O'Neill EC, Kong YX, Connell PP et al., Gaze behavior among experts and trainees during optic disc examination: does how we look affect what we see?. Investigative ophthalmology & visual science. 2011 Jun 1;52(7):3976-83.
- Özyurt J, Greenlee MW. Neural correlates of inter-and intra-individual saccadic reaction time differences in the gap/overlap paradigm. Journal of neurophysiology. 2011 May;105(5):2438-47.
- Patel DE, Cumberland PM, Walters BC et al., Study of Optimal Perimetric Testing in Children (OPTIC): evaluation of kinetic approaches in childhood neuro-ophthalmic disease. British Journal of Ophthalmology. 2019 Aug 1;103(8):1085-91.
- Patel SC, Friedman DS, Varadkar P et al., Algorithm for interpreting the results of frequency doubling perimetry. American journal of ophthalmology. 2000 Mar 1;129(3):323-7.

- Peinkhofer C, Knudsen GM, Moretti R et al., Cortical modulation of pupillary function: systematic review. PeerJ. 2019 May 7;7:e6882.
- Pel JJ, Manders JC, Van der Steen J. Assessment of visual orienting behaviour in young children using remote eye tracking: methodology and reliability. Journal of Neuroscience Methods. 2010 Jun 15;189(2):252-6.
- Pel JJ, van Beijsterveld MC, Thepass G et al., Validity and repeatability of saccadic response times across the visual field in eye movement perimetry. Translational vision science & technology. 2013 Nov 1;2(7):3-.
- Perperidis A, McTrusty AD, Cameron LA, Murray IC, Brash HM, Fleck BW, Minns RA, Tatham AJ. The assessment of visual fields in infants using saccadic vector optokinetic perimetry (SVOP): A feasibility study. Translational Vision Science & Technology. 2021 Mar 1;10(3):14-.
- Perry VH, Cowey A. The ganglion cell and cone distributions in the monkey's retina: implications for central magnification factors. Vision research. 1985 Jan 1;25(12):1795-810.
- Pierrot-Deseilligny CH, Ploner CJ, Müri RM et al., Effects of cortical lesions on saccadic: eye movements in humans. Annals of the New York Academy of Sciences. 2002 Apr;956(1):216-29.
- Pierrot-Deseilligny C, Müri RM, Ploner CJ et al., Cortical control of ocular saccades in humans: a model for motricity. Progress in brain research. 2003 Jan 1;142:3-17.
- Pillai MR, Sinha S, Aggarwal P et al., Quantification of RAPD by an automated pupillometer in asymmetric glaucoma and its correlation with manual pupillary assessment. Indian Journal of Ophthalmology. 2019 Feb;67(2):227.
- Poletti M, Rucci M. Eye movements under various conditions of image fading. Journal of vision. 2010 Mar 1;10(3):6-.
- Quigley HA. Identification of glaucoma-related visual field abnormality with the screening protocol of frequency doubling technology. American journal of ophthalmology. 1998 Jun 1;125(6):819-29.
- Radzius A, Welch P, Cone EJ et al., A portable pupilometer system for measuring pupillary size and light reflex. Behavior Research Methods, Instruments, & Computers. 1989 Nov;21(6):611-8.
- Ramey NA, Ying HS, Irsch K et al., A novel haploscopic viewing apparatus with a three-axis eye tracker. Journal of American Association for Pediatric Ophthalmology and Strabismus. 2008 Oct 1;12(5):498-503.
- Rayner K, Li X, Williams CC et al., Eye movements during information processing tasks: Individual differences and cultural effects. Vision research. 2007 Sep 1;47(21):2714-26.
- Reulen JP, Sanders EA, Hogenhuis LA. Eye movement disorders in multiple sclerosis and optic neuritis. Brain. 1983 Mar 1;106(1):121-40.

- Reulen JP. Latency of visually evoked saccadic eye movements. Biological cybernetics. 1984 Jul;50(4):251-62.
- Rukmini AV, Milea D, Gooley JJ. Chromatic pupillometry methods for assessing photoreceptor health in retinal and optic nerve diseases. Frontiers in neurology. 2019 Feb 12;10:76.
- Sadun AA. Neuroanatomy of the human visual system: Part I Retinal projections to the LGN and pretectum as demonstrated with a new method. Neuro-ophthalmology. 1986 Jan 1;6(6):353-61.
- Said FS, Sawires WS. Age dependence of changes in pupil diameter in the dark. Optica Acta: International Journal of Optics. 1972 May 1;19(5):359-61.
- Salman MS, Sharpe JA, Eizenman M et al., Saccades in children. Vision Research. 2006 Apr 1;46(8-1
- Schnitzler EM, Baumeister M, Kohnen T. Scotopic measurement of normal pupils: Colvard versus Video Vision Analyzer infrared pupillometer. Journal of Cataract & Refractive Surgery. 2000 Jun 1;26(6):859-66.
- Sharma P, Sample PA, Zangwill LM et al., Diagnostic tools for glaucoma detection and management. Survey of ophthalmology. 2008 Nov 1;53(6):S17-32.
- Shin YD, Bae JH, Kwon EJ et al., Assessment of pupillary light reflex using a smartphone application. Experimental and Therapeutic Medicine. 2016 Aug 1;12(2):720-4.
- Shwe-Tin A, Smith GT, Checketts D et al., Evaluation and calibration of a binocular infrared pupillometer for measuring relative afferent pupillary defect. Journal of Neuro-Ophthalmology. 2012 Jun 1;32(2):111-5.
- Smeets JB, Hooge IT. Nature of variability in saccades. Journal of neurophysiology. 2003 Jul;90(1):12-20.
- Smith ND, Glen FC, Crabb DP. Eye movements during visual search in patients with glaucoma. BMC ophthalmology. 2012 Dec;12(1):1-1.
- Soans RS, Grillini A, Saxena R et al., Eye-movement–based assessment of the perceptual consequences of glaucomatous and neuro-ophthalmological visual field defects. Translational Vision Science & Technology. 2021 Feb 5;10(2):1-.
- Stangor C, Walinga J. Introduction to psychology-1st Canadian edition. 2014
- Szczepanowska-Nowak WI, Hachol A, Kasprzak H. System for measurement of the consensual pupil light reflex. Opt Appl. 2004 Jan 1;34(4):619-34.
- Takagi M, Frohman EM, Zee DS. Gap-overlap effects on latencies of saccades, vergence and combined vergence-saccades in humans. Vision Research. 1995 Dec 1;35(23-24):3373-88.
- Takizawa G, Miki A, Maeda F et al., Relative afferent pupillary defects in homonymous visual field defects caused by stroke of the occipital lobe using pupillometer. Neuro-Ophthalmology. 2018 May 4;42(3):139-45.

- Tamietto M, Morrone MC. Visual plasticity: blindsight bridges anatomy and function in the visual system. Current Biology. 2016 Jan 25;26(2):R70-3.
- Tatham AJ, Murray IC, McTrusty AD et al., A case control study examining the feasibility of using eye tracking perimetry to differentiate patients with glaucoma from healthy controls. Scientific Reports. 2021 Jan 12;11(1):1-0.
- Tekin K, Sekeroglu MA, Kiziltoprak H et al., Static and dynamic pupillometry data of healthy individuals. Clinical and Experimental Optometry. 2018 Sep 1;101(5):659-65.
- Tham YC, Li X, Wong TY et al., Global prevalence of glaucoma and projections of glaucoma burden through 2040: a systematic review and meta-analysis. Ophthalmology. 2014 Nov 1;121(11):2081-90.
- Thepass G, Pel JJ, Vermeer KA, Creten O, Bryan SR, Lemij HG, van der Steen J. The effect of cataract on eye movement perimetry. Journal of ophthalmology. 2015 Jan 1;2015.
- Thepass G, Lemij HG, Vermeer KA et al., Slowed Saccadic Reaction Times in Seemingly Normal Parts of Glaucomatous Visual Fields. Frontiers in Medicine. 2021;8.
- Thomas R, Bhat S, Muliyil JP et al., Frequency doubling perimetry in glaucoma. Journal of glaucoma. 2002 Feb 1;11(1):46-50.
- Thomas R, Loibl K, Parikh R. Evaluation of a glaucoma patient. Indian journal of ophthalmology. 2011 Jan;59(Suppl1):S43.
- Trope GE, Eizenman M, Coyle E. Eye movement perimetry in glaucoma. Canadian Journal of ophthalmology. Journal Canadien D'ophtalmologie. 1989 Aug 1;24(5):197-9.
- Toepfer A, Kasten E, Guenther T et al., Perimetry while moving the eyes: implications for the variability of visual field defects. Journal of Neuro-Ophthalmology. 2008 Dec 1;28(4):308-19.
- Varma R, Lee PP, Goldberg I et al., An assessment of the health and economic burdens of glaucoma. American journal of ophthalmology. 2011 Oct 1;152(4):515-22.
- Vaswani RS, Mudgil AV, Gleicher D. Correlation of pupil size to iris color in children. Journal of Refractive Surgery. 2002 Mar 1;18(2):189-.
- Vikesdal GH, Langaas T. Optically induced refractive errors reduces fixation stability but saccade latency remains stable. Journal of Eye Movement Research. 2016, 9 (7)
- Voets NL, Bartsch A, Plaha P. Brain white matter fibre tracts: a review of functional neuro-oncological relevance. Journal of Neurology, Neurosurgery & Psychiatry. 2017 Dec 1;88(12):1017-25.
- Vogel AC, Gutmann DH, Morris SM. Neurodevelopmental disorders in children with neurofibromatosis type 1. Developmental Medicine & Child Neurology. 2017 Nov;59(11):1112-6.
- Wade NJ. Pioneers of eye movement research. i-Perception. 2010 Aug;1(2):33-68.

- Warren DE, Thurtell MJ, Carroll JN et al., Perimetric evaluation of saccadic latency, saccadic accuracy, and visual threshold for peripheral visual stimuli in young compared with older adults. Investigative ophthalmology & visual science. 2013 Aug 1;54(8):5778-87.
- Weinreb RN, Khaw PT. Primary open-angle glaucoma. The lancet. 2004 May 22;363(9422):1711-20.
- Wiencken-Barger, A. E., and V. A. Casagrande. "Visual system development and neural activity." (2002): 791-804.
- Wilhelm H, Schabet M. The diagnosis and treatment of optic neuritis. Deutsches Ärzteblatt International. 2015 Sep;112(37):616.
- Winn B, Whitaker D, Elliott DB et al., Factors affecting light-adapted pupil size in normal human subjects. Investigative ophthalmology & visual science. 1994 Mar 1;35(3):1132-7.
- Wirtschafter JD, Hard-Boberg AL, Coffman SM. Evaluating the usefulness in neuro-ophthalmology of visual field examinations peripheral to 30 degrees. Transactions of the American Ophthalmological Society. 1984;82:329.
- Wilson-Pauwels L, Akesson EJ, Stewart PA et al., Cranial nerves in health and disease. PMPH USA (BC Decker); 2002.
- Woodhouse JM, Campbell FW. The role of the pupil light reflex in aiding adaptation to the dark. Vision research. 1975 Jun 1;15(6):649-53.
- Woods DL, Wyma JM, Yund EW et al., Factors influencing the latency of simple reaction time. Frontiers in human neuroscience. 2015 Mar 26;9:131.
- Yamagishi S, Furukawa S. Factors Influencing Saccadic Reaction Time: Effect of Task Modality, Stimulus Saliency, Spatial Congruency of Stimuli, and Pupil Size. Frontiers in Human Neuroscience. 2020 Nov 26;14:571893.
- Yang Q, Bucci MP, Kapoula Z. The latency of saccades, vergence, and combined eye movements in children and in adults. Investigative Ophthalmology & Visual Science. 2002 Sep 1;43(9):2939-49.
- Yang GZ, Dempere-Marco L, Hu XP et al., Visual search: psychophysical models and practical applications. Image and vision computing. 2002 Apr 1;20(4):291-305..
- Yoo YJ, Yang HK, Hwang JM. Efficacy of digital pupillometry for diagnosis of Horner syndrome. PloS one. 2017 Jun 2;12(6):e0178361.
- Yoo H, Mihaila DM. Neuroanatomy, pupillary light reflexes and pathway. InStatPearls [Internet] 2021 Aug 11. StatPearls Publishing.
- Yu HH, Rosa MG. A simple method for creating wide-field visual stimulus for electrophysiology: mapping and analysing receptive fields using a hemispheric display. Journal of Vision. 2010 Dec 1;10(14):15-.
- Zele AJ, Gamlin PD. The pupil: behavior, anatomy, physiology and clinical biomarkers. Frontiers in Neurology. 2020 Apr 9;11:211.

PORTFOLIO

PhD Student: Najiya Sundus Kadavath Meethal	PhD Period: October 2017 – June 2022
Erasmus MC Department: Neuroscience	Promotor: Prof. Dr. J. van der Steen
	Dr. R.J. George
Research School: ONWAR	Co-Promotor: Dr. ir. J.J.M. Pel

1. PhD Training	**Years**	**Workload (ECTS)**
General/specific Courses:		
▪ Data management for clinical research, certification issued by Vanderbilt University (Online program, Coursera)	2017	1.00
▪ Glaucoma - evaluation & diagnostics (Glaucoma department, Medical Research Foundation, Chennai, India)	2017-2018	2.00
▪ Research methodology - Scientific literature search & critical review, scientific research (Medical Research Foundation, Chennai, India)	2017-2019	3.00
▪ Biostatistics - Statistical tool packages (Medical Research Foundation, Chennai, India)	2017-2019	1.50
▪ Scientific/technical writing (Medical Research Foundation, Chennai, India)	2017-2019	1.50
▪ Medical & Surgical Management of Glaucoma under Glaucoma management (Glaucoma department, Medical Research Foundation, Chennai, India)	2018	0.50
▪ Scientific Integrity - Best & professional practices in research, intellectual honesty, adherence to ethical considerations & good clinical practice (Medical Research Foundation, Chennai, India)	2018-2019	1.00

▪	Good Clinical Practice (GCP), certification issued by NIDA Clinical Trails Network	2021	2.00
▪	MATLAB – Basics & programming (Department of Neuroscience, Erasmus MC, Rotterdam, The Netherlands)	2022	1.00

Institutional visits:

▪	VU University Medical Centre, Amsterdam, The Netherlands	2017	0.50
▪	Lamirus, Ede, The Netherlands	2017	0.50
▪	Vasan Institute of Ophthalmology & Research, Malappuram, Kerala, India	2017	0.50
▪	Manipal School of Allied Health Sciences, Manipal, India	2018	0.50
▪	Bulbitech AS, Trondheim, Norway	2018	0.50
▪	The Department of Optometry & Vision Science, University of Melbourne, Australia	2019	0.50
▪	The Department of Optometry & Vision Science, SRM Institute of Science & Technology, Chennai, India	2021	0.50

2. Scientific participations	**Years**	**Workload (ECTS)**

(Inter) national conference presentations (as a presenting author):

▪	Vision 2017 (12th International conference by the ISLRR), The Hague, The Netherlands	2017	1.00
▪	Sankara Nethralaya Glaucoma Meet (SANGAM), Chennai, India	2017	1.00
▪	World Congress of Optometry (2nd WCO), Hyderabad, India	2017	1.00
▪	Indian Eye Research Group – ARVO - India Chapter (25th IERG-ARVO-IC), Hyderabad, India	2018	1.00

▪ World Glaucoma Congress (8th WGC), Melbourne, Australia	2019	1.00
▪ Indian Eye Research Group – ARVO - India Chapter (26th IERG-ARVO-IC), Chennai, India	2019	1.00
▪ India Vision Institute (IVI) symposium, India	2021	1.00
▪ India Vision Institute (2nd IVI International optometry conference), India	2021	1.00

(Inter) national conference presentations (as a co-author):

▪ Vision 2017, 12th International conference by the ISLRR, The Hague, The Netherlands (2nd author)	2017	0.50
▪ Sankara Nethralaya Glaucoma Meet (SAN-GAM), Chennai, India (2nd author)	2017	0.50
▪ World Congress of Optometry (WCO), Hyderabad, India (2nd author)	2017	0.50
▪ World Glaucoma Congress (8th WGC), Melbourne, Australia (2nd author)	2019	0.50
▪ Kongsberg Vision Meeting 2019, Kongsberg, Norway	2019	0.50
▪ Dr. E.V. Memorial Scientific session (19th Dr. EVM) Chennai, India (2x as 2nd author)	2021	1.00
▪ India Vision Institute (2nd IVI International optometry conference), India (4x as 2nd author)	2021	2.00
▪ Indian Eye Research Group – ARVO - India Chapter (27th IERG-ARVO-IC), India (2x as 2nd author)	2021	1.00
▪ Dr. E.V. Memorial Scientific session (20th Dr. EVM) Chennai, India (2x as 2nd author)	2022	1.00

Workshops/Seminars/Lectures (as an invited speaker):

▪ Research Methodology workshop series, 8x (Elite School of Optometry, Chennai, India)	2017 - 2020	1.00

▪ Guest lecture on Primary care in glaucoma (Vasan institute for ophthalmology & research, Kerala, India)	2017	2.00
▪ Workshop on glaucoma detection & referral How & When (The Sankara Nethralaya Academy & Optometric Association of Tamil Nanbargal, Chennai, India)	2018	1.00
▪ Invited talk on neuro-ophthalmology, State annual conference & scientific seminar (Indian Optometrists Association, Kerala, India)	2018	2.00
▪ Glaucoma workshop (Optometric Association of Tamil Nanbargal, Chennai, India)	2018	1.00
▪ Workshop on Research Methodology for Diplomate of National Board candidates in Ophthalmology (Sankara Nethralaya, Chennai, India)	2019	1.00
▪ Webinar on neuro-ophthalmology (Malabar Institute of Optometry, Thrissur, Kerala, India)	2020	2.00
▪ Webinar on perimetry (Optometric Association of Tamil Nanbargal, Chennai, India)	2020	2.00
▪ Webinar on neuro-ophthalmology (Optometry Association of Assam, India)	2020	2.00
▪ Webinar on scientific research (Paathshala – learning platform, India)	2021	2.00
▪ ResMeet 2022 (India Vision Institute symposium, India)	2022	2.00

(Inter) national conferences/Workshops/Seminars/Lectures (as an attendee):

▪ Dr. E. Vaithilingam Memorial Scientific Sessions, (Elite School of Optometry, a unit of Medical Research Foundation, Chennai, India)	2017-2019, 2021	1.00

▪	Pedagogy & assessment workshop for optometrist (3-day workshop) (Department of Medical Education, Kasturba Medical College, Manipal, India)	2018	1.00
▪	Google AI: Artificial Intelligence in ophthalmic diagnostics - In collaboration with Medical & Vision Research Foundation & Google	2019	0.50
▪	Pupil examination & assessment: A skill must for an optometrist Speaker: Dr. Rashmin Gandhi (Optometric Association of Tamil Nanbargal, Chennai, India)	2020	0.50
▪	Role of optometrist in Occupational health – Speaker: Dr. Krishnakumar R. (Optometric Association of Tamil Nanbargal, Chennai, India)	2020	0.50
▪	An overview of Research Methodology for clinicians (Dr. Shroff's eye care hospital, India)	2020	0.50
▪	How to start a research? Speaker: Dr. Kalpa Negiloni (Optometry Association of Assam, India)	2020	0.50
▪	Ophthalmic imaging in Glaucoma diagnosis Speaker: Dr. Rashima Asokan (Optometry Association of Assam, India)	2020	0.50
▪	Enhancing research capacities for ophthalmologists (Medical & Vision Research Foundation, Chennai, India)	2020	0.50
▪	Low vision care: A community based approach Speaker: Ms. Devi D. R. (Optometric Association for Tamil Nanbargal, India)	2020	0.50

Department talks/Lectures:

▪	Research cell meetings (attendance: 2x) Medical Research Foundation, Chennai, India	2017, 2019	0.50

▪ Neuroscience lab talks (Presenter: 5x) Erasmus MC, Rotterdam, The Netherlands	2017-2021	2.50
▪ Glaucoma department talks (Presenter: 5x) Medical Research Foundation, Chennai, India	2017-2021	2.50
▪ Glaucoma department talks (Attendance: 48x) Medical Research Foundation, Chennai, India	2018-2021	6.00

Technical write-ups:

▪ A guest column titled: Envisioning the brink beyond refraction Opsis - a magazine, The Indian Optometrists Association (IOA), Kerala	2018	0.25
▪ A guest column titled: Eye-tracking Technology in Ophthalmic practice Vision Science Academy (VSA), London, UK	2021	0.25
▪ A Technical write-up titled: Channelising your competency in optometry Lumos - an e-magazine, The Optometry Association of Assam, India	2021	0.25
▪ A Technical write-up titled: Mendeley reference manager: A Step-by-step Guide e-Ophtha (Online portal), India	2021	0.25
▪ A Technical write-up titled: Zotero: A quick start Guide e-Ophtha (Online portal), India	2021	0.25
▪ A Technical write-up titled: The clinical pearls in astigmatic refractive care e-Ophtha (Online portal), India	2021	0.25

Others:

▪ Member and facilitator of research methodology workshop series (Elite School of Optometry, a unit of Medical Research Foundation, Chennai, India)	2017-2020	4.00

	Years	Workload (ECTS)
■ Member of the research advisory board for the project: Development of a prototype eye tracking technology to evaluate oculomotor functions. (Bulbi-Tech, Trondheim, Norway)	2017-Present	1.50
■ Organiser & facilitator for 'Ideas to Reality' – as seminary conducted as a part of the 18th Dr. E. Vaithilingam Memorial Scientific Session. (Elite School of Optometry, a unit of Medical Research Foundation, Chennai, India)	2019	0.50
■ Executive member of the scientific committee in 18th Dr. E. Vaithilingam Memorial Scientific Session. (Elite School of Optometry, a unit of Medical Research Foundation, Chennai, India)	2019	0.50
■ Certificate of recognition: World Glaucoma Association for special & distinct service	2021	0.50

3. Academic participations	Years	Workload (ECTS)
Lecturing/Teaching:		
■ 'Glaucoma': 3rd year Bachelor students of Optometry Elite School of Optometry, A unit of Medical Research Foundation, Chennai, India	2017	0.50
■ Examiner for 'Optometric Optics': 2nd year Bachelor students of Optometry Elite School of Optometry, A unit of Medical Research Foundation, Chennai, India	2017	0.50
■ 'Common clinical conditions': 3rd year Bachelor students of Optometry Elite School of Optometry, A unit of Medical Research Foundation, Chennai, India.	2017-2019	1.50

▪ Moderator for the 'Inter-College Continuous Medical Education & case discussion': 3rd & 4th year Bachelor students of Optometry Elite School of Optometry, A unit of Medical Research Foundation, Chennai, India	2017-2018	1.00
▪ Co-editor & first author (Four chapters) for the EcSelO (ESO's Case Scenario based e-learning in Optometry) Elite School of Optometry, A unit of Medical Research Foundation, Chennai, India	2017-2018	2.50
▪ Clinical mentoring: 4th year Bachelor students of Optometry Elite School of Optometry, A unit of Medical Research Foundation, Chennai, India	2017-2019	1.50
▪ Examiner for 'The clinical evaluation of visual system': 2nd year Bachelor students of Optometry SRM Institute of Science & Technology, Chennai, India	2019	0.50

Supervision/Guidance:

▪ Evaluator for the undergraduate theses in various Optometry specialties – 3rd year Bachelor of Science in Optometry (5x) (Elite School of Optometry, A unit of Medical Research Foundation, Chennai, India)	2017	1.25
▪ Evaluator for the undergraduate theses in various Optometry specialties – 3rd year Bachelor of Science in Optometry (11x) (Elite School of Optometry, A unit of Medical Research Foundation, Chennai, India)	2017-2018	2.75

▪	Supervised Research protocol writing - Bachelor in Medical electronics engineering (College of Engineering, Anna University, Chennai, India)	2018	0.25
▪	Supervision of Master's in Optometry research thesis titled: 'The evaluation and preference of visual field staging classification systems in glaucoma by Eye Care Practitioners' (The Sankara Nethralaya Academy, Chennai, India)	2019-2021	2.00
▪	Supervision of Master's in Optometry research thesis titled: 'Construction and validation of a low-cost visual field screener for glaucoma' (The Sankara Nethralaya Academy, Chennai, India)	2019-2021	2.00
▪	Supervision of Master's in Optometry research thesis titled: 'The evaluation of Low Contrast Visual Acuity as an outcome measure in Optic Neuritis' (The Sankara Nethralaya Academy, Chennai, India)	2019-2021	2.00
▪	Supervision of Master's in Optometry research thesis titled: 'Quality of life among patients with glaucoma and the impact of low vision services' (The Sankara Nethralaya Academy, Chennai, India)	2020-2022	2.00
▪	Evaluator for the undergraduate theses in various Optometry specialties - Bachelor of Science in Optometry, Defense presentation (15x) (SRM Institute of Science & Technology, Chennai, India)	2021	3.75

Total ECTS: 100.5

LIST OF PUBLICATIONS

Original articles ---

- **Meethal NS**, Mazumdar D, Asokan R, Panday M, van der Steen J, Vermeer KA, Lemij HG, George RJ, Pel JJ. *Development of a test grid using eye movement perimetry for screening glaucomatous visual field defects.* Graefe's Archive for Clinical and Experimental Ophthalmology. 2018 Feb; 256(2):371-9.

- **Meethal NS**, Pel JJ, Mazumdar D, Asokan R, Panday M, van der Steen J, George R. *Eye Movement Perimetry and Frequency Doubling Perimetry: clinical performance and patient preference during glaucoma screening.* Graefe's Archive for Clinical and Experimental Ophthalmology. 2019 Jun; 257(6):1277-87.

- Mazumdar D, **Meethal NS**, Panday M, Asokan R, Thepass G, George RJ, van der Steen J, Pel JJ. *Effect of age, sex, stimulus intensity, and eccentricity on saccadic reaction time in eye movement perimetry.* Translational Vision Science & Technology. 2019 Jul 1; 8(4):13-.

- **Meethal NS**, Lokapavani V, Asokan R, Vijaya L, George RJ. *SITA standard testing with Humphrey visual field analyzer versus full threshold testing with frequency doubling perimetry: a comparison of patient preference and perception.* Asian Journal of Ophthalmology. 2019; 17(1):45-55.

- Mazumdar D, Pel JJ, **Meethal NS**, Asokan R, Panday M, George R. *Visual field plots: A comparison study between standard automated perimetry and eye movement perimetry.* Journal of Glaucoma. 2020 May 21; 29(5):351-61.

- Mazumdar D, **Meethal NS**, George R, Pel JJ. *Saccadic reaction time in mirror image sectors across horizontal meridian in eye movement perimetry.* Scientific Reports. 2021 Jan 29; 11(1):1-1.

- **Meethal NS**, Mazumdar D, Morshchavka S, Robben J, van der Steen J, George R, Pel JJ. *A haploscope based binocular pupillometer system to quantify the dynamics of direct and consensual Pupillary Light Reflex.* Scientific reports. 2021 Oct 26; 11(1):1-3.

- **Meethal NS**, Robben J, Mazumdar D, Loudon S, Naus N, Polling JR, van der Steen J, George R, Pel JJ. *Detection of visual field defects using Eye Movement Pediatric Perimetry in children with intracranial lesions: feasibility and applicability*. Heliyon. 2022 Nov 17:e11746.

Book chapters ---

- *Automated Perimetry interpretation in glaucoma.* Atlas of Glaucoma, Springer (in Press)

- *Visual field progression,* Atlas of Glaucoma, Springer (in Press)

- *Optic Nerve Head evaluation and imaging in glaucoma*, Atlas of Glaucoma, Springer (in Press)

LIST OF AWARDS AND ACCOLADES

- 2017: Dr. Narasimhan memorial award for the Best Research in Optometry, instituted by Elite School of Optometry (ESO), a unit of Medical Research Foundation (MRF), Chennai, India, for the research work titled: "*Development of a test grid using Eye Movement Perimetry for screening glaucomatous visual field defects*"

- 2017 (Co-author): Travel grant of amount $1,100, offered by the Association for Research in Vision and Ophthalmology (ARVO), Baltimore, Maryland, US, for the research work titled: *"Variability of Saccadic Reaction Time across the visual field on an Eye-tracker based perimeter"*

- 2018: Award for the paper to publication during Dr. E. Vaithilingam memorial scientific session, instituted by Elite School of Optometry (ESO), a unit of Medical Research Foundation (MRF), Chennai, India, for the research work titled: *"Development of a test grid using Eye Movement Perimetry for screening glaucomatous visual field defects*"

- 2019: Young clinical mentor award instituted by Elite School of Optometry (ESO), a unit of Medical Research Foundation (MRF), Chennai, India for the "*Contribution towards the education and training in Optometry & Vision Science*"

- 2019 (Co-author): Ruby Banik endowment award for the Best Research in Clinical Ophthalmology, instituted by Vision Research Foundation (VRF), Chennai, India, for the research work titled: *"Evaluation of Saccadic Reaction Time within Glaucoma Hemifield Test in Eye Movement Perimetry"*

- 2020: Ruby Banik endowment award for the Best Research in Clinical Ophthalmology, instituted by Vision Research Foundation (VRF), Chennai, India, for the research work titled: *"A haploscope based automated binocular pupillometer to quantify the dynamics of direct and consensual Pupillary Light Reflex: methodology & feasibility"*

- 2021 (Co-author): Award for the best presentation, Dr. E. Vaithilingam memorial scientific session, instituted by Elite School of Optometry (ESO), unit of Medical Research Foundation (MRF), Chennai, India, for the research work titled: *"Monocular and binocular visual field evaluation based on Saccadic Reaction Times using an Eye Movement Perimeter: An exploratory Approach"*

- 2021: Award for the best presentation under the category of Optometry Advances during the 2nd International Optometry Conference, instituted by India Vision Institute (IVI), India, for the research work titled: "*Quantification of pupillary dynamics in light and dark irides using a haploscope based pupillometer*"

- 2022 (Co-supervisor): Best performer award in Research project, instituted by The Sankara Nethralaya Academy (TSNA), Chennai, India for the research project titled: *"Construction and validation of a low-cost visual field screener for glaucoma"*

- 2022 (Co-author): Award for the best presentation under the category of Low vision and rehabilitation during the 3rd International Optometry Conference, instituted by India Vision Institute (IVI), India, for the research work titled: "*Practice and preference pattern of low vision services in glaucoma and its impact on individuals' quality of life*"

- 2022 (Co-author): Dr. Narasimhan memorial award for the Best Research in Optometry, instituted by Elite School of Optometry (ESO), a unit of Medical Research Foundation (MRF), Chennai, India, for the research work titled: *"Impact of monocular and binocular visual function parameters on vision-related quality of life in glaucoma"*

- 2022 (Co-supervisor): Best performer award in Research project, instituted by The Sankara Nethralaya Academy (TSNA), Chennai, India for the research project titled: *"Quality of life among patients with glaucoma and the impact of low vision services"*

ACKNOWLEDGMENTS

CURRICULUM VITAE

Najiya Sundus K. Meethal
born and raised in Kerala, India, acquired her Bachelor's and Master's degree in Optometry from Elite School of Optometry (ESO), Chennai, India in affiliation with Birla Institute of Technology and Science (BITS), Pilani, India. She achieved the institutional awards for the 'Best outgoing student' during her Bachelor's as well as the Master's programs along with various other academic excellence awards.

During the final quarter of the year 2017, she commenced her Doctor of Philosophy (Ph.D.) studentship by undertaking a translational research project titled "The functional biomarkers to assess visual system integrity: an eye tracking based approach". This was an Indo-Dutch collaborative endeavour between the Vestibular and Ocular Motor Research group at the Department of Neuroscience, Erasmus Medical Centre (EMC), Rotterdam, The Netherlands, and Sankara Nethralaya, A unit of Medical Research Foundation (MRF), Chennai, India. Najiya was also a member of the research advisory team of BulbiTech AS, Trondheim, Norway, which focuses on the prototype development of an eye-tracking technology based neuro-ocular diagnostic device and validation of its measurement protocols/interfaces. She could present her scientific research outcomes on several (inter) national platforms around the globe that were later in time successfully transformed into peer-reviewed publications in various scientific journals. During her Ph.D. tenure, she was the proud recipient of certain prestigious awards and accolades pertaining to scientific research. Najiya has successfully earned the designation of Fellowship at the American Academy of Optometry (FAAO) under the scientific category. In parallel, she was also dynamically engaged in providing academic guidance and supervision in clinical and research activities of undergraduate and postgraduate optometry students at the ESO and The Sankara Nethralaya Academy (TSNA), Chennai, India. She was honoured with the 'Young clinical mentor award for the year 2018-19 for her contributions towards optometric education & teaching at her alma mater.

SYNOPSIS

Our eyes are exquisitely evolved to function as a physical portal through which details from the external environment are captured by their neural components. This visual information is then translated into the brain's internal language thus aiding us in perceiving the real world. Any assault on the elements involved in this capture and transfer process, as in glaucoma or any neuro-ophthalmic conditions, can lead to visual function deficits. These eventually limit real-life independence and brings about a variety of public health, social and economic burdens, particularly in underdeveloped/developing countries. Conventional ophthalmic evaluation entails various methods to assess the visual system integrity, including the visual field and pupillary evaluation. They play a vital role in disease diagnosis and monitoring. However, these approaches raise some challenges, thereby compromising the reliability of the outcome measures. With the advancements in technology over the past decades, the capabilities have increased enormously, among which Eye Tracking Technology (ETT) is one such approach that offers one of the most potent ways of assessing visual functional biomarkers. This thesis aimed to quantify potential functional biomarkers to assess the integrity of the visual system on the basis of ETT. The research findings support the possibility of applying ETT at eye care centres to provide a supplementary/surrogate way of studying the integrity of visual functions, thereby further enhancing the existing clinical methods.